01 Feb 1969

Three-bolt in-line connections with low ductility light-gage steel

D. W. Popowich

S. J. Errera

George Winter

Department of Structural Engineering

School of Civil Engineering

Cornell University

Report No. 2

Three-Bolt In-Line Connections with Low Ductility Light-Gage Steel

by

D. W. Popowich

and

S. J. Errera

George Winter

Project Director

Final report of an ad hoc investigation for the

American Iron and Steel Institute

Ithaca, New York February, 1969

TABLE OF CONTENTS

	Page
1. Introduction	1
2. Procedure	1
3. Results	3
4. Discussion	4
5. Conclusions	5
References	6
Notation	7
List of Tables	
Table I - Connection Dimensions	8
Table II - Test Results	8
Table III - Elongation Data	9
List of Figures	
Figure 1 - Typical Connection Specimen	
Figure 2 - Scoring Pattern for Plates	
Figure 3 - Tension Failure Comparison for Three-Bolt In-Line Connections	
Figure 4 - Tension Failure Comparison for One-Bolt Connections	
Figure 5 - Plate and Bolt Hole Elongation Profile	
Figure 6 - Stress-Strain Diagram	
Figure 7 - Load-Deformation Diagram	

1. Introduction

In order to investigate the influence of ductility on the strength and behavior of bolted connections, Dhalla[1] conducted tests on single bolt lap joints using "low ductility" steels. As part of a separate investigation, Popowich[2] conducted tests on single, double, and triple bolt in-line lap joints using "high ductility" steels. The investigation reported herein was performed in order to compare the performance of 3 bolt in-line connections of high ductility steels (21 to 53% elongation in a 2 inch gage length) with that of similar 3 bolt in-line connections of low ductility steels (nominally 5 and 10% elongation in a 2 inch gage length).

2. Procedure

Eight test specimens were prepared for this investigation. Fig. 1 illustrates the typical specimen arrangement used in these tests. Specimens Nos. 16051A and 16052A were made from 16 gage, 5% ductility steel, Nos. 16101A and 16102A were made from 16 gage, 10% ductility steel, and Nos. 7085S, 7091S, 7092S, and 7093S were made from 7 gage, 8.5 to 9% ductility steel. (These steels were specially prepared for research on the influence of ductility.) No. 16051A of the 5% ductility specimens used three 1/2 inch bolts in line, while the 5% ductility specimen No. 16052A used three 3/4 inch bolts in line. The same geometry was used for the 10% ductility steel, Nos. 16101A and 16102A. The steel specimens Nos. 7085S, 7091S, 7092S, and 7093S used three 5/8 inch bolts in line and varied s (width of plate) in order to obtain different d/s values. The steel

properties, obtained from coupon tests, are given in the first three columns of Table II, as follows: The nominal 5% ductility steel had a tension coupon ultimate stress σ_t of 84.9 ksi, a yield point σ_y of 84.9 ksi, and an actual elongation of 4.91% in a gage length of 2 inches. The nominal 10% ductility steel had σ_t = 79.3 ksi, σ_y = 75.6 ksi, and an actual elongation of 10.7% in a gage length of 2 inches. The 7 gage low ductility steels had σ_t = 85 and 86 ksi, σ_y = 85 and 86 ksi, and elongations of 8.5 and 9.2% in a 2 inch gage length, respectively. All connection specimens were designed to fail by transverse tearing. Tables I and II give all pertinent data for the connection specimens.

One of the plates in each of the 5 and 10% ductility steel specimens was painted with machinist's ink and scribed as shown in Fig. 2-a, while both plates in the 7 gage low ductility steel specimens were painted with machinist's ink and scribed as shown in Fig. 2-b. The longitudinal scribe line was made adjacent to the hole perimeter, as shown in the figures. A toolmakers' microscope was used to measure the spacing of the lines, as well as the size of the holes in each plate. After the specimen failed, the scribed plates and the hole sizes were again measured, in order to observe the elongation patterns of the specimens.

The assembled specimens were connected with high strength bolts, completely threaded, with an ultimate shear stress of 120 ksi. The bolts were torqued: 40 ft-lb for the 1/2 inch bolts, 50 ft-lb for the 5/8 inch bolts, and 110 ft-lb for the

3/4 inch bolts. The holes in the plates were drilled and washers were placed under the head and nut of the bolt. Shims were used in the grips of the testing machine to reduce the load eccentricity.

The tests were conducted using the 80 kip range of a 400 kip capacity Baldwin Southwark hydraulic testing machine.

3. Results

All test specimens failed by transverse tearing, as they were designed to do. The results of the tests are given in Table II. Table III gives the data on the elongation of the plates and holes.

In order to make a comparison of all the three bolt in-line connection tests, the results were plotted in Fig. 3. In Fig. 3 the ratio of average stress on the net section to the tensile strength of a coupon is plotted versus the ratio of bolt diameter to the width of the plate. The test results are also compared with the failure criterion suggested in Reference 2 for tension failures,

$$\frac{\sigma_{NET}}{\sigma_t} = 1.0 - 0.9r + 3.0rd/s$$

where σ_{NET} is the stress across the net section of the specimen, σ_t is the tensile stress of a coupon, r is the ratio of the force transmitted by the bolt to the tension force in the member at the critical section, d is the diameter of the bolt, and s is the width of the plate. From this graph it is seen that the low ductility steels behaved the same or slightly more favorably than did the high ductility steel. Because of

this finding, a similar graph was plotted for the one bolt tests previously performed (see Fig. 4). Again the low ductility steel behaved as well as or slightly better than the high ductility steel.

In Fig. 5 graphs are constructed in order to show the elongation profile of the test specimens. These graphs were obtained by measuring the elongations within the variable gage lengths (1/2 and 1/4 inches), shown in Fig. 2. Two plots are used to show this: the percent elongation along the length of the plate, and the elongation of each of the three holes. The elongation of the bolt holes was obtained by measuring the clear distance between the ends of the longitudinal diameter.

4. Discussion

The behavior in tension on the net section indicates that the low elongation steels used have adequate local ductility to distribute the stresses both laterally across the net section and longitudinally along the specimen as effectively as, if not better than, do high ductility steels. This is probably true, because in spite of the fact that one steel is much more ductile than the other, the low elongation steel still is quite ductile, as compared to a brittle material. Fig. 6 illustrates typical stress-strain diagrams for the 5 and 10% ductility coupons and the 7 gage steel coupons, while Fig. 7 illustrates the load-deformation relationship of the connections made from the 5 and 10% ductility steels and the 7 gage steels, respectively. The gage

length in Fig. 7 is equal to 4e + 2d'.

The elongation profile graphs shown in Fig. 4 suggest that the longitudinal distribution of load was accomplished mainly by local bearing deformation at the bolt holes. Table II shows that some bearing stresses were as high as 2.3 times the tensile strength; yet failure occurred in net section tension rather than bearing.

A reason for the slightly superior behavior of the low ductility steels may possibly be found in the absence of a strain-hardening range in these unusual steels. The comparisons in Figs. 3 and 4 are based only on tensile strength. The real behavior of a complex connection probably depends on the shape of the complete stress-strain curve rather than on one single property.

5. Conclusions

The behavior in tension on the net section of connections with three in line bolts indicates that the low ductility light gage steels used have adequate local ductility to distribute the tension stresses laterally across the net section and longitudinally along the specimen as effectively as do high ductility steels. The longitudinal distribution probably was accomplished mainly by local bearing deformation at the bolt holes.

REFERENCES

1. Dhalla, A. K., and Errera, S. J., "Influence of Ductility on the Structural Behavior of Light-Gage Cold-Formed Steel Members", First Progress Report, February, 1968, Department of Structural Engineering, Cornell University, Ithaca, New York.

2. Popowich, D. W., and Errera, S. J., "Tension Capacity of Bolted Connections in Light-Gage Steel", Report, June, 1968, Department of Structural Engineering, Cornell University, Ithaca, New York.

NOTATION

d = diameter of bolt, in.

d' = size of hole in sheet, in.

e = longitudinal spacing between bolts or distance between bolt and edge of sheet, in.

P_{Fail} = failure load of connection, lb.

r = force transmitted by the bolt or bolts at the section considered, divided by the tension force in the member at that section.

s = width of sheet, in.

t = thickness of sheet, in.

σ_b = bearing stress in the connection, psi.

σ_{NET} = average tension stress on net section, psi.

σ_t = ultimate strength of coupon, psi.

σ_y = yield strength of coupon, psi.

TABLE I

CONNECTION DIMENSIONS

Specimen	t in.	d in.	d' in.	s in.	e in.
16051A	0.06	1/2	9/16	4.00	2
16052A	0.06	3/4	13/16	4.00	1 3/4
16101A	0.06	1/2	9/16	4.00	2
16102A	0.06	3/4	13/16	4.00	1 3/4
7085S	0.184	5/8	11/16	3.22	3 1/8
7091S	0.182	5/8	11/16	3.30	3 1/8
7092S	0.183	5/8	11/16	4.23	4 1/4
7093S	0.185	5/8	11/16	4.23	4 1/4

TABLE II

TEST RESULTS

Specimen	σ_y ksi	σ_t ksi	% Elong. in 2" %	P_{FAIL} kips	σ_{NET} ksi	σ_b ksi	$\frac{\sigma_{NET}}{\sigma_t}$	$\frac{\sigma_b}{\sigma_y}$	d/s
16051A	84.9	84.9	4.91	17.5	85.0	194	1.00	2.29	0.125
16052A	84.9	84.9	4.91	19.2	100	142	1.18	1.67	0.1875
16101A	75.6	79.3	10.7	16.7	81.0	186	1.02	2.46	0.125
16102A	75.6	79.3	10.7	16.5	86.4	122	1.09	1.61	0.1875
7085S	85	85	8.55	40.2	86.4	116.5	1.016	1.37	0.194
7091S	86.25	86.25	9.23	40.2	84.8	118	0.983	1.37	0.190
7092S	86.25	86.25	9.23	54.9	84.75	160	0.983	1.855	0.148
7093S	86.25	86.25	9.23	54.8	83.6	158	0.970	1.83	0.148

TABLE III-a

ELONGATION DATA

Gage Mark	16051A L_o in.	L_f in.	ΔL in.	% Elong. %	16052A L_o in.	L_f in.	ΔL in.	% Elong. %
1	0.492	0.500	0.008	1.63	0.465	0.446	-0.019	-4.09
2	0.486	0.500	0.014	2.88	0.500	0.499	-0.001	-0.20
3	0.489	0.489	0	0	0.501	0.501	0	0
4	0.250	0.250	0	0	0.256	0.256	0	0
5	0.251	0.251	0	0	0.246	0.246	0	0
6	0.250	0.251	0.001	0.400	0.256	0.257	0.001	0.39
7	0.201	0.202	0.001	0.498	0.248	0.248	0	0
8	0.553	0.553	0	0	0.493	0.493	0	0
9	0.565	0.565	0	0	0.562	0.562	0	0
10	0.499	0.499	0	0	0.498	0.498	0	0
11	0.274	0.274	0	0	0.256	0.256	0	0
12	0.223	0.223	0	0	0.248	0.248	0	0
13	0.252	0.252	0	0	0.248	0.248	0	0
14	0.248	0.248	0	0	0.256	0.256	0	0
15	0.502	0.502	0	0	0.498	0.498	0	0
16	0.556	0.555	-0.001	-0.18	0.564	0.564	0	0
17	0.500	0.500	0	0	0.500	0.500	0	0
18	0.250	0.254	0.004	1.60	0.250	0.250	0	0
19	0.250	0.249	-0.001	-0.40	0.248	0.249	0.001	0.403
20	0.252	-	-	-	0.253	0.255	0.002	0.79
21	0.248	0.249	0.001	0.403	0.249	0.249	0	0
22	0.499	0.249	0	0	0.500	0.500	0	0
Holes								
1	0.565	0.598	0.033	5.85	0.805	0.805	0	0
2	0.569	0.629	0.060	10.53	0.805	0.805	0	0
3	0.563	0.700	0.137	24.40	0.804	0.805	0.001	0.124
1'	0.562	0.599	0.037	6.59	0.804	0.804	0	0
2'	0.563	0.600	0.037	6.57	0.804	0.804	0	0
3'	0.560	0.595	0.035	6.25	0.804	0.910	0.106	13.2

Failure not in scored plate.

TABLE III-b

ELONGATION DATA

Gage Mark	16101A L_o in.	16101A L_f in.	16101A ΔL in.	16101A % Elong. %	16102A L_o in.	16102A L_f in.	16102A ΔL in.	16102A % Elong. %
1	0.460	0.460	0	0	0.483	0.461	-0.022	-4.56
2	0.498	0.498	0	0	0.492	0.491	-0.001	-0.204
3	0.501	0.501	0	0	0.506	0.507	0.001	0.198
4	0.250	0.250	0	0	0.254	0.253	-0.001	-0.394
5	0.251	0.251	0	0	0.244	0.243	-0.001	-0.410
6	0.250	0.250	0	0	0.255	0.257	0.002	0.785
7	0.247	0.247	0	0	0.247	0.247	0	0
8	0.501	0.501	0	0	0.504	0.502	-0.002	-0.398
9	0.592	0.592	0	0	0.557	0.558	0.001	0.179
10	0.468	0.468	0	0	0.473	0.472	-0.001	-0.212
11	0.249	0.250	0.001	0.402	0.276	0.276	0	0
12	0.252	0.252	0	0	0.253	0.253	0	0
13	0.251	0.250	-0.001	-0.402	0.246	0.245	-0.001	-0.406
14	0.253	0.253	0	0	0.256	0.257	0.001	0.391
15	0.522	0.522	0	0	0.497	0.496	-0.001	-0.201
16	0.532	0.532	0	0	0.557	0.559	0.002	0.359
17	0.501	0.501	0	0	0.501	0.501	0	0
18	0.250	0.252	0.002	0.800	0.250	0.250	0	0
19	0.249	0.247	-0.002	-0.803	0.250	0.261	0.011	4.40
20	0.250	0.269	0.019	7.6	0.250	0.390	0.140	56.0
21	0.250	0.250	0	0	0.250	0.256	0.006	3.40
22	0.499	0.498	-0.001	-0.201	0.500	0.500	0	0
Holes								
1	0.564	0.619	0.055	9.75	0.805	0.806	0.001	0.124
2	0.578	0.662	0.084	14.51	0.804	0.805	0.001	0.124
3	0.563	0.681	0.118	21.00	0.805	0.970	0.165	20.5
1'	0.565	0.630	0.065	11.50	0.800	0.800	0	0
2'	0.577	0.680	0.103	17.85	0.800	0.800	0	0
3'	0.562	0.830	0.268	47.70	0.800	0.800	0	0

Failure not in scored plate.

TABLE III-c

ELONGATION DATA

Gage Mark	7085S L_o in.	7085S L_f in.	7085S ΔL in.	7085S % Elong. %	7091S L_o in.	7091S L_f in.	7091S ΔL in.	7091S % Elong. %
1	0.500	0.500	0	0	0.499	0.499	0	0
2	0.501	0.501	0	0	0.501	0.501	0	0
3	0.249	0.249	0	0	0.250	0.250	0	0
4	0.247	0.247	0	0	0.250	0.250	0	0
5	0.500	0.500	0	0	0.500	0.500	0	0
6	0.500	0.500	0	0	0.500	0.500	0	0
7	0.625	0.625	0	0	0.624	0.624	0	0
8	0.501	0.501	0	0	0.500	0.500	0	0
9	0.498	0.498	0	0	0.499	0.499	0	0
10	0.254	0.254	0	0	0.249	0.249	0	0
11	0.247	0.247	0	0	0.249	0.249	0	0
12	0.499	0.499	0	0	0.501	0.501	0	0
13	0.499	0.499	0	0	0.501	0.501	0	0
14	0.625	0.625	0	0	0.619	0.619	0	0
15	0.501	0.501	0	0	0.504	0.504	0	0
16	0.500	0.500	0	0	0.498	0.500	0.002	0.500
17	0.248	0.402	0.154	62.0	0.251	0.285	0.034	13.75
18	0.250	0.277	0.027	10.4	0.249	0.416	0.166	66.5
19	0.508	0.508	0	0	0.498	0	0	0
20	0.491	0.491	0	0	0.505	0	0	0
Holes								
1	0.692	0.712	0.020	2.89	0.690	0.694	0.004	0.580
2	0.691	0.704	0.013	1.95	0.688	0.699	0.011	1.60
3	0.699	0.904	0.205	29.4	0.685	0.899	0.214	31.2
1'	0.697	0.711	0.014	2.01	0.690	0.702	0.012	1.67
2'	0.697	0.711	0.014	2.01	0.689	0.689	0.009	1.23
3'	0.702	0.721	0.019	2.71	0.690	0.707	0.017	2.54

TABLE III-d

ELONGATION DATA

Gage Mark	7092S L_o in.	7092S L_f in.	7092S ΔL in.	7092S % Elong. %	7093S L_o in.	7093S L_f in.	7093S ΔL in.	7093S % Elong. %
1	0.500	0.500	0	0	0.502	0.502	0	0
2	0.499	0.501	0.002	0.400	0.499	0.499	0	0
3	0.248	0.248	0	0	0.250	0.250	0	0
4	0.247	0.247	0	0	0.250	0.250	0	0
5	0.501	0.502	0.001	0.300	0.250	0.250	0	0
6	0.498	0.498	0	0	0.498	0.498	0	0
7	-	-	-	-	-	-	-	-
8	0.500	0.500	0	0	0.499	0.499	0	0
9	0.500	0.503	0.003	0.600	0.501	0.503	0.002	0.400
10	0.247	0.249	0.002	0.606	0.249	0.249	0	0
11	0.251	0.251	0	0	0.249	0.249	0	0
12	0.498	0.498	0	0	0.501	0.501	0	0
13	0.498	0.498	0	0	0.500	0.500	0	0
14	-	-	-	-	-	-	-	-
15	0.500	0.500	0	0	0.501	0.501	0	0
16	0.501	0.507	0.006	1.20	0.496	0.504	0.008	1.51
17	0.247	0.688	0.189	37.9	0.250	0.270	0.020	8.00
18	0.252				0.252	0.403	0.151	60.00
19	0.497	0.497	0	0	0.498	0.599	0.101	20.3
20	0.499	0.499	0	0	0.502	0.502	0	0
Holes								
1	0.688	0.734	0.046	6.69	0.682	0.741	0.059	8.65
2	0.685	0.748	0.063	9.20	0.683	0.734	0.051	7.39
3	0.685	0.915	0.230	33.4	0.685	0.946	0.261	38.1
1'	0.697	0.735	0.038	5.45	0.681	0.743	0.062	9.10
2'	0.686	0.749	0.063	9.18	0.688	0.747	0.059	8.65
3'	0.685	0.766	0.081	11.8	0.686	0.747	0.061	8.96

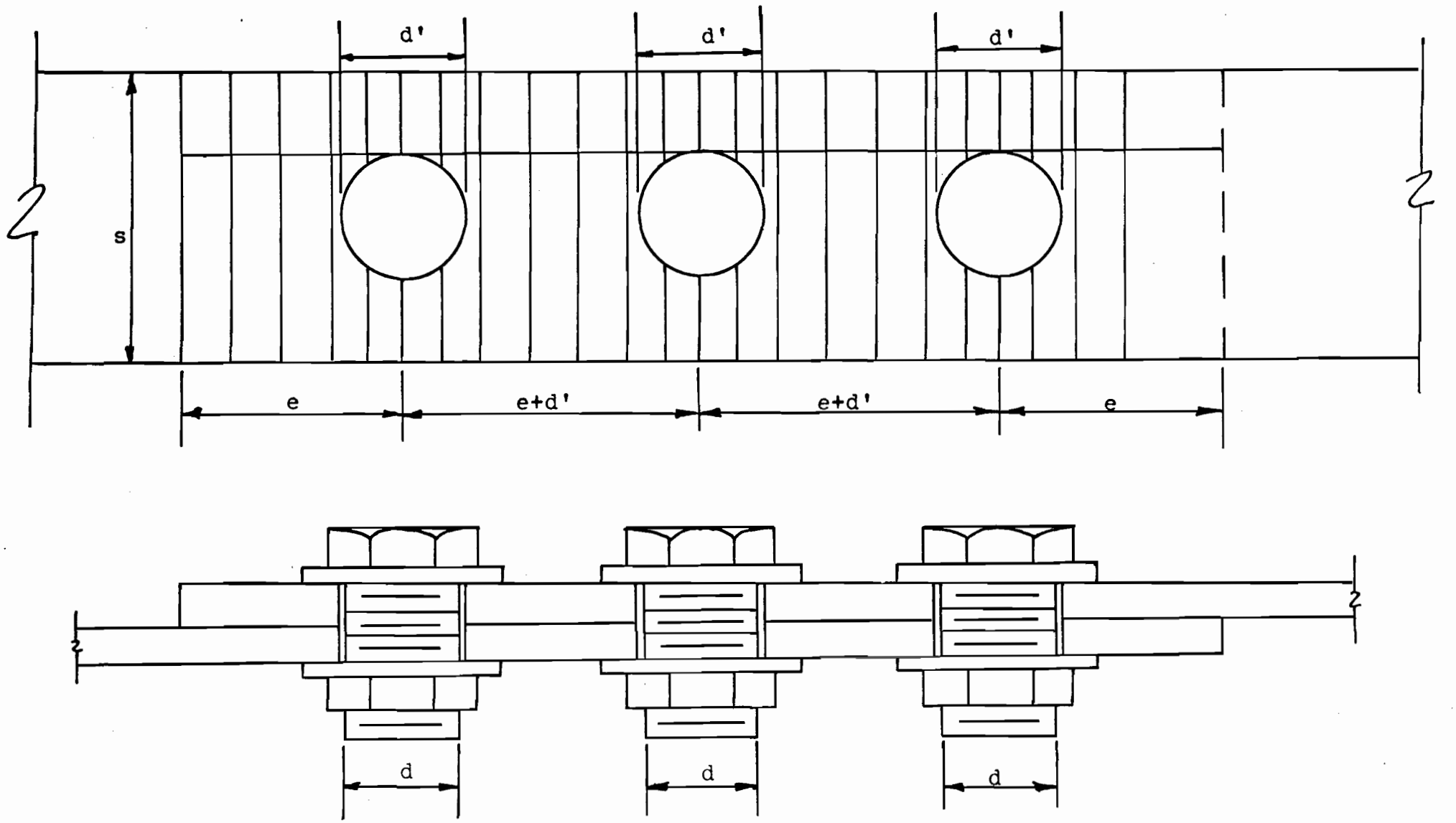

FIG. 1 - TYPICAL CONNECTION SPECIMEN.

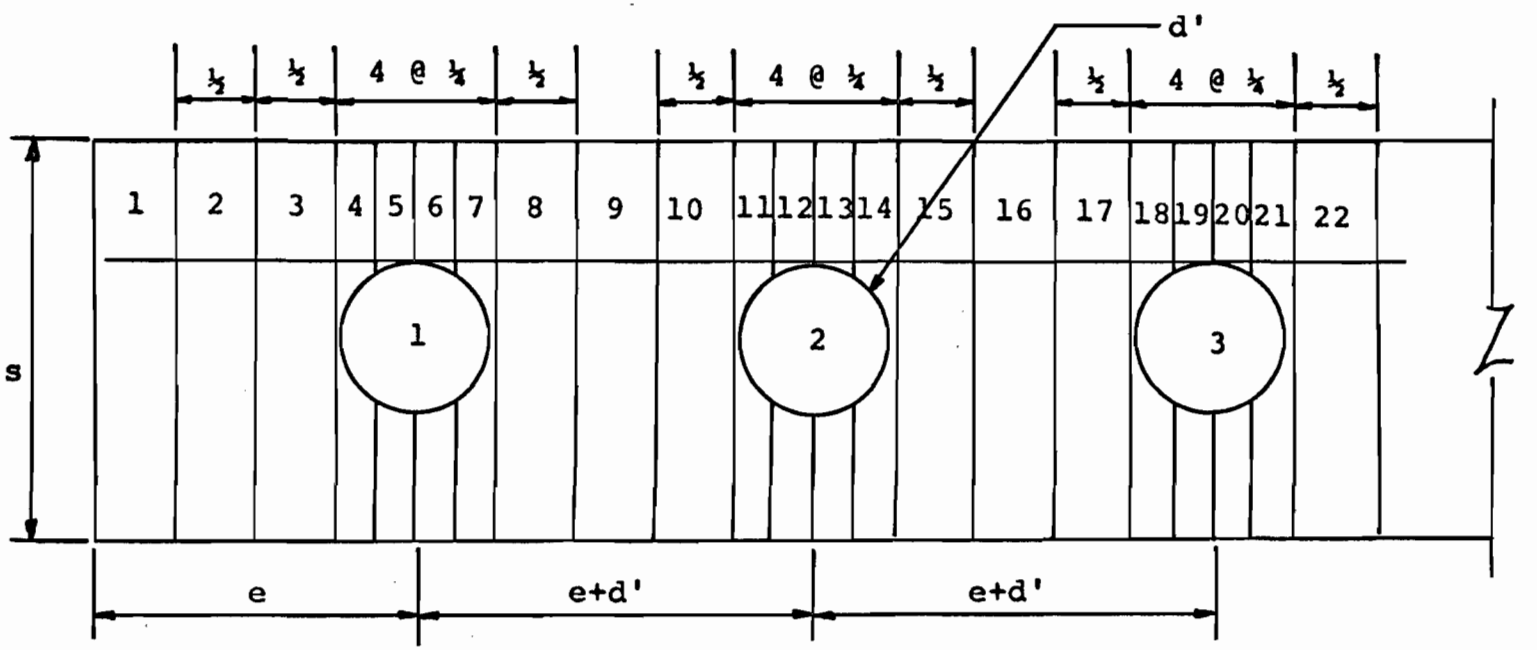

Scoring For Plates: 16051A
16052A
16101A
16102A

FIG. 2a - SCORING PATTERN (A) FOR PLATES.

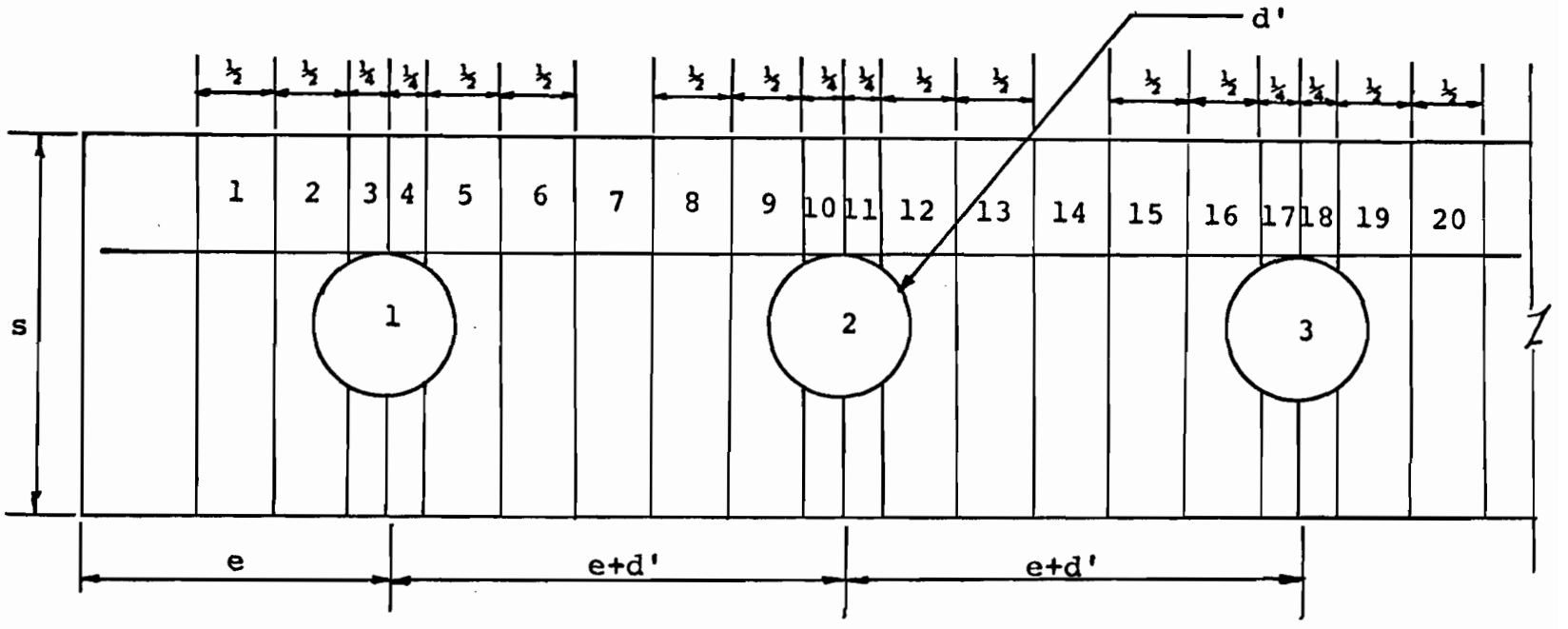

Scoring for Plates: 7085S
7091S
7092S
7093S

FIG. 2b - SCORING PATTERN (B) FOR PLATES.

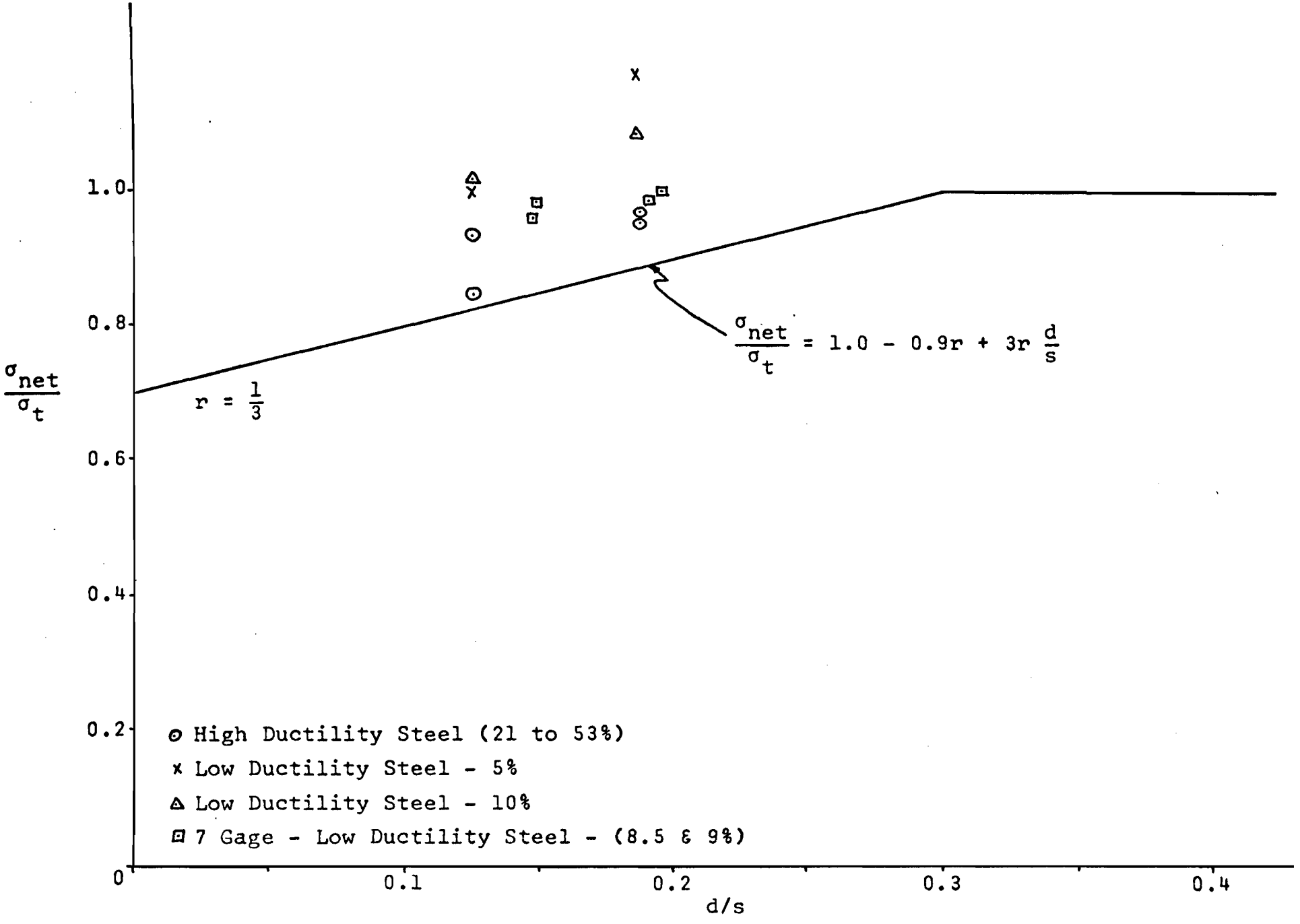

FIG. 3 - TENSION FAILURE COMPARISON FOR THREE BOLT IN-LINE CONNECTIONS.

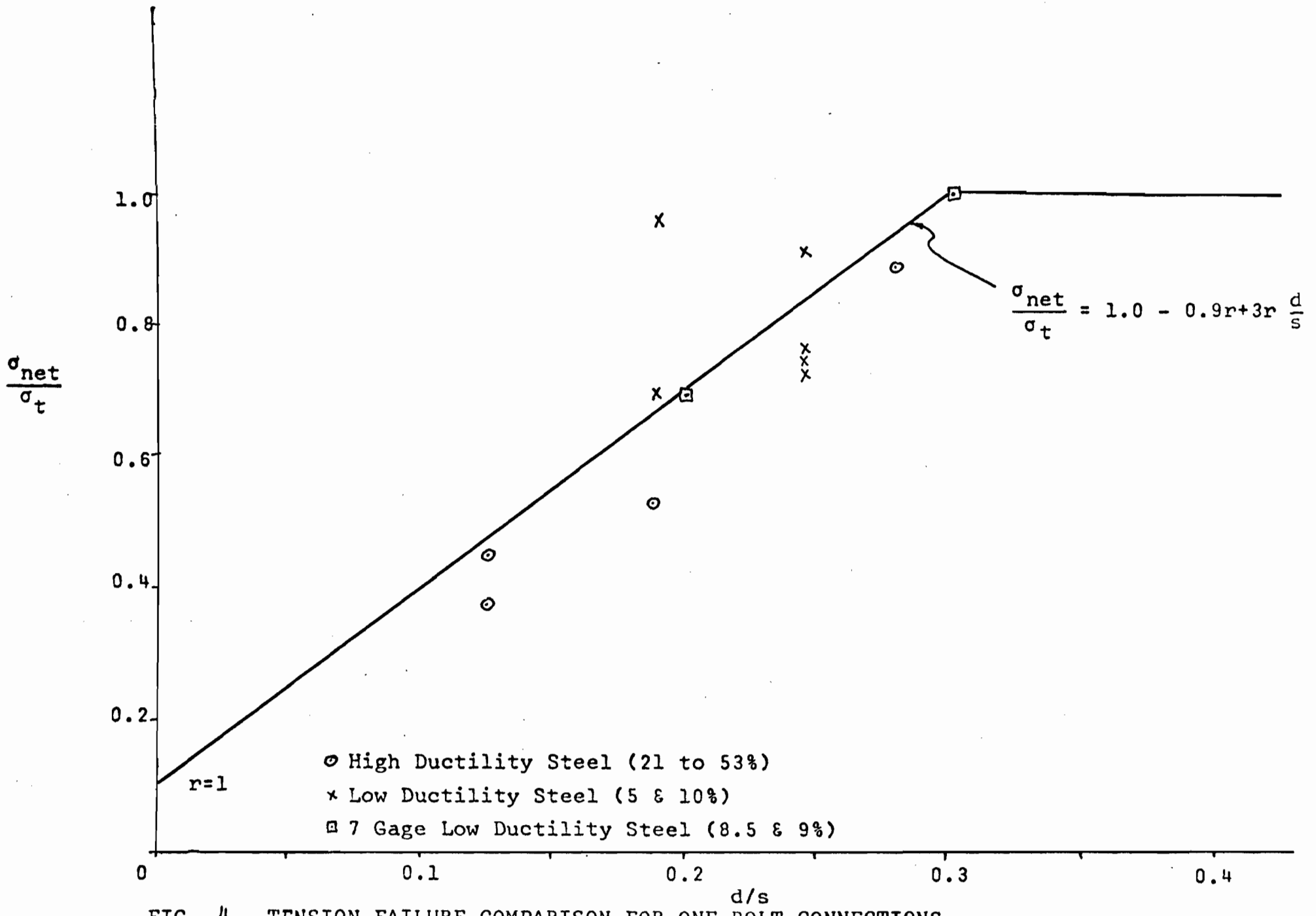

FIG. 4 - TENSION FAILURE COMPARISON FOR ONE BOLT CONNECTIONS.

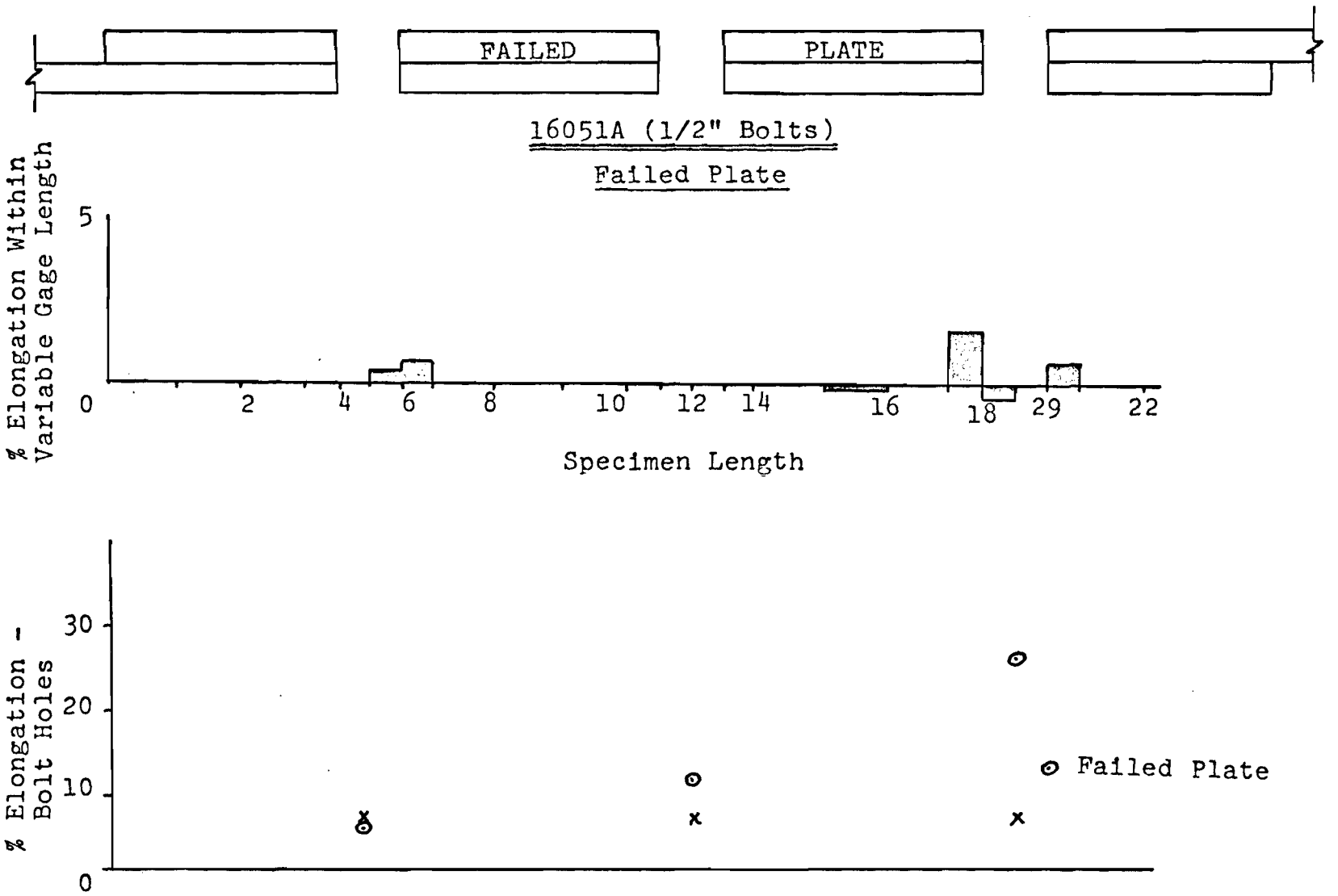

FIG. 5a - PLATE AND BOLT HOLE ELONGATION PROFILE.

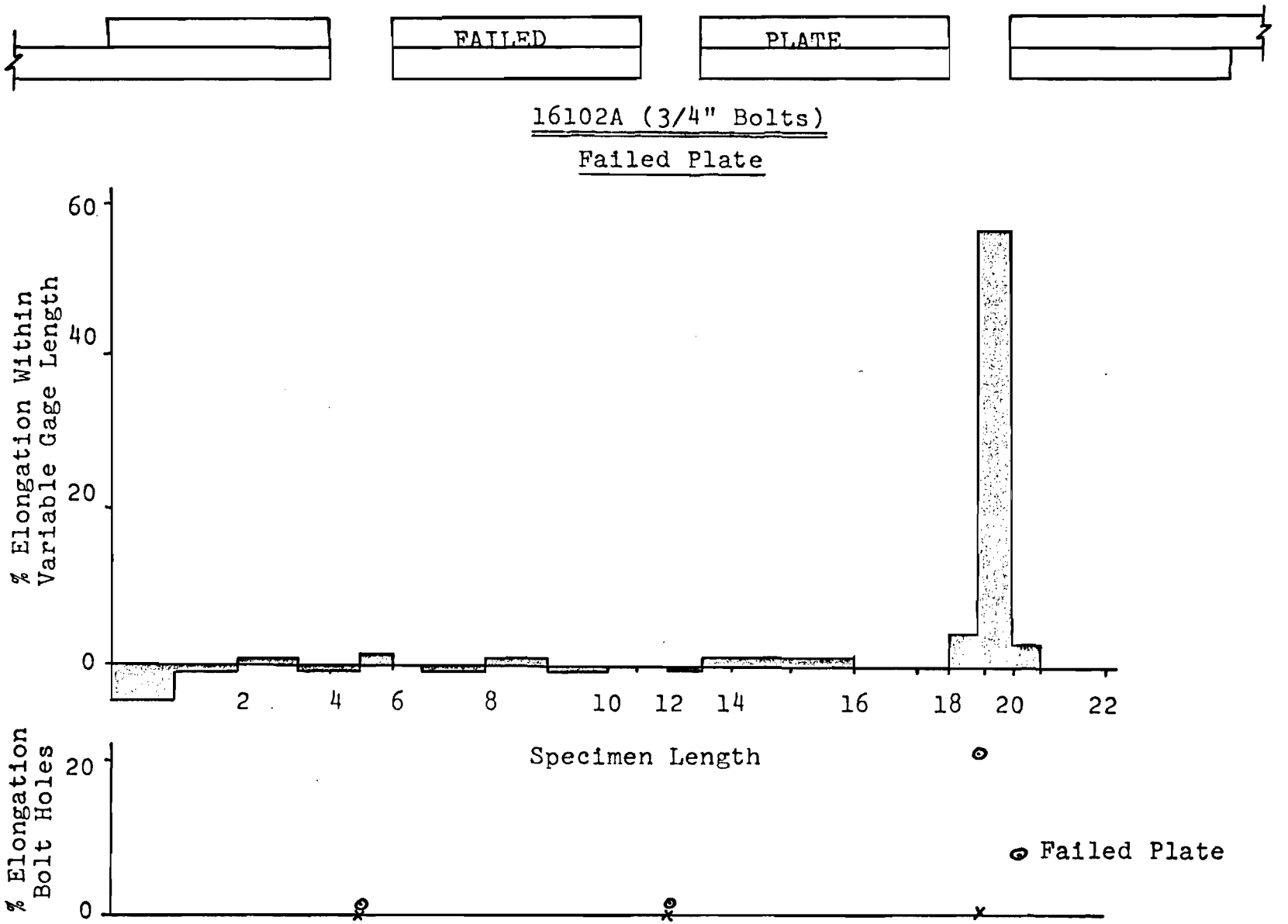

FIG. 5b - PLATE AND BOLT HOLE ELONGATION PROFILE.

7092S (5/8" Bolts)

Failed Plate

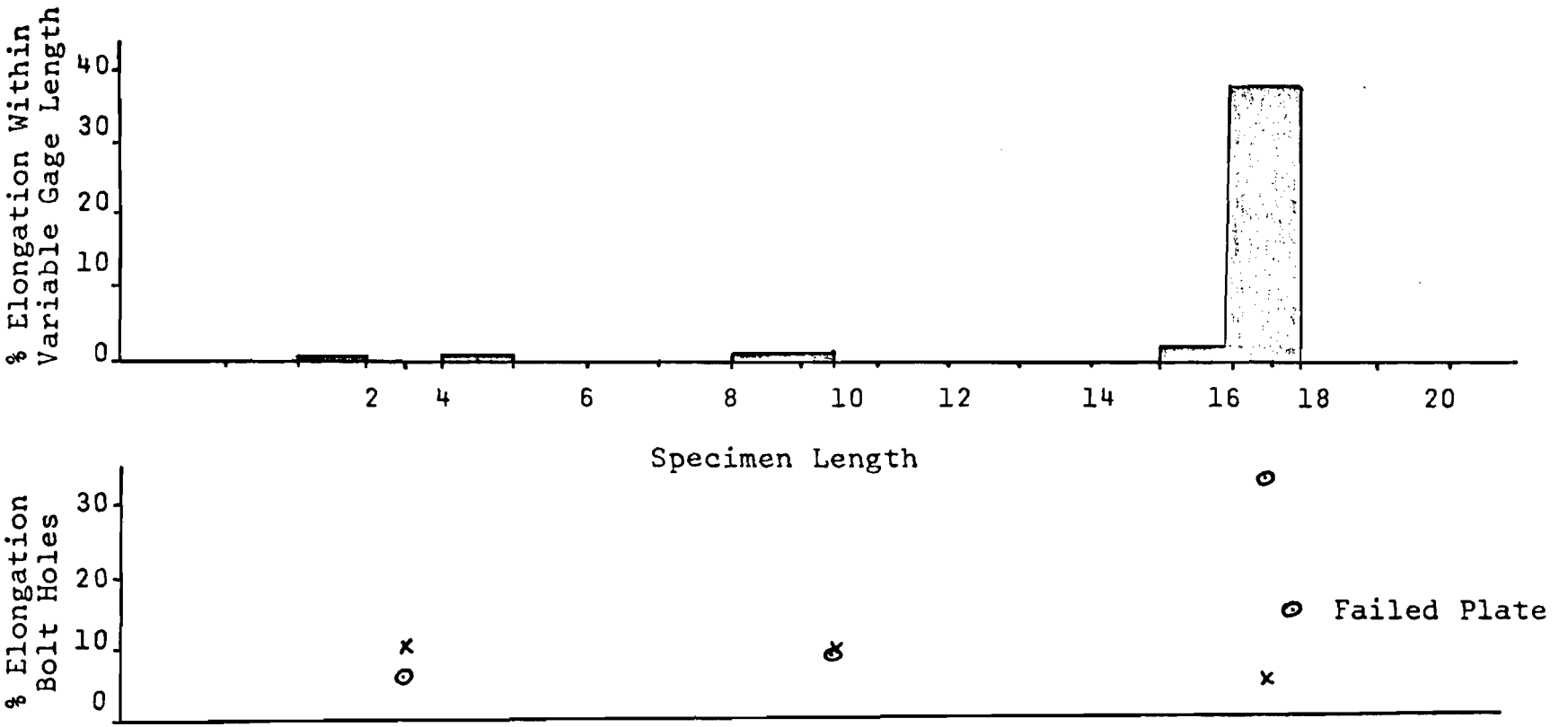

FIG. 5c - PLATE AND BOLT HOLE ELONGATION PROFILE.

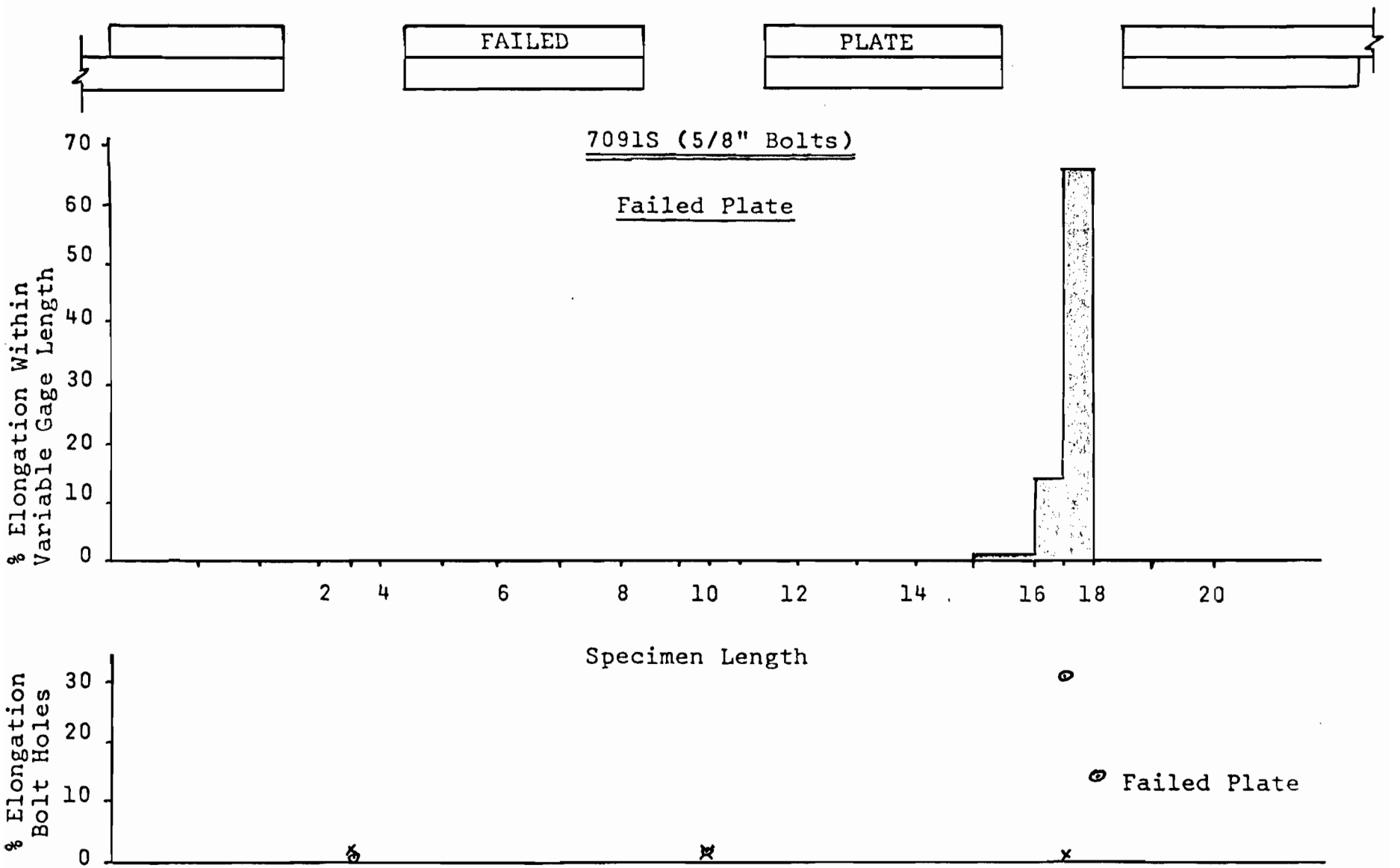

FIG. 5d - PLATE AND BOLT HOLE ELONGATION PROFILE.

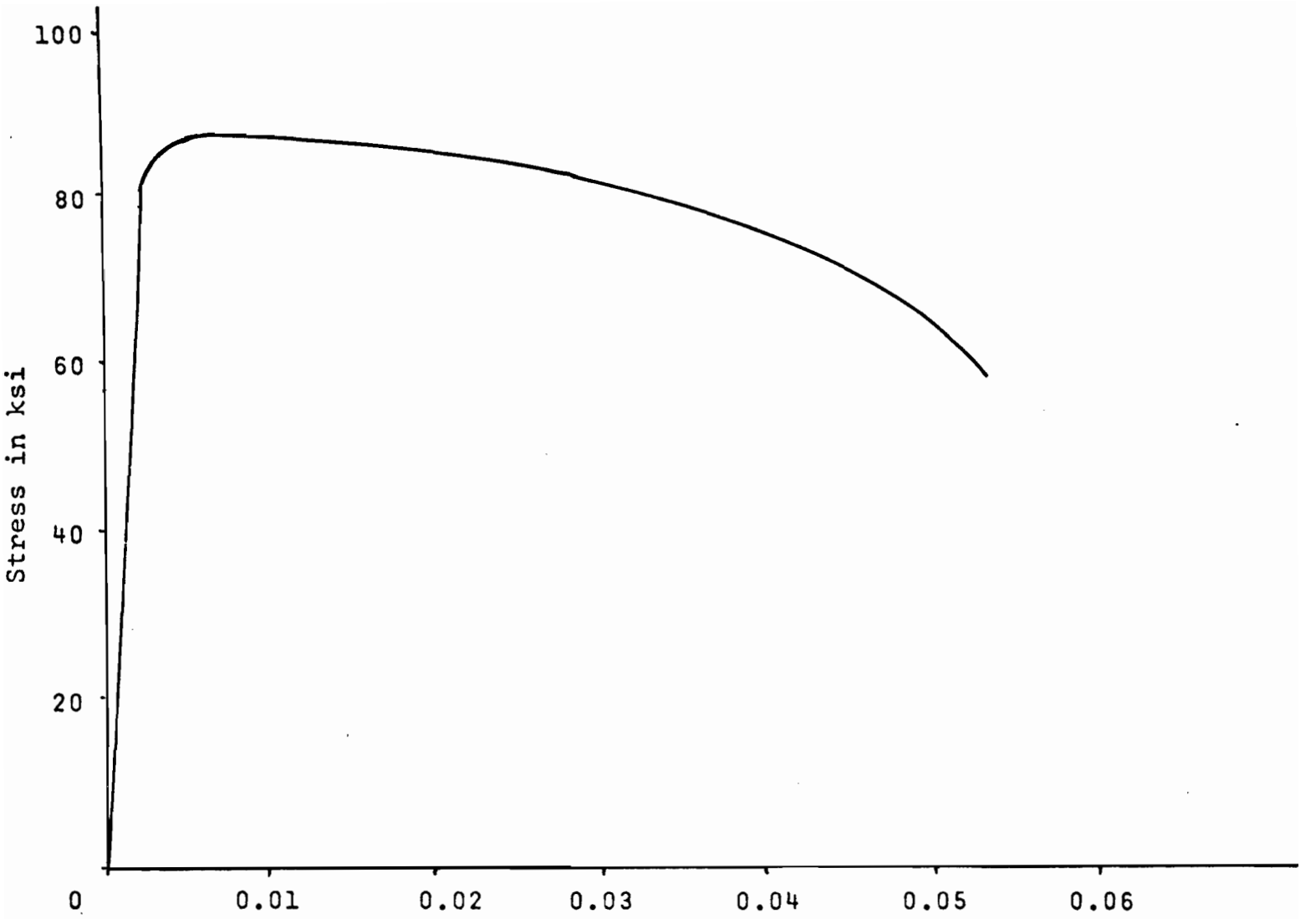

FIG. 6a - STRESS-STRAIN DIAGRAM FOR SPECIMEN NO. 16051A.

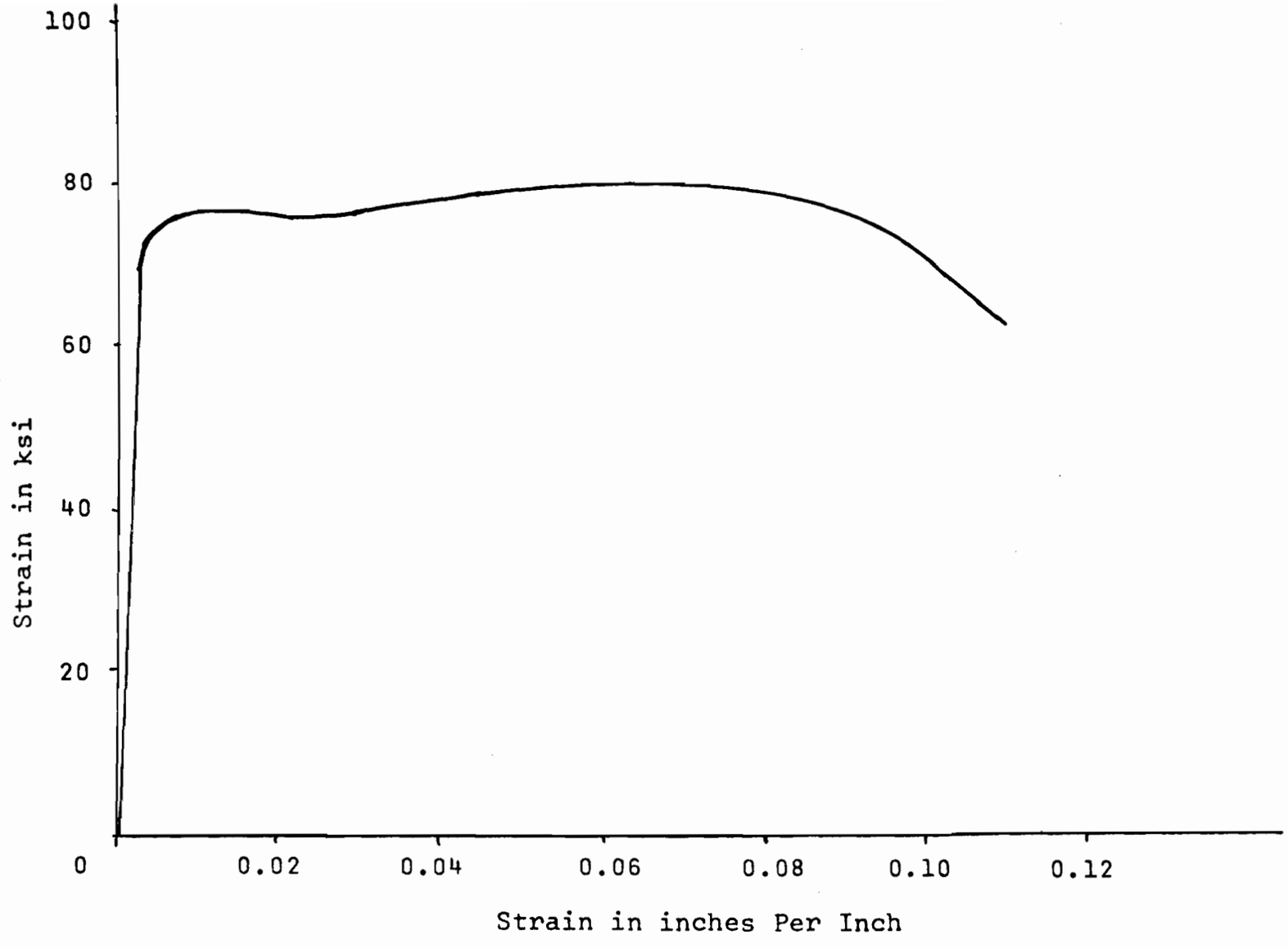

FIG. 6b - STRESS-STRAIN DIAGRAM FOR SPECIMEN NO. 16102A.

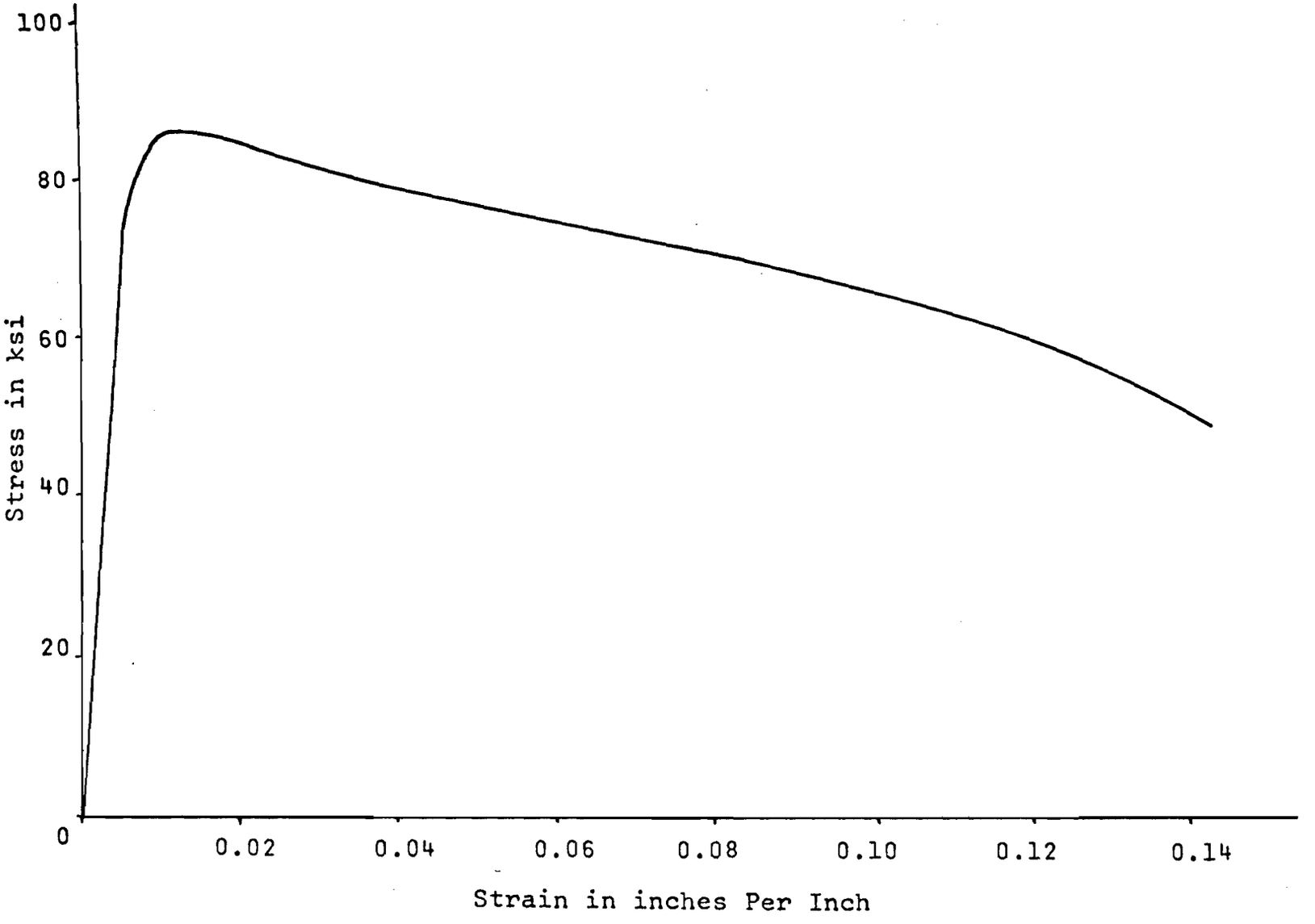

FIG. 6c - STRESS-STRAIN DIAGRAM FOR SPECIMEN NO. 7092S.

Specimen # 16051A

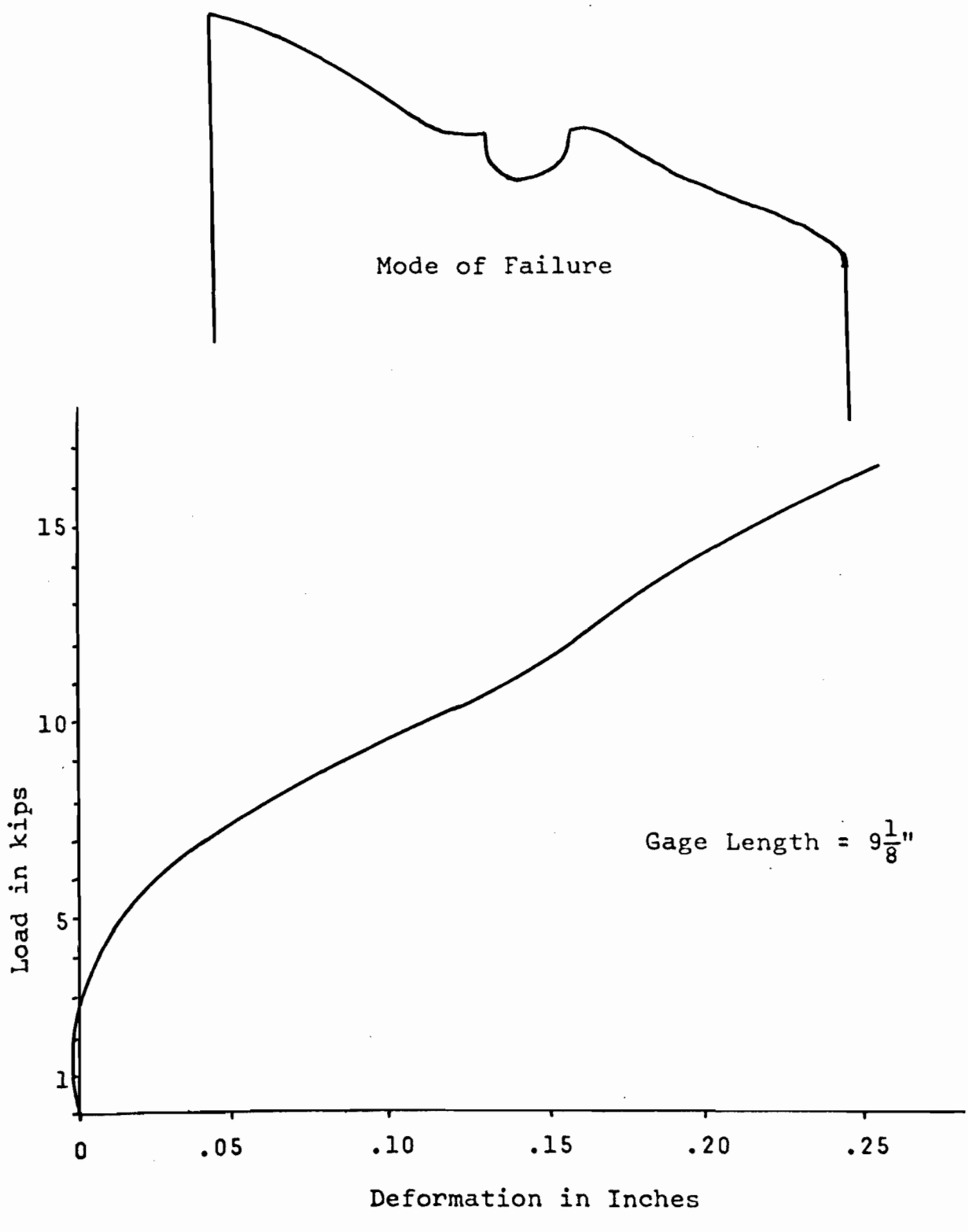

FIG. 7a - LOAD-DEFORMATION DIAGRAM.

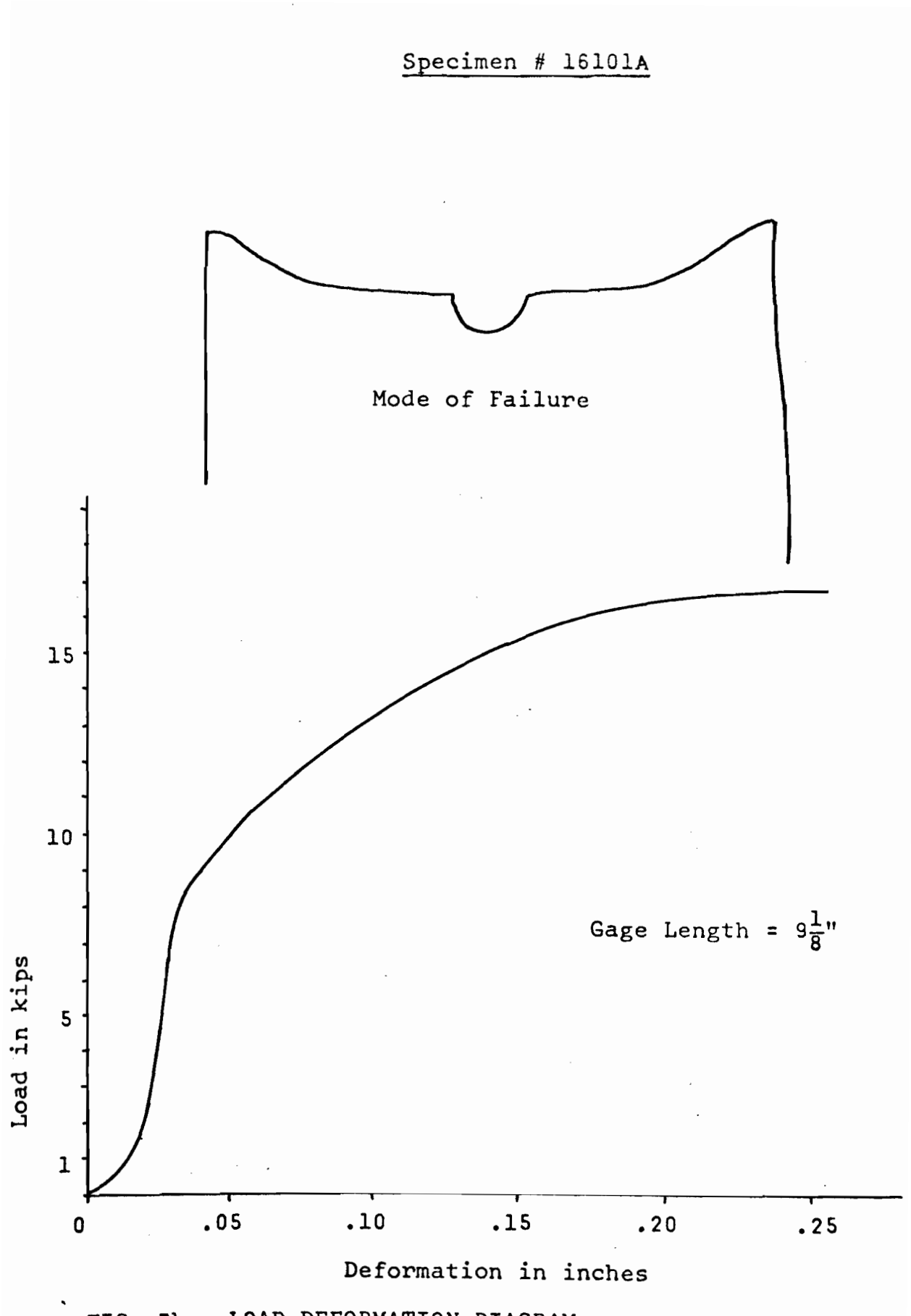

FIG. 7b - LOAD-DEFORMATION DIAGRAM.

Specimen # 7091S

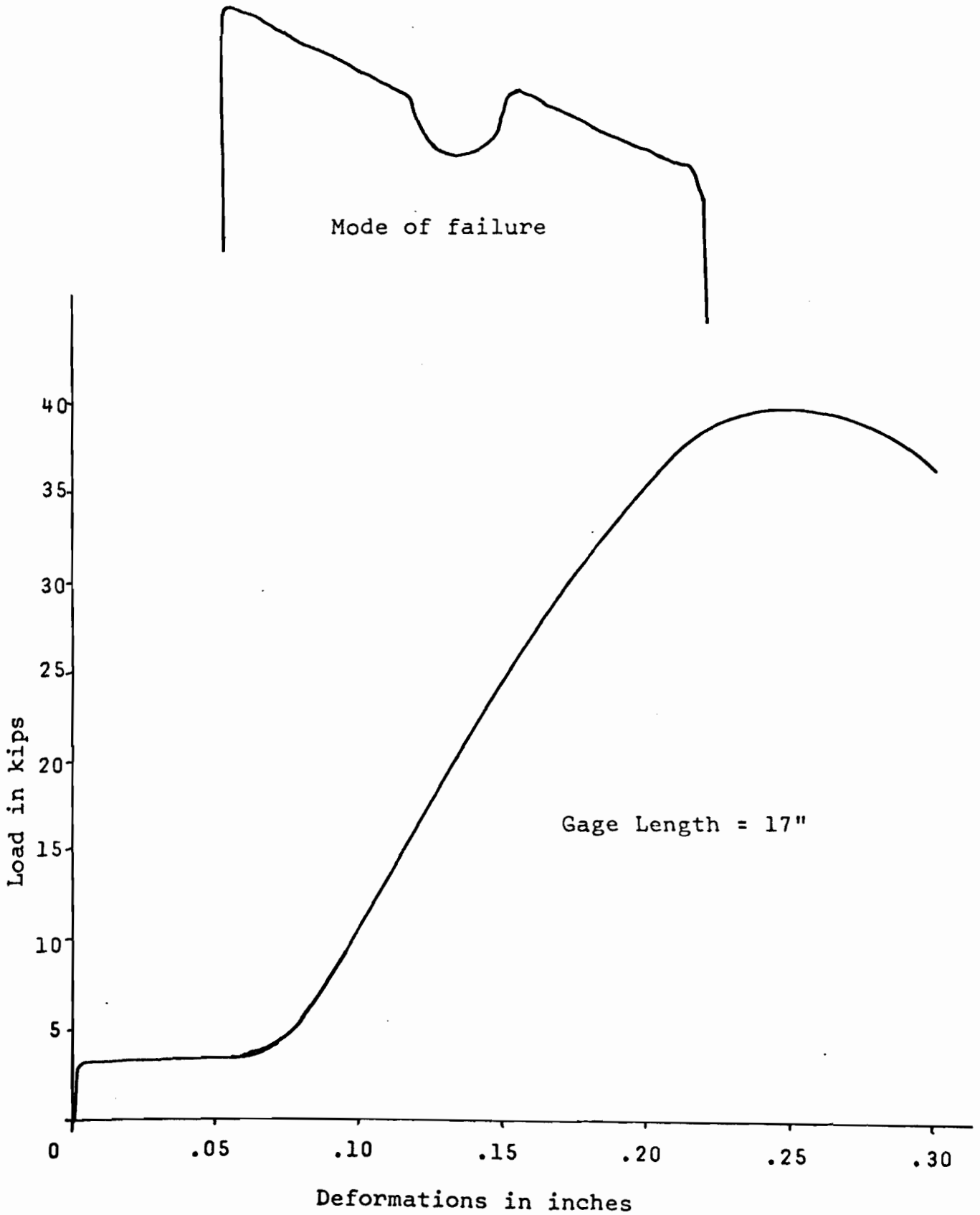

FIG. 7c - LOAD-DEFORMATION DIAGRAM.

May 8, 1969

Informal Memo

To: Prof. Winter

From: A. K. Dhalla

Subject: "Influence of Ductility on the Structural Behavior of Light Gage Cold Formed Steel Members".

Progress since October 1968

TABLE OF CONTENTS

		Page
1.	Abstract	1
2.	Introduction	2
3.	Material Properties	3
4.	Tension Tests on Rectangular Plates	5
5.	Bolted Connection Tests	7
6.	Welded Connections	10
7.	Formability of Corners	14
8.	Conclusions	15
9.	References	17

1. ABSTRACT

Ductility parameters defined in Second Progress Report, were obtained by conducting tension coupon tests on especially produced (A and S) steel. In this memo, tension coupon tests are reported on a 20 gage commercial low ductility steel, i.e. an ASTM Grade E Steel, herein designated as Steel B. Its behavior is compared with that of the especially rolled A and S steels with the intention to test the validity of conclusions arrived at in the second progress report. Test programs were set up to study the behavior of B steel (under static tension loading), one program for single bolted connections and another for rectangular plates with holes. Here again the behavior of B steel is compared with A and S steels.

Longitudinal fillet welded connections (A and S steel only) are also investigated. Finally a few brief remarks are made regarding corners formed from A and S steel.

2. INTRODUCTION

It was mentioned in the First Progress Report[1] that the strength of low ductility steel tension members under static loading is not affected by the presence of stress raisers in the member. Formulas for single bolted connection were also developed in that report from the tests conducted on A and S steel, which was along the lines of earlier work done by Winter[2]. In this memo the single bolted connection tests and rectangular tension plates with holes in them on commercial steel (B Steel), is studied, to confirm and to compare with the results obtained in the first progress report.

Under essentially static loading the parameters necessary to define the ductility of steel were reported in second progress report[3]. In this memo the material properties of commercial steel (B Steel) is studied. The material was tested, and the results are tabulated in the same manner as in the second progress report wherein the conducting of test and reporting of the results were standardized, here again the validity of conclusions reached in second progress report are tested.

Weldability of the material is also investigated qualitatively. A few longitudinal fillet weld connection tests are also reported herein. The formability of the material is also investigated in a restricted sense, since only corners instead of the full cross-sections were formed in the press brake. At present no corner tension coupon tests have been conducted but the behavior of the corner during the forming process is discussed briefly.

3. MATERIAL PROPERTIES

Coupons for standard tension tests were prepared as per current ASTM-E8-65T Specification. The main aim of testing commercial steel was to test the conclusions arrived at in second progress report. Table 1 compares various ductility criterias for commercial steel (B Steel) and especially produced steel (A and S Steel). Stress strain curves of A, S and B steel are plotted in Fig. 1. The following two equations, which were derived by Oliver,[4] are mentioned in the second progress report.

$$e\% = K'L^{\alpha} \qquad (1)$$

and

$$e\% = K\left(\frac{L}{A}\right)^{\alpha} \qquad (2)$$

where e = Percent elongation in gage length L.

A = Cross-sectional area of the coupon.

K, K' and α are constants.

The numerical value of α is the measure of overall ductility of the material, while K (or K') is a measure of local ductility of the material. K, K', and α can be obtained by plotting Eqs. 1 and 2 on log-log scale. Figs. 2 and 3 show the log-log plot for A, S and B steel.

Comparing commercial (B) steel with special rolled (A or S) steel, it can be seen that B steel has more overall ductility (α = -0.6), than A or S low ductility steel (α = -0.9); but A or S steel has more local ductility (K = 45) than B steel (K = 20). Another way of looking at overall and local ductility is to observe the values of percent elongation in 2 1/2" gage length excluding neck and percent elonga-

tion in 1/4" gage length which includes the fractured section. Here again it could be pointed out that B steel has more overall ductility (% elongation in 2 1/2" = 2.7) than A or S steel (% elongation in 2 1/2" = 0.4); but B steel has lower local ductility (% elongation in 1/4" = 14) than A or S steel (% elongation in 1/4" ≅ 45). The above view is reinforced by looking at the value of tensile/yield ratio and percent reduction in area. Since B steel has a tensile yield ratio greater than one, it has better capacity to distribute the strain over the length of the coupon, than A or S steel (T/y = 1.00). But lower percent reduction in area in B steel (58.5 %) indicates that less local deformation took place at the fractured cross section, than that occurred in A or S steel.

Observing the complete stress strain curves in Fig. 1, for the commercial (B) steel and especially produced (A or S) steel it can be said that in B steel, the major portion of percent elongation (in 2" G.L) occurred just before the necking started in the coupon, and less percent elongation occurred after the necking process started. The opposite is true for A or S steel.

4. TENSION TESTS ON RECTANGULAR PLATES WITH HOLES

In the First Progress Report, it was observed that the strength of a rectangular plate of low ductility steel with a hole is not affected by the presence of stress raiser. At present no attempt is made to put a lower bound on the ductility parameters, but for a given material the effect of ductility on strength or carrying capacity of the member is investigated. Hence neglecting the effect of stress raiser, the following equation can be written

$$P_{ult} = \sigma_t A_{net} \qquad (3)$$

where σ_t = ultimate tensile strength of material under uniaxial tension

A_{net} = net cross-sectional area of the member

P_{ult} = ultimate load on the member.

The tests presented herein are an extension of tension tests conducted on rectangular plates in first progress report. More than one hole is drilled in the material in longitudinal direction to investigate the following points:

(1) Longitudinal plastic strain distribution, after fracture, in the tension member.

(2) Comparison of local ductility of tension member with that obtained from the standard tension coupon test.

(3) Effects that overall ductility has on the deformation characteristics of the tension member.

(4) Investigation of whether or not the total member deformation is increased by the introduction of extra holes in the longitudinal direction.

In Table 2 the nominal dimensions of the specimen are shown. Steel A specimens are from 1210-T-L1 to 1210-T-L5 and steel B specimens are from 20B-T-L6 to 20B-T-L10. Table 3 shows the results of the tension test on the specimens. Observing the ratio of tensile strength of plate at ultimate load (σ_{tt}) to the tensile strength of coupon (σ_t) it can be seen that the plate is able to develop the full strength as given by Equation (3). In Table 3 the total deformation of the member is reported which was measured (after fracture) in gage length equal to the center to center distance between holes in longitudinal direction plus one inch. By increasing the number of holes in the longitudinal direction total deformation of the member can be increased.[5] Because overall ductility of the material allows the cross-section to enter plastic range at holes other than the one where initial yielding took place. Fig. 4 shows the deformation curves of 20B-T-L2 and 20B-T-L3 specimens, indicating that total deformation is higher in plates with three holes than those with one hole. In Table 3, one can compare the values of percent elongation in 1/4" gage length obtained from coupon test with that of tension test on rectangular plate. It can be seen that local ductility in both cases is quite comparable, though in the coupon the local ductility is higher than that in tension test mainly due to biaxial stress condition in the rectangular plate, and the width of the plate more than that in the coupon.

5. BOLTED CONNECTION TESTS

Single bolted connection tests were conducted on commercial steel (B-Steel) to compare the behavior of these specimens with that of A and S steel reported in first progress report. The equations derived therein have been used to design the specimens. The nominal dimensions of the specimen are shown in Table 4. As before the types of failure considered are:

(i) Longitudinal shearing of sheet along two practically parallel planes whose distance is equal to bolt diameter.

(ii) Bearing failure with considerable elongation of the hole and material "piling up" in front of the bolt.

(iii) Transverse tension-tearing across the sheet.

Results of the connection test are presented in Table 5. Shear, bearing and tension type of failure was represented by the following equations, in first progress report[1].

$$P_{shear} = P_s = 0.9\ e\ \sigma_t\ t \qquad (4)$$

$$P_{bearing} = P_b = 3.0\ \sigma_t d\ t \qquad (5)$$

$$P_{tension} = P_s = (0.1 + 3\tfrac{d}{s})\ \sigma_t(A_{net}) \leq \sigma_t A_{net} \qquad (6)$$

where e = edge distance of the plate in longitudinal direction measured from the center of the plate

t = thickness of the plate

d = diameter of the bolt

s = width of the plate

A_{net} = net cross-sectional area of the plate through the center of plate.

Graphical representation of equations 4, 5 and 6 is given in Figs. 5, 6 and 7 respectively. Figs. 5, 6, and 7 are reproduced from first progress report and the test points obtained for B steel are indicated therein. Observing the points plotted in Fig. 6 for B steel it can be seen that the bearing strength of B steel is lower than that of A or S steel. Actually this may be due to the small thickness of the plate and it is quite possible that bearing strength of thicker sheets is higher than that of thinner ones. Hence equation could be modified to

$$P_{bearing} = P_b = 2.0\ \sigma_t\ dt \qquad (5a)$$

But the data points are not sufficient to justify this observation at present.

Stresses in the specimen at failure can be given by the following equations

$$\tau_{sf} = \frac{P_{ult}}{2e\ \ t} \qquad (7)$$

$$\sigma_{bf} = \frac{P_{ult}}{d\ t} \qquad (8)$$

$$\sigma_{tf} = \frac{P_{ult}}{A_{net}} \qquad (9)$$

From equations 4 and 5 for type (i) and type (ii) failure respectively, the following equations give the maximum shear and bearing stress in the material at ultimate load.

$$(\tau_s)_{max} = 0.45\ \sigma_t \qquad (10)$$

$$(\sigma_b)_{max} = 3.0\ \sigma_t \qquad (11)$$

Similarly the tension stress on the net section for type (iii) failure is given by equation 4 in the following form

$$(\sigma_{net})_{max} = (0.1 + 3\frac{d}{s})\ \sigma_t \leq \sigma_t \qquad (12)$$

In Table 5 the values of shear bearing and tension stress according to Eqs. 7 to 12 are given. When the failure is by shearing of the plate, type (i); τ_{sf} is quite close to $(\tau_s)_{max}$. For $\frac{d}{s} \geq 0.3$ σ_{tf} is also quite close to σ_t for tension tearing of plate, type (iii) failure. But when the bearing failure is predominant, i.e., when e/d is around 3 (say) the bearing strength of the plate at ultimate load (Eq. 8) is less than that predicted by equation 11.

Load deformation characteristics for specimens 20B-L3 and 20B-L4 is indicated in Fig. 8.

6. WELDED CONNECTIONS

Longitudinal fillet weld connections are designed here in the conventional way (i.e. disregarding effect of stress concentration) to develop the full strength of the connected plate. Failure modes considered were Type A, transverse tension tearing of the plate; Type B, shear failure in the weld. Fig. 9 indicates the basic dimension of a design specimen.

Table 6 shows the nominal dimensions of the specimens along with the average mechanical properties of the material. The design is broken down in three groups, Group I (Specs. 7S-W100-L3 to 12FA-W70-L7) in which the plate failure is predicted; Group II (Specs 7S-W100-L8 to 12FA-W70-L12); in which the shearing failure (in weld) is expected, and Group III which is designed such that the failure may either occur in the weld or the plate. Connections in Group I were designed to develop the full strength of the plate, where the value of yield strength (σ_{yA}) of welding electrode is as given by ASTM (A316) Specification, which is equivalent to AISC 1968 Draft Specification (1.5.3) where allowable shear strength for the electrode is given. The weld strength for the connections in Group II were taken to be the tensile strength of the electrode as given by the manufacturers (σ_{tM}). The weld length required by this design to develop the full strength of the plate was then reduced by about 10% so that the failure would occur in the weld and not in plate. In Group III the weld length was designed to develop the full strength of the plate, where the strength of the welding electrode was assumed to be that given by the yield strength as per manufacturer's specification

(σ_{yM}) which is approximately equivalent to tensile strength value (σ_{tA}) as given in ASTM (A316) specifications.

Results of the connection test are presented in Table 7. The failure mode in Group I is by tearing of the plate as was predicted before the test. Comparing columns 2 and 5 it can be observed that the connected plate (width b_n) developed σ_{tt} which is approximately 0.95 (σ_t) where σ_t is the tensile strength obtained from uniaxial tension coupon test. Also looking at Columns 3 and 9 it can be seen that the local ductility (% elongation in 1/4") of the plate is quite close to the local ductility of the material obtained in uniaxial tension.

Failure in Group II specimens occurred by shearing of the weld, as was desired in the design of those specimens. Comparing the values of weld strength (σ_{tw}) with the value of weld strength as given by ASTM or manufacturers specifications, it can be observed that the σ_{tw} is closer to value σ_{yM} (σ_{yield} specified by manufacturers) which is equivalent to σ_{tA} (tensile strength specified by ASTM specifications). The failure in 12 gage 5% A steel (1205-W100-L10) occurred prematurely. This may be due to defective welding since the failure in only one side of the plate occurred instead of the failure (or slip due to shearing) occurring in the fillet welds on both sides of the plate simultaneously. The behavior of 12 gage full annealed A steel was quite different from that observed in low ductility specimens. The plates of 12 gage full annealed specimen bulged out of the plane of plate intro-

ducing extraneous effects, causing rather unpredictable failure behavior.

In Group III where the weld length was designed such that it is between that given by Group I and Group II design, the failure occurred either by tearing of the plate (as in 7S-W100-L13) or by shearing of the weld (as in 12S,1205, and 1605 specimens). In this group σ_{tt}/σ_t ratio (material strength) is approximately 0.85 while $\frac{\sigma_{ym}}{\sigma_{tw}}$ ratio (weld strength) is approximately 0.95.

In Groups II and III the maximum percent elongation cannot be reliably measured. If the gage lines are marked too close to the edge they would be destroyed or wiped off during testing. On the other hand, the strain measurements taken away from the edge cannot be satisfactory since the maximum strain occurs at the edge and falls off very rapidly away from it.

Member deformation is measured by the automatic recorder where the gage distance is equal to lap length (L) of the connection plus 3 inches. The total deformation measured after fracture is noted in column 8 of Table 7. Maximum member deformation recorded is for group III specimens. Minimum member deformation is reported for Group I specimens. In Group I the major portion of total deformation occurs in the plate and in low ductility steel percent elongation is not large. But in Group III if the failure occurs by shearing of weld the deformation not only takes place in the plate (due

to higher tensile stress in plate than in Group II), but also there is relative slip between the two plates when the weld starts failing in shear.

7. FORMABILITY OF CORNERS

The corners were formed in a press-brake. The variables used were (a) radius of the corner (b) angle of opening at the corner and (c) ductility. A few brief observations can be made here regarding the qualitative behavior of the corner, brake pressed from low ductility material as compared to that of high ductility material.

(1) Softer material (12 and 16 gage full annealed steel) wrapped around the die very nicely. Consequently, it formed truer inside and outside radius. On the other hand the harder material (7, 12, and 16 gage 5% A steel) did not wrap around the die so well, hence it was not possible to obtain a smooth curve on the inside as well as outside of the material.

(2) The harder material showed small microscopic cracks at the outside curve, the effects of which can be gauged only after tension coupon tests are completed.

(3) It was not possible to bend 7 gage S steel to a 90° bend with radius = t (thickness of material), since the specimen cracked (the outside of the corner) under the application of load in the press brake.

8. CONCLUSIONS

(1) Ductility of commercial low ductility steel (designated as B steel), can be characterized by the parameters defined in the second progress report.

(2) Comparison of B steel can be made with especially produced steel (designated as A and S steel), as shown in Table 1.

(3) Under monotonically increasing static loading it is possible to develop the full tension strength of a rectangular plate with a hole (stress-raiser) in it.

(4) Increasing the number of holes in the longitudinal direction increases the total member deformation (or "member ductility").

(5) For A, S, and B steel the local ductility parameter, % elongation in 1/4" G.L. correlates satisfactorily with the local ductility of rectangular plate.

(6) Single bolted connections of commercial low ductility steel (B Steel) behave essentially in the same manner as those of the especially produced steel (S Steel). Shear and tension type failures of B Steel, but not bearing failures of single bolted connection in single shear can be predicted by the same equations that were derived for S steel in first progress report. Bearing strength of B steel is less than that reported for S steel. It is quite possible that bearing strength varies with the thickness of the material.

(7) Due to the lower bearing strength of B steel, the connection has a substantial amount of deformation before failure occurs, either in tension or in shear type of failure.

(8) With a careful design, a single bolted connection can be made to behave as a ductile connection in a tension member using low ductility steel.

(9) For low ductility A and S steel a longitudinal fillet weld connection can be designed to develop the full strength of the plate. There are no visible ill effects due to stress concentration at the corners of the connected plate. Failure in the connected plate starts from one of those points.

(10) When the weld length is too small, the failure occurs by shearing of the weld along the entire length of the longitudinal fillet weld. This behavior is in no way affected by the low ductility of steel used for the specimen. This behavior may be due to beneficial effects of the welding process on the material adjacent to the fillet weld. At higher load levels the material adjacent to the weld forms a "plastic boundary layer" which eventually allows complete separation of the two connected plates.

(11) A and S steel is "weldable" in the sense that no noticeable defects in the lab welded connection were observed.

REFERENCES

1. Dhalla, A. K. and Errera, S. J., "Influence of Ductility on the Structural Behavior of Light-Gage Cold-Formed Steel Members", First Progress Report, Cornell University, Ithaca, N.Y., Feb. 1968.

2. Winter, G., "Tests on Bolted Connections in Light Gage Steel". Proc. ASCE, Vol. 82, Paper No. 920, March 1956.

3. Dhalla, A. K., "Influence of Ductility on the Structural Behavior of Light-Gage Cold-Formed Steel Members", Second Progress Report, Cornell University, Ithaca, N.Y., Oct. 1968.

4. Oliver, D. A., "Proposed New Criteria of Ductility From a New Law Connecting the Percentage Elongation with Size of Test Piece", Inst. of Mech. Engineers, Vol. II, 1928.

5. Van Den Broek, J. A.,"Effect of Connections and Rivet Holes on Ductility and Strength of Steel Angles", Civil Engineering, Feb. 1940.

TABLE 1.

COMPARATIVE STUDY OF DUCTILITY CHARACTERISTICS.

DUCTILITY PARAMETERS	20B-L3	125-L3 *	1205-L2 *	1605-L3 *	16FA-L1 *
ELONGATION IN 2", %	4.25	5.13	5.58	6.84	52.20
REDUCTION IN AREA, %	58.50	65.20	69.40	59.00	83.80
TENSILE/YIELD RATIO	1.10	1.01	1.00	1.00	1.48
ELONGATION IN 1/4" (INCLUDING NECK), %	14.30	38.40	44.40	35.20	85.60
ELONGATION IN 2 1/2" (EXCLUDING NECK), %	2.69 ±	0.33	0.40	1.28	38.00
K	20.50	45.00	46.00	45.00	120.00
α	−0.601	−0.974	−0.983	−0.795	−0.335

NOTE : * THE VALUES REPORTED IN COLUMN ARE TAKEN FROM TABLE 7 OF SECOND PROGRESS REPORT.

± THIS VALUE IS FOR % ELONGATION IN 2" EXCLUDING NECK.

TABLE – 2

NOMINAL DIMENSIONS OF RECTANGULAR PLATES WITH HOLES

(A.S and B steel).

TABLE 2.

SPEC. DESIGNATION	GEOMETRIC PROPERTIES OF SPECIMEN						AV. MATERIAL PROPERTIES.		
	DIA OF HOLE	NO. OF HOLES		WIDTH OF PLATE	THICKESS OF PLATE	$\frac{d}{s}$			% ELONG. IN
		LONG.	TRASVEASE				σ_y	σ_t	1/4" G.L.
	d (in)	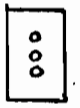	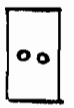	s (in)	t (in)		(ksi)	(ksi)	(%)
1210-T-L1	1/2	–	Two	3.50	0.107	0.263	76.2	76.9	–
1210-T-L2	1/2	Three	–	4.25	0.107	0.118	71.6	74.6	49.0
1210-T-L3	3/16	Three	–	4.25	0.107	0.044	71.6	74.6	49.0
1205-T-L4	1/2	Three	–	4.25	0.107	0.118	72.2	72.2	47.0
1205-T-L5	3/16	Three	–	4.25	0.107	0.044	72.2	72.2	47.0
20B-T-L6	13/16	One	–	2.52	0.038	0.323	75.5	81.7	15.5
20B-T-L7	9/16	One	–	4.25	0.038	0.133	"	"	"
20B-T-L8	1/2	Three	–	4.25	0.038	0.118	"	"	"
20B-T-L9	3/16	Three	–	4.25	0.038	0.044	"	"	"
20B-T-L10	1/2	–	Two	3.52	0.038	0.142	"	"	"

TABLE - 3

RESULTS OF TENSION TEST PERFORMED ON RECTANGULAR PLATES WITH HOLES. (A, S and B steel)

TABLE-3

SPEC. DESIGNATION	$\frac{d}{s}$	AV. MAT'L PROPERTIES		EXPERIMENTAL RESULTS.				
		σ_t (ksi)	% ELONG in 1/4" (%)	P_{ULT} (kip)	σ_{tt} (ksi)	% ELONG in 1/4" %	TOTAL MEMBER DEFORMATION (in)	$\frac{\sigma_{tt}}{\sigma_t}$
1210-T-L1	0.263	76.9	—	22.30	81.5	35.2	0.09	1.06
1210-T-L2	0.118	74.6	49.0	30.70	75.5	37.2	0.19	1.01
1210-T-L3	0.044	74.6	49.0	32.80	75.6	34.8	0.18	1.01
1205-T-L4	0.118	72.2	47.0	32.20	79.4	28.6	0.11	1.10
1205-T-L5	0.044	72.2	47.0	32.70	74.5	27.6	0.08	1.03
20B-T-L6	0.323	81.7	15.5	5.28	81.2	21.7	0.06	0.99
20B-T-L7	0.133	"	"	12.42	88.0	17.1	0.04	1.08
20B-T-L8	0.118	"	"	12.80	90.0	12.9	0.06	1.10
20B-T-L9	0.044	"	"	13.70	88.8	11.5	0.05	1.09
20B-T-L10	0.142	"	"	8.90	95.6	14.3	0.03	1.17

TABLE – 4

NOMINAL DIMENSIONS OF SINGLE BOLTED CONNECTION TESTS

(TB – STEEL)

TABLE-4

SPEC. DESIGNATION	Edge Dist. e (in)	Bolt Dia d (in)	Width of Tp s (in)	& σ_y (ksi)	σ_t (ksi)	$\frac{e}{d}$	$\frac{d}{s}$
20TB-L1	1.75	1/2 – S.S.	1.50	75.5	81.7	3.50	0.33
20B-L2	1.00	1/2 – S.S.	1.50	"	"	2.00	0.33
20B-L3	1.50	3/4 – S.S.	2.50	"	"	2.00	0.30
20B-L4	2.25	3/4 – S.S.	2.50	"	"	3.00	0.30
20B-L5	1.00	1/2 – D.S.	2.50	"	"	2.00	0.20
20B-L6	1.50	1/2 – D.S.	2.50	"	"	3.00	0.20
20B-L7	0.47	3/16 – D.S.	2.00	"	"	2.50	0.09
20B-L8	0.66	3/16 – D.S.	2.00	"	"	3.50	0.09

(1) S.S. = SINGLE SHEAR D.S. = DOUBLE SHEAR
(2) ALL HOLES DRILLED
(3) FINGER TIGHT BOLTS
(4) WASHER ON EACH SIDE OF BOLT.

TABLE - 5

RESULTS OF SINGLE BOLTED CONNECTION TEST

(B - STEEL)

SPEC. DESIGNATION	$\frac{e}{d}$	$\frac{d}{s}$	P_{ULT} (KIP)	MODE OF FAILURE (TYPE)	STRESSES PREDICTED AS PER EQS. 10 (τ_s) 11 (σ_b) and 12 (σ_{net})		STRESSES CALCULATED FROM ULT. LOAD. AS PER EQS. 7 (τ_{sf}) 8 (σ_{bf}) 9 (σ_{tf})		INCREASE IN HOLE SIZE. (in)
					EQ. NO.	STRESS (KSI)	EQ. NO.	STRESS (KSI)	
20B-L1	3.50	0.33	3.12	(iii)	10 11 12	36.75 245.50 81.70	7 8 9	22.85 160.0 85.0	0.19
20B-L2	2.00	0.33	2.74	(ii) + (i)	-DO-	-DO-	7 8 9	35.1 140.4 74.7	0.49
20B-L3	2.00	0.30	4.20	(ii) + (i)	-DO-	-DO-	7 8 9	35.8 143.2 63.6	0.54
20B-L4	3.00	0.30	3.84	(ii)	-DO-	-DO-	7 8 9	21.8 131.0 58.0	0.69
20B-L5	2.00	0.20	2.55	(i)	10 11 12	36.75 245.50 57.20	7 8 9	32.7 130.8 33.2	0.64
20B-L6	3.00	0.20	2.68	(ii)	-DO-	-DO-	7 8 9	29.5 167.0 45.6	1.20
20B-L7	2.50	0.09	1.43	(i)	10 11 12	36.75 245.50 30.20	7 8 9	39.1 192.0 30.2	0.37
20B-L8	3.50	0.09	1.50	(ii) + (i)	10 11 12	36.75 245.50 30.20	7 8 9	29.2 206.0 21.2	0.56

TABLE - 6

AVERAGE MATERIAL PROPERTIES AND NOMINAL DIMENSIONS OF LONGITUDINAL FILLET WELDED CONNECTIONS (A and S STEEL SPECIAL ROLLING).

1	2	3	4	5	6	7	8	9	10
SPEC. DESIGNATION	GEOMETRIC PROPERTIES OF SPECIMEN					AVERAGE MECHANICAL PROPERTIES OF MAT'L			
	t (in)	b_w (in)	b_n (in)	L (in)	ELECTRODE (ASTM SPEC. A-316)	σ_y (ksi)	σ_t (ksi)	% ELONG in 2" G.L. (%)	% ELONG in 1/4" G.L. (%)
PRILIMINARY TESTS									
7S-W70-L1	0.183	3.50	2.50	3.00	E-7018	81.8	83.3	8.40	47.0
7S-W70-L2	0.183	3.75	2.50	5.00	E-10018	"	"	"	"
GROUP I TESTS									
7S-W100-L3	0.183	4.75	2.50	3.25	"	"	"	"	"
12S-W100-L4	0.106	4.25	3.00	3.25	"	82.5	82.5	4.38	31.4
1205-W100-L5	0.109	4.25	3.00	3.25	"	84.1	84.1	4.70	29.9
1605-W100-L6	0.063	4.25	3.00	3.75	"	98.0	98.0	4.98	26.6
12FA-W70-L7	0.108	5.00	4.00	3.75	"	31.5	45.0	49.80	105.0

NOTE : REFER FIG. 9 FOR NOMENCLATURE.

TABLE - 6 (CONT'D).

1	2	3	4	5	6	7	8	9	10
	GEOMETRIC PROPERTIES OF SPECIMEN					AVERAGE MECHANICAL PROPERTIES OF MAT'L.			
GROUP II ↓									
7S-W100-L8	0.183	4.75	2.50	2.25	E - 10018	81.8	83.3	8.40	47.0
12S-W100-L9	0.106	4.25	3.00	2.25	E - 10018	82.5	82.5	4.38	31.4
1205-W100-L10	0.109	4.25	3.00	2.25	E - 10018	84.1	84.1	4.70	29.9
1605-W100-L11	0.063	4.25	3.00	2.75	E - 10018	98.0	98.0	4.98	26.6
12FA-W100-L12	0.108	5.00	4.00	1.50	E - 7018	29.6	44.6	49.30	105.0
GROUP III ↓									
7S-W100-L13	0.183	4.75	2.50	2.75	E - 10018	81.8	83.3	8.40	47.0
12S-W100-L14	0.106	4.25	3.00	2.75	E - 10018	82.5	82.5	4.38	31.4
1205-W100-L15	0.109	4.25	3.00	2.75	E - 10018	84.1	84.1	4.70	29.9
1605-W100-L16	0.063	4.25	3.00	3.25	E - 10018	98.0	98.0	4.98	26.6
12FA-W100-L17	0.108	5.00	4.00	2.00	E - 7018	29.6	44.6	49.30	105.0

TABLE - 7

RESULTS OF LONGITUDINAL FILLET WELDED CONNECTION TESTS.
(A AND S STEEL - SPECIAL ROLLING)

1	2	3	4	5	6	7	8	9	10
SPEC. DESIGNATION	PROPERTIES OF MAT'L.		EXPERIMENTAL RESULTS						
					AV. WELD STRESS @ FAILURE		MEMBER DEFORMATION IN 1/4" OF ℄	MAX % ELONG	TYPE OF FAILURE
	σ_t (ksi)	% ELONG IN 1/4" G.L. (%)	P_{ULT} (kip)	σ_{tt} (ksi)	σ_{sw} (ksi)	σ_{tw} (ksi)	(in)	(%)	
PRELIMINARY TESTS									
7S-W70-L1	83.3	47.0	37.25	81.5	48.0	83.1	0.49	15.4	B
7S-W70-L2	"	"	38.90	85.0	30.0	52.5	—	—	A
GROUP II TESTS									
7S-W100-L3	"	"	38.30	83.7	45.4	78.6	0.40	49.8	A
12S-W100-L4	82.5	31.4	24.90	78.8	51.0	88.4	0.16	27.6	A
1205-W100-L5	84.1	29.9	25.80	79.6	51.8	89.8	0.15	32.4	A
1605-W100-L6	98.0	26.6	16.60	89.5	50.1	86.8	0.10	21.7	A
12FA-WTQ-L7	45.0	105.0	16.80	39.6	29.2	51.0	0.75	102.0	A

FOR E-10018 ELECTRODES σ_{YA} = 87.0 ksi σ_{tA} = 100.0 ksi σ_{ym} = 98.0 ksi σ_{tm} = 109.0 ksi τ_{SA} = 30.0 ksi

FOR E-7018 ELECTRODES σ_{YA} = 57.0 ksi σ_{tA} = 70.0 ksi σ_{ym} = 72.0 ksi σ_{tm} = 80.0 ksi τ_{SA} = 21.0 ksi

TOTAL MEMBER DEFORMATION MEASURED AFTER FRACTURE.

REFER FIG. 9A FOR NOMENCLATURE. ON WELD STRENGTH.

TABLE - 7 (CONT'D)

1	2	3	4	5	6	7	8	9	10
GROUP II ↓	PROPERTIES OF MAT'L		EXPERIMENTAL RESULTS.						
7S-W100-L8	83.3	47.0	33.80	74.0	58.1	100.8	0.30	16.8	B
12S-W100-L9	82.5	31.4	19.40	61.0	57.4	99.5	0.54	—	B
1205-W100-L10	84.1	29.9	16.40	50.5	47.6	82.5	0.77	38.0	B
1605-W100-L11	98.0	26.6	14.30	76.8	58.8	101.8	0.30	—	B
12FA-W100-L12	44.6	~~49.30~~ 105.0	9.80	23.3	42.7	74.0	—	25.6	A+B
GROUP III	TESTS ↓								
7S-W100-L13	83.3	47.0	37.50	82.0	52.6	91.2	0.13	20.2	A
12S-W100-L14	82.5	31.4	22.25	70.0	54.0	93.6	0.61	—	B
1205-W100-L15	84.1	29.9	23.80	73.5	57.5	98.0	0.77	—	B
1605-W100-L16	98.0	26.6	16.20	85.7	56.4	97.5	0.41	5.6	B
12FA-W70-L17	44.6	105.0	11.80	28.2	38.5	66.6	—	24.6	A+B

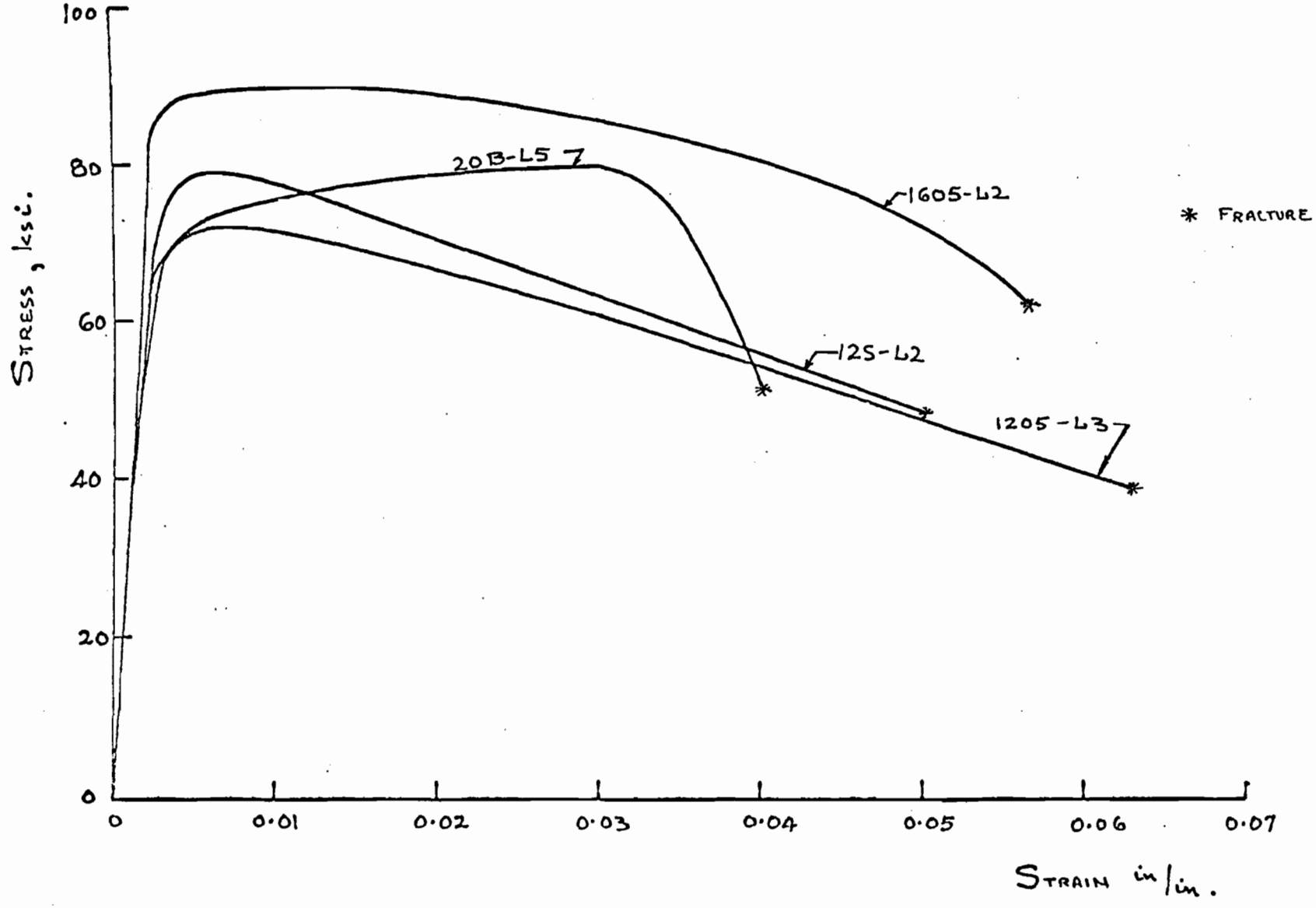

Fig. 1. Complete Stress Strain Curves Of A, S, and B Steel

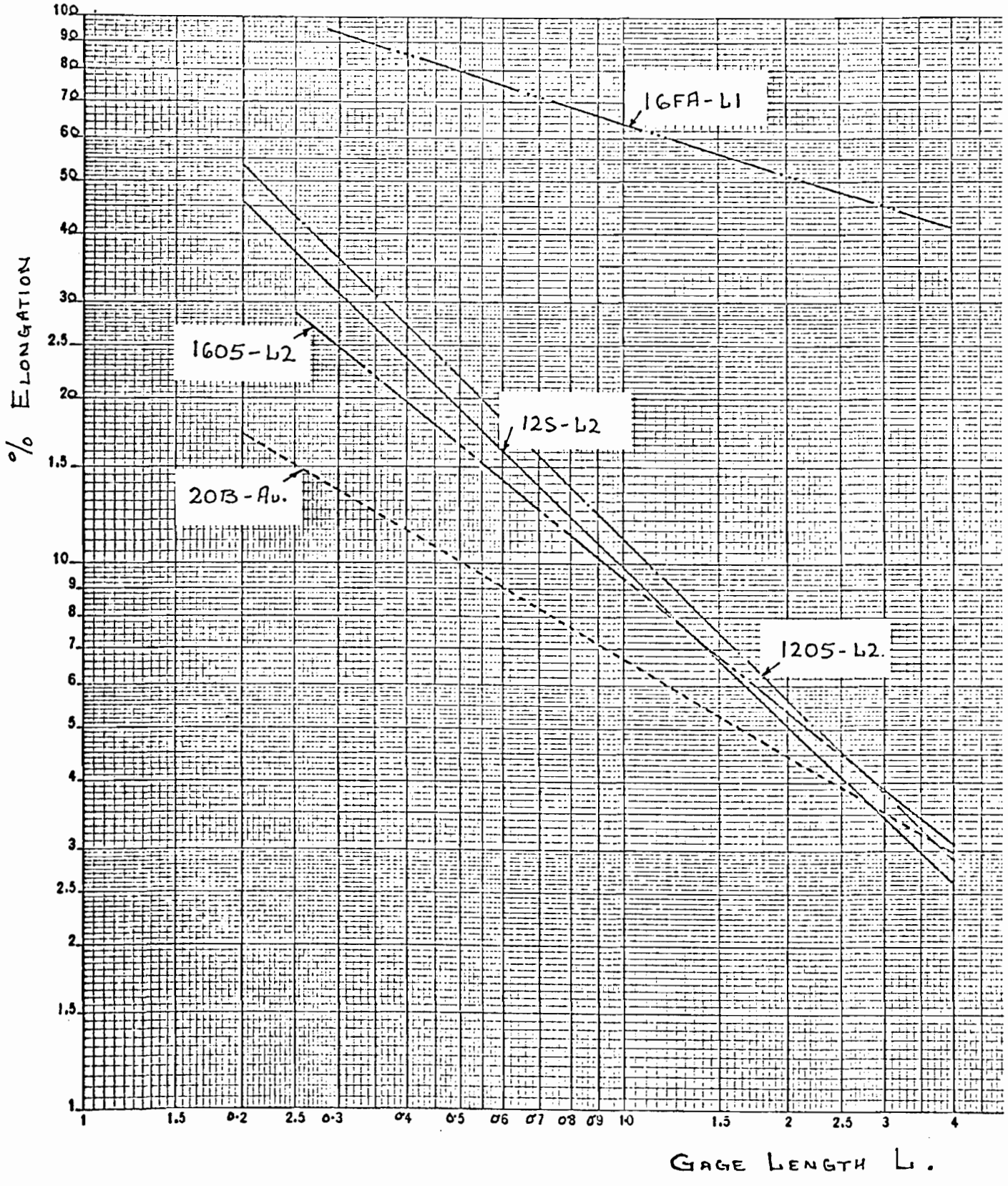

FIG. 2. LOGERITHMIC RELATION BETWEEN ELONGATION LENGTH AND GAGE LENGTH FOR A, S, AND B STEEL

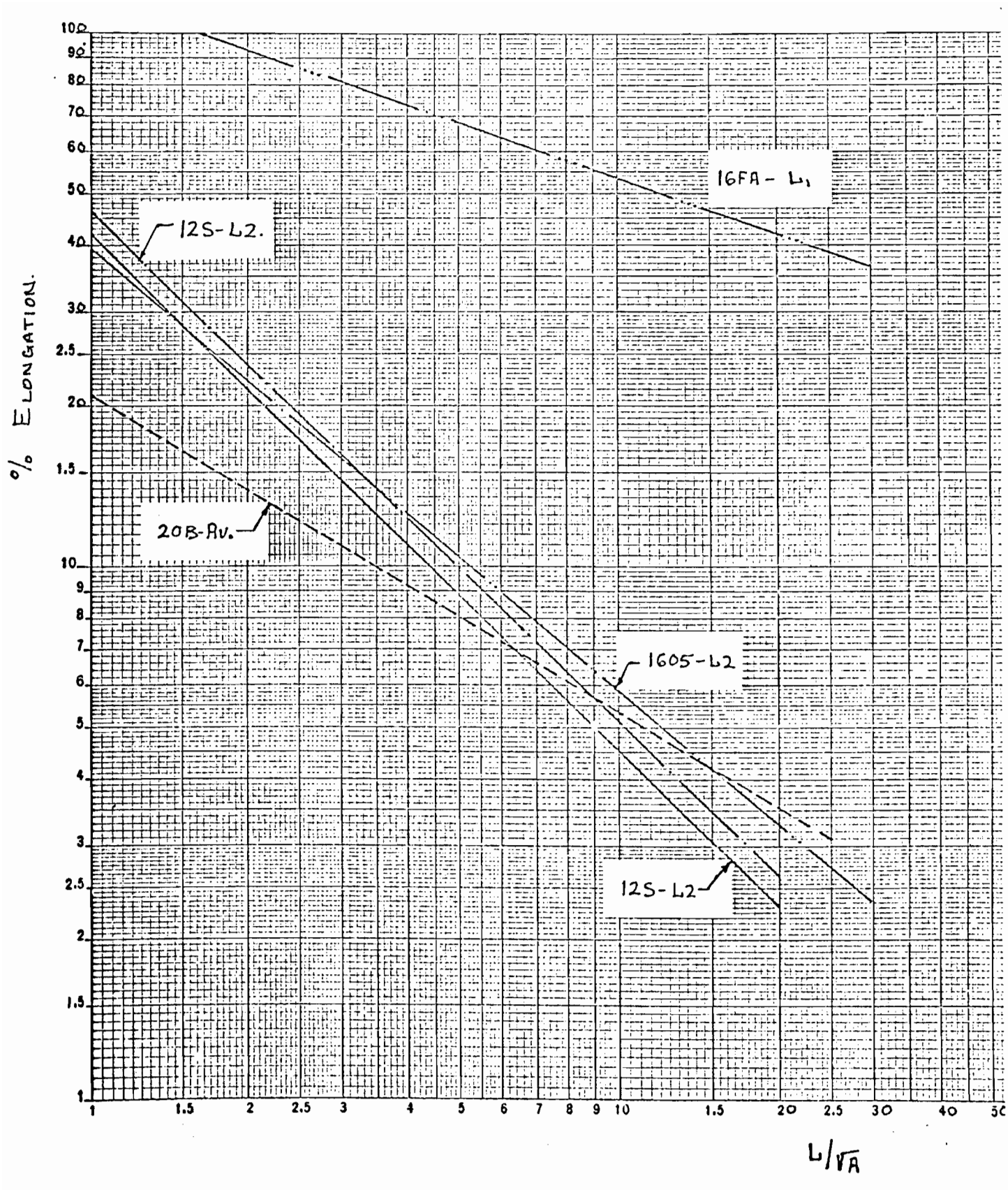

Fig. 3. Results Of A, S, and B Steel Plotted on Logarithmic Co-ordinates.

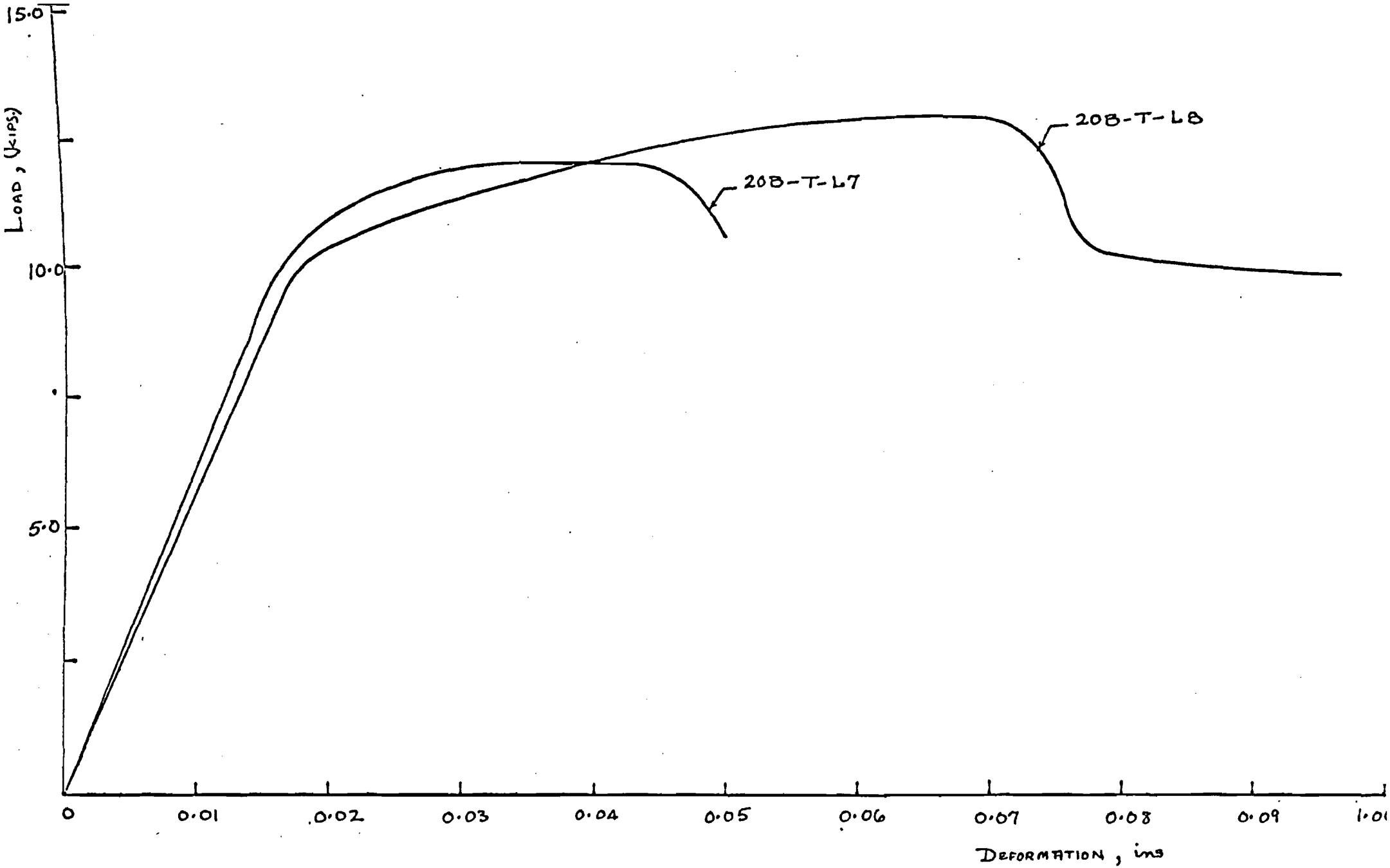

FIG. 4. LOAD - DEFORMATION CURVES OF 20B-T-L7 AND 20B-T-L8 SPECIMENS.

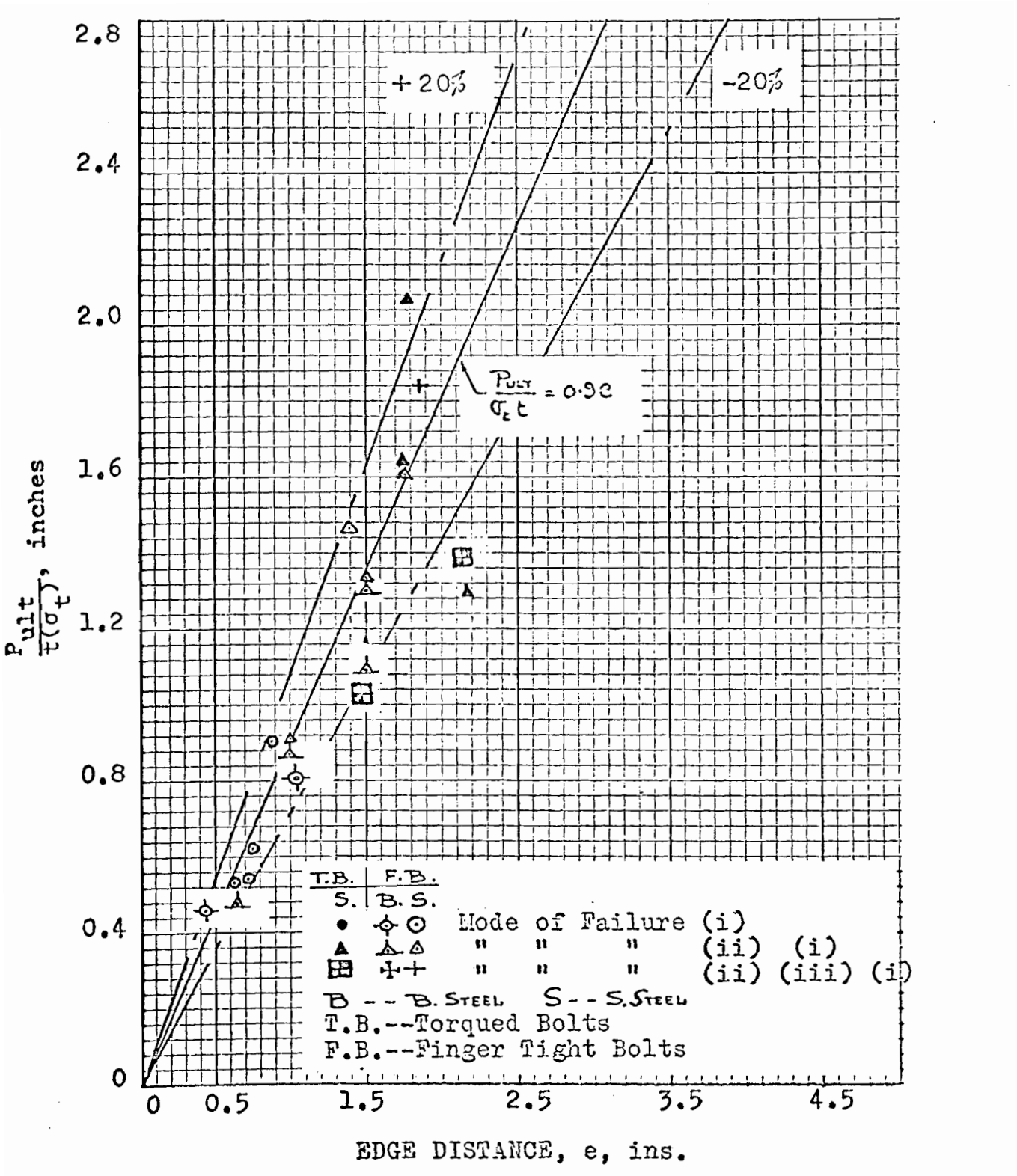

Fig. 5. Type (i) failures.

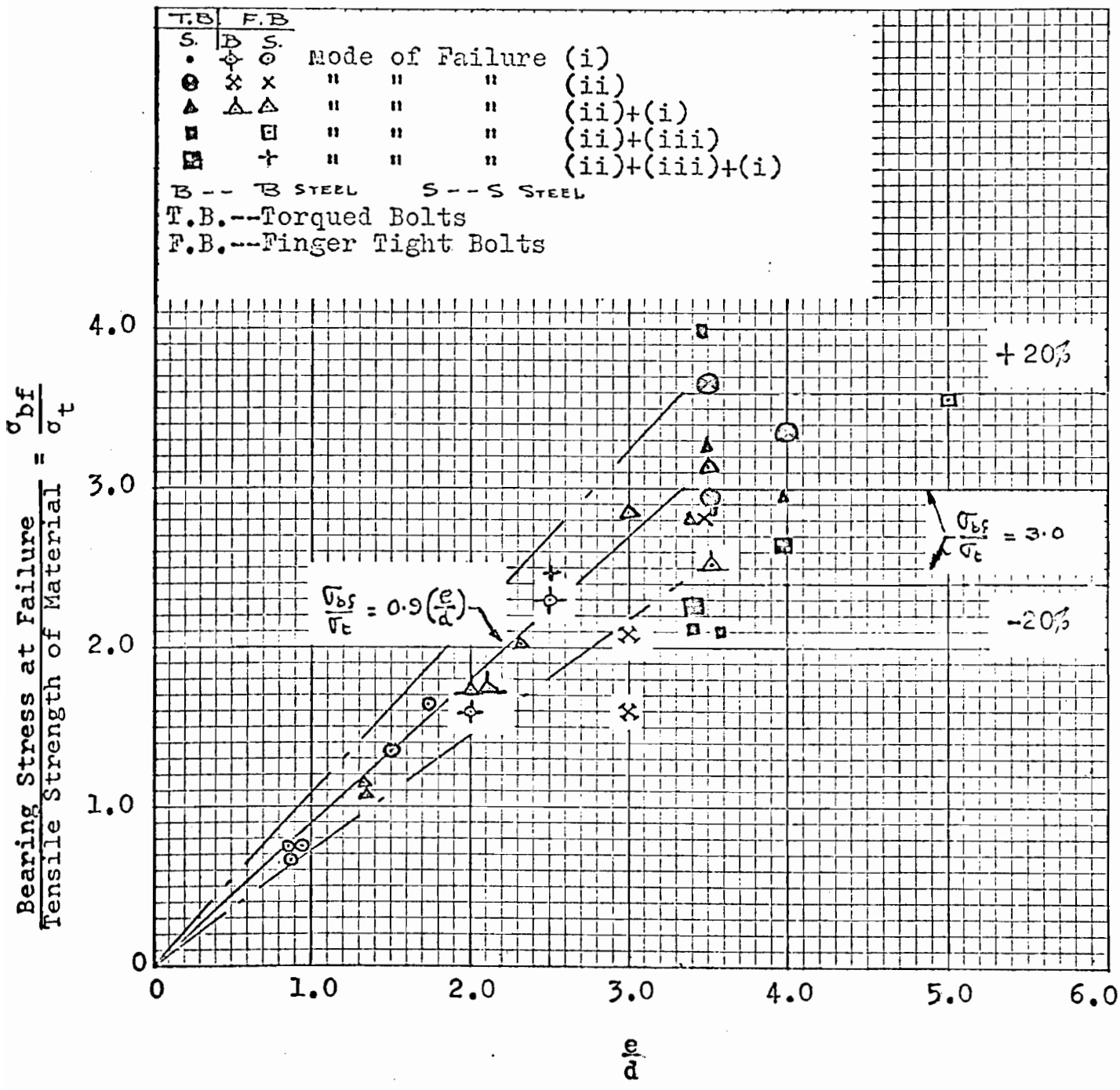

Fig. 6. Type (i) and (ii) failures.

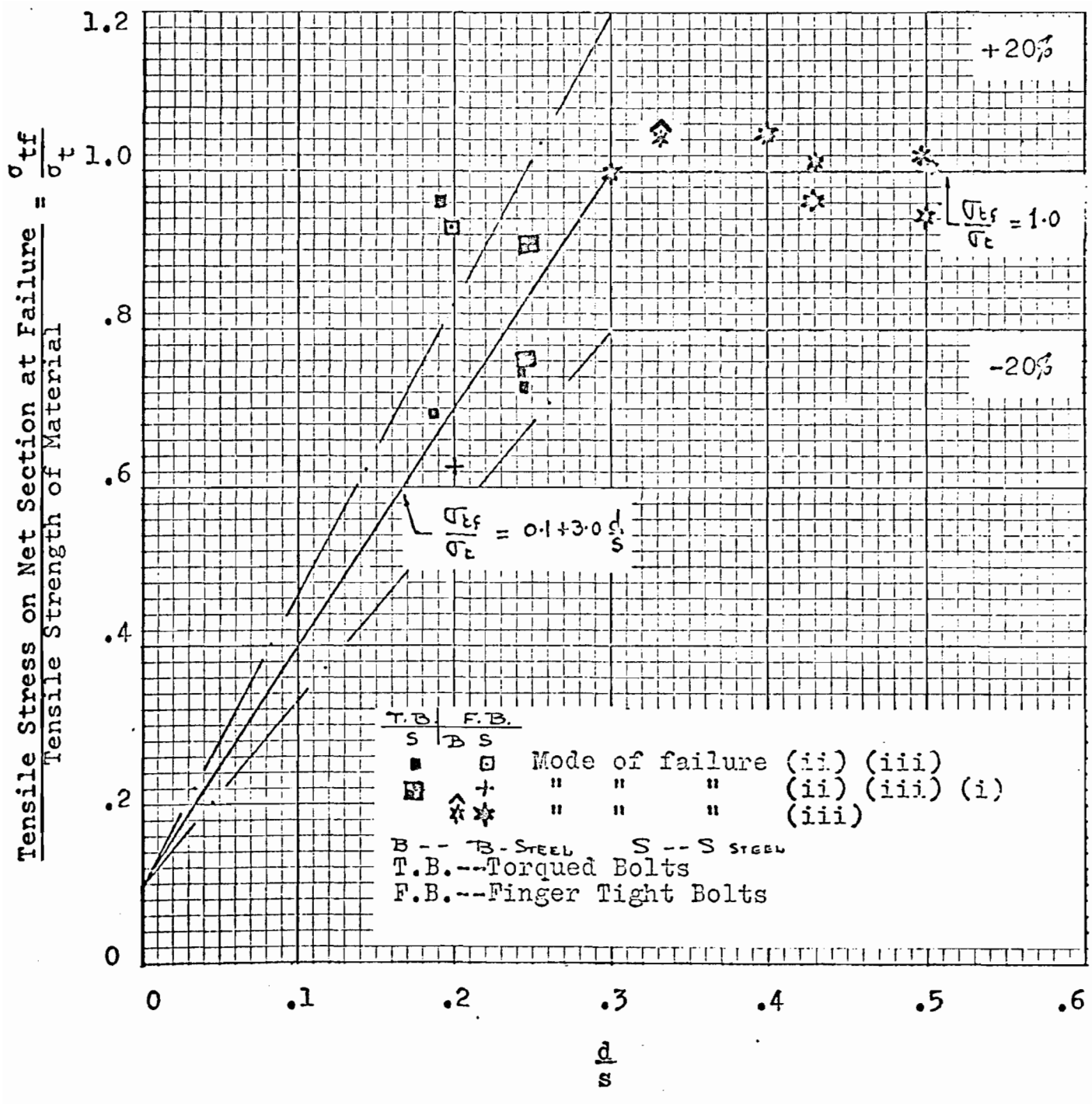

Fig. 7. Type (iii) failures.

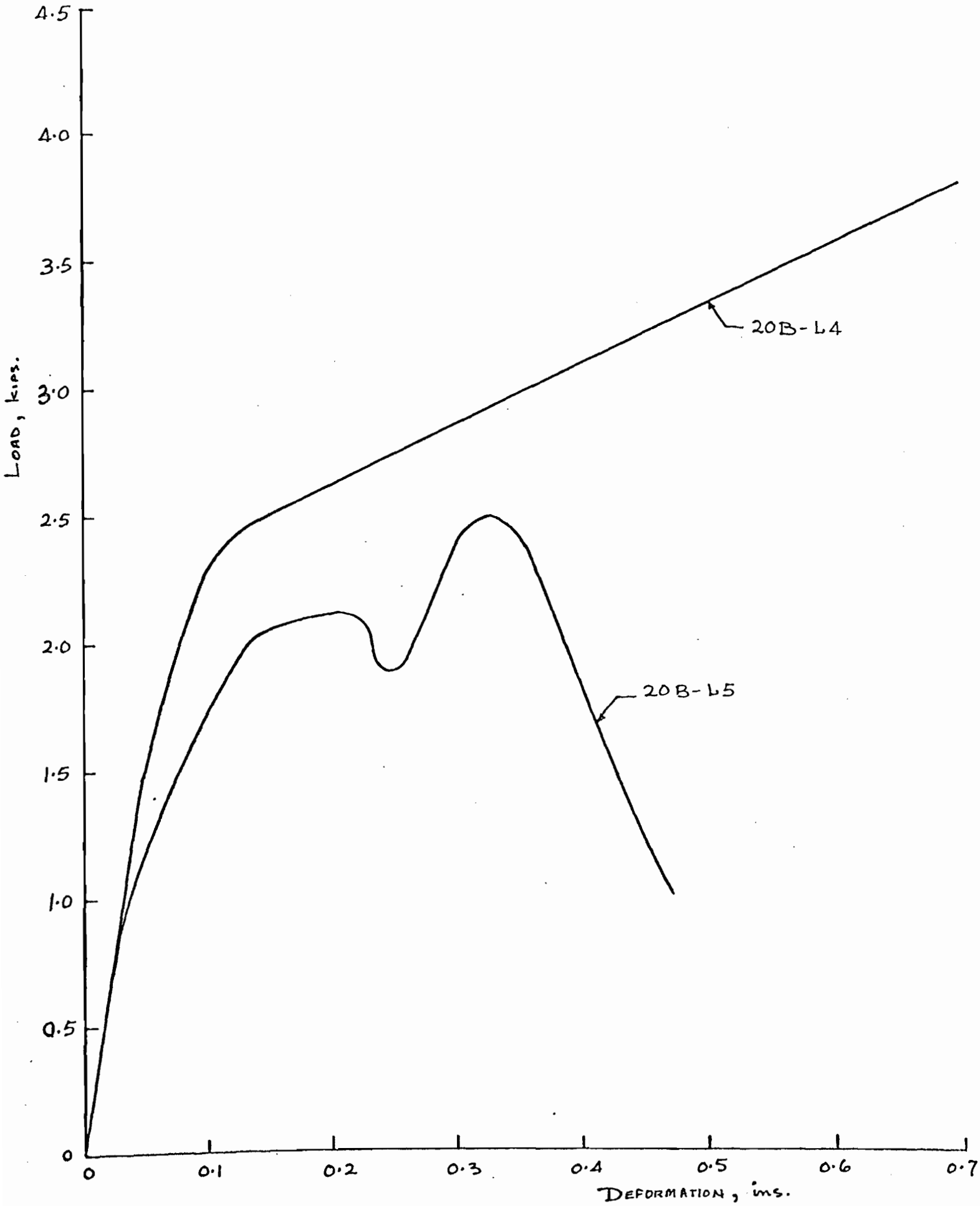

FIG. 8. LOAD-DEFORMATION CURVES FOR 20 GAGE B-STEEL SINGLE BOLTED CONNECTION SPECIMENS.

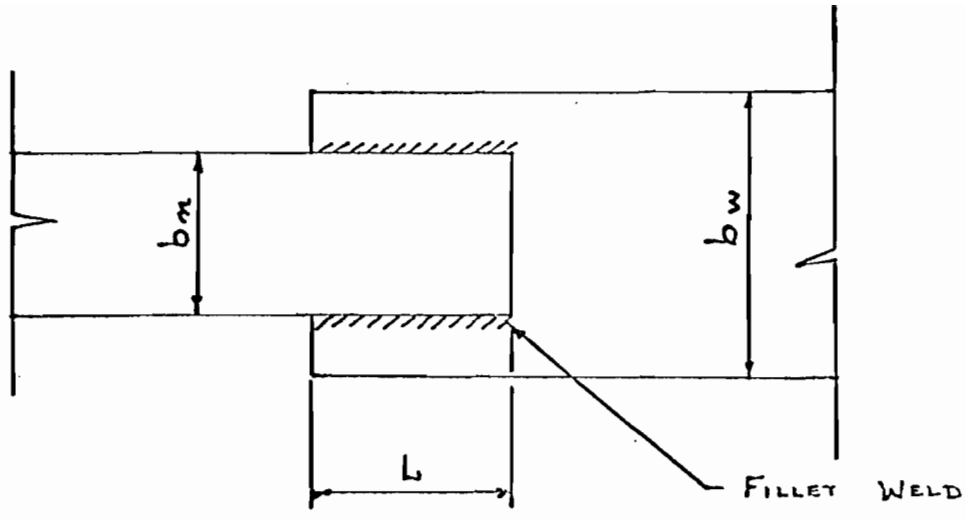

FIG. 9 LONGITUDINAL FILLET WELD CONNECTION

NOMENCLATURE USED IN TABLE 7 TO DEFINE WELD STRENGTH.

σ_{yA} = YIELD STRENGTH OF ELECTRODE AS PER ASTM SPECS. (A 316).
σ_{tA} = TENSILE STRENGTH " " " " " " " ".
σ_{yM} = YIELD STRENGTH OF ELECTRODE AS PER MANUFACTURER'S SPECS.
σ_{tM} = TENSILE STRENGTH " " " " " " ".
τ_{SA} = ALLOWABLE SHEAR STRENGTH OF ELECTRODE AS PER AISC SPECS (1.5.3)
τ_{SW} = ACTUAL " " " " " CALCULATED FROM P_{ULT}.
σ_{tW} = ACTUAL TENSILE STRENGTH " " " " " ".

FIG. 9A. NOTATION USED FOR WELD STRENGTH.

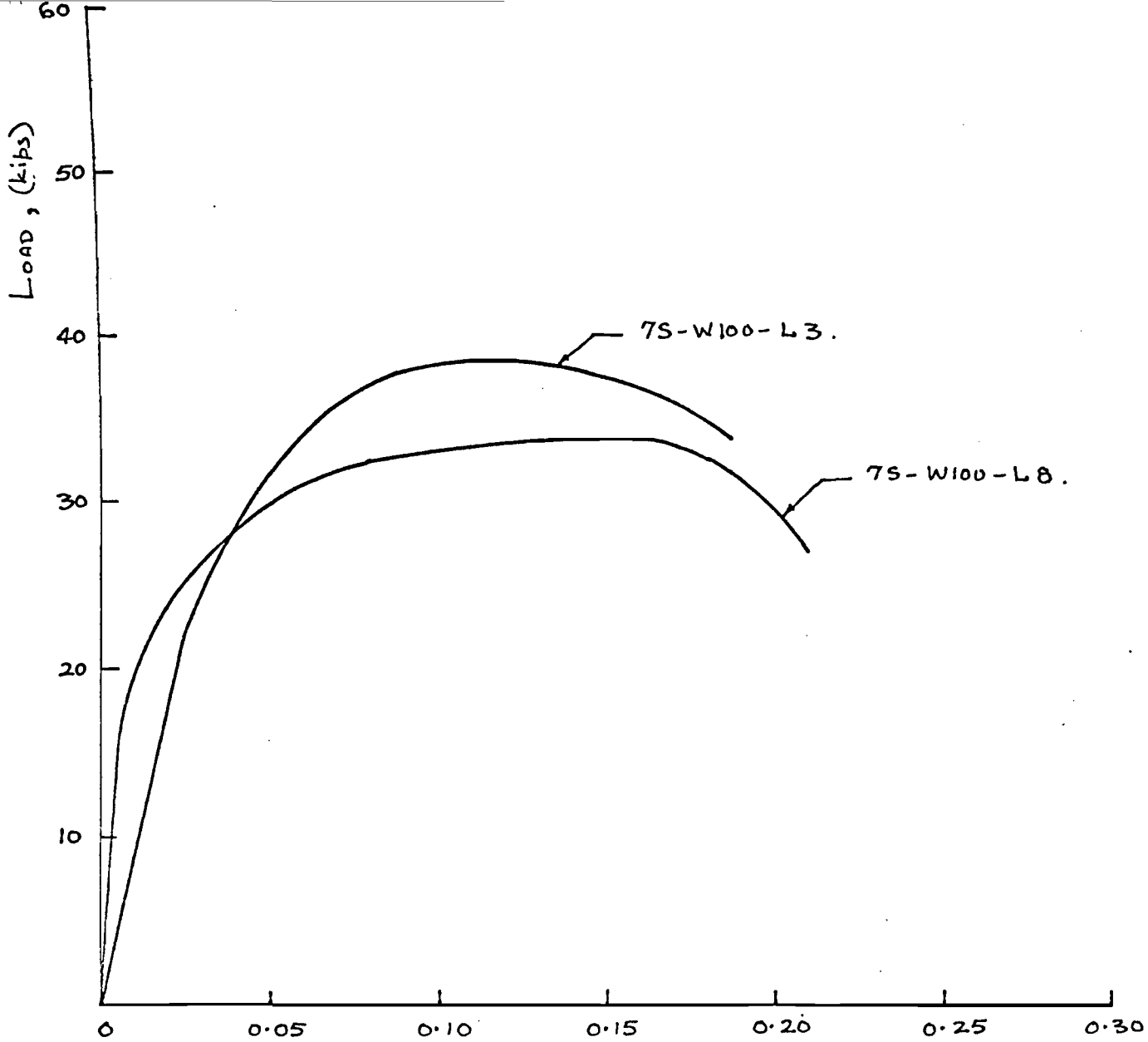

FIG. 10. LOAD-DEFORMATION CURVE OF LONGITUDINAL FILLET WELDED SPECIMENS.

October 2, 1969

To: G. Winter

From: A. K. Dhalla and S. J. Errera

Subject: Influence of Ductility on the Structural Behavior of Cold-Formed Steel Members

Summary of Investigation and

Plans for Immediate Future

Table of Contents

1. Introduction 1
2. Material Properties 1
3. Rectangular Plates with Holes 4
4. Single Bolted Connection Tests 5
5. Longitudinal Fillet-Welded Connections 6
6. Finite Element Analysis 8

References 10

List of Tables:

1. Comparative Study of Ductility Characteristics of A, B, and S Steel
2. Typical Results of Tension Tests on Rectangular Plate with Holes
3. Results of Longitudinal Lap Welded Connection Tests

List of Figures:

1. Complete Stress Strain Curves of A, B, and S Steel
2. Distribution of Longitudinal Strain in Tension Coupon
3. Logarithmic Relationship Between Elongation and $L/\sqrt{A}$ for A, S and B Steel.
4. Longitudinal Strain Distribution After Fracture in Rectangular Plate with Holes.
5. Bearing and Shear or Combined Failures (Low Ductility Steel).
6. Transverse Tearing or Combination of Bearing and Tension Failure (Low Ductility Steel).
7. Load-Deformation Curve of Longitudinal Fillet Welded Specimens.

1. Introduction

In order to determine the "suitability of steel"[1] for cold-formed construction one needs to know, in addition to other mechanical properties of the material, performance characteristics such as ductility, formability and weldability. Ductility is the ability of a material to undergo large plastic deformations without fracture. It reduces the harmful effect of stress concentrations, permits large local strains without serious damage, and helps achieve uniform stress or load distribution in connections.

There are different tests specified by ASTM to measure ductility, the chief of them being the percent elongation after fracture in a specified gage length, usually 2" or 8". The minimum acceptable for structural use, according to ASTM standards, varies a great deal. Two of the low ductility steels used in this investigation were specially rolled and made available by the manufacturers. These are designated as A and S steels, and had between 5 and 10 percent elongation in 2" gage length, well below the "ductility" required by ASTM for structural steels in general use in load carrying members. The third steel investigated to date is a 20 gage commercial low ductility steel, ASTM A-446 Grade E, herein designated as Steel B, with a specified minimum elongation of 1.5% in 2". Grade E steel is used primarily for cold formed panels.

2. Material Properties

The parameters which can be used to define the ductility

of steel were discussed in the Second Progress Report. These include elongation in 2", reduction in area, tensile-yield strength ratio, elongation in 1/4", and elongation in some gage length which excludes the fracture zone. These parameters were measured from standard tension tests wherein the coupons were prepared and tested in accordance with ASTM Specification E8-65T. The A and S steel coupon test results were presented in the first and second progress reports. B steel coupons were tested subsequently.

Typical complete stress-strain curves for 12 and 16 gage A steel, 12 gage S steel and 20 gage B steel are shown in Fig. 1. An important fact indicated by the figure is that B steel has a strain hardening range while the other two steels do not. The B steel shows about 4% elongation in 2", which is considerably more than the 1.5% required by ASTM for the A-446 Grade E. Fig. 2 shows the distribution of longitudinal strains in typical coupons of each of the steels.

In the earlier tests of A and S steels it was observed that though the elongation in 2" G.L. was around 5 to 8 percent, the elongation in 1/4" G.L. was around 30 to 45 percent. Hence the measure of ductility was separated into two parts; one was designated as local ductility and the other as overall ductility. The total percentage strain is given by the following equation[2]:

$$e = K \left(\frac{L}{\sqrt{A}}\right)^{\alpha} \qquad (1)$$

where e = the percent elongation in gage length L

A = cross sectional area of the specimen

K and α = constants related to local and overall ductility, respectively

One advantage of the above relationship is that the constants K and α are independent of the size and shape of the test specimen used.

Table 1 presents ductility parameters obtained from representative standard tension coupon tests of A, S and B steels, wherein percent reduction of area, percent elongation in 1/4" G.L. and K are indicators of local ductility of the material, while tensile-to-yield ratio, percent elongation in 2 1/2" G.L. excluding neck, and α are indicators of overall ductility of the material. Higher algebraic values indicate greater ductility in all cases. Comparison of the algebraic values given in Table 1 indicates that A and S steels have more local ductility and less overall ductility than that obtained in B steel.

Fig. 3 is a graph of Eq. 1 for each of the steels using the values of K and α from Table 1, and includes also the results for full annealed A steel taken from the Second Progress Report. In Fig. 3 higher values of the intercept on the elongation axis indicate greater local ductility, and flatter slopes indicate greater overall ductility. Table 1 and Figs. 2 and 3 all indicate that B steel has less local ductility than the low ductility A or S steels; but B steel has greater overall ductility.

The overall ductility of B steel is a consequence of its strain-hardenability. This permits sufficient strain hardening at that portion or portions of the member at which localized first yielding begins, so that yielding spreads to other portions of the specimen rather than causing necking at the location of initial yielding.

3. Rectangular Plates with Holes

Tests of rectangular plates of A, S and B steel with one or more holes in line of stress showed that these plates developed their full tensile strength as calculated on the net cross sectional area; that is

$$\frac{\sigma_{tt}}{\sigma_t} \geq 1 \qquad (2)$$

where σ_{tt} = tensile stress calculated on the net area

σ_t = tensile strength of coupon in uniaxial tension

Typical results are given in Table 2. The local ductility determined from tests of plates with holes compares reasonably well with the local ductility measured in the coupon tests. For A steel the average elongation in 1/4" G.L. at the hole in the plate was approximately 32 percent, while that of the tension coupon was 48 percent. For B steel elongation in 1/4" G.L. in the tension coupon was 15.5 percent, while at the hole in the rectangular plate it was 12.9 percent. Fig. 4 shows the longitudinal strain distribution for plates of A and B steel with three holes in line of stress. The greater local ductility of the A steel is again evident.

The above tests indicate that the effects of the elastic stress concentration produced by a hole are eventually wiped out due to the good local ductility of these "low ductility" steels.

4. Single Bolted Connection Tests

Single bolted connection tests were conducted using each of the project steels. The experimental set up and the presentation of results are similar to those given by Winter[3] in an earlier paper. The types of failure and form of the prediction equations also are similar to those obtained from Winter's tests which were performed on high ductility steels.

Variables considered in the program in addition to the type of steel used were: edge distance e, bolt diameter d, sheet thickness t, plate width s, and coupon tensile strength σ_t. The connection failures are divided into three main types:

(i) Longitudinal shearing of the plate along two practically parallel planes whose distance is equal to the bolt diameter

(ii) Bearing failure with considerable elongation of the hole and material "piling up" in front of the bolt

(iii) Transverse tension-tearing across the plate

Test results for the low ductility steels are presented in Fig. 5 for bearing, shear and combined failures, and in Fig. 6 for tension and combined failures. The failure loads can be represented by the following equations:

$$P_{shear} = P_{sh} = 0.9\ e\ \sigma_t\ t \tag{4}$$

$$P_{bearing} = P_b = 3.0\ \sigma_t\ dt \tag{5}$$

$$P_{tension} = P_t = (0.1 + 3\ \frac{d}{s})\ \sigma_t\ A_{net} \leq \sigma_t\ A_{net} \tag{6}$$

where A_{net} = net cross sectional area of the plate through center of the hole

σ_t = tensile strength of the material as obtained from the coupon test

One of the main differences in the behavior of Winter's tests and the current ones is that the bearing strength of the low ductility material is a lower multiple of σ_t (by about 20%) than previously obtained for high ductility connection specimens. On the other hand, the expression for tension failure of connections of low ductility steel is identical to Winter's expression for high ductility steels. Tests of three-bolt in-line connections with low ductility steel gave similar results[4].

Dimensional analysis has been used in an attempt to refine the strength prediction of bolted connections under mixed modes of failure; this study is continuing.

5. Longitudinal Fillet-Welded Connections

Tests of longitudinal fillet welded connections using A and S steel have been conducted. Variables considered in the program were: lap length L, thickness of material t, and type of steel. The connections were designed to fall into three groups. Group I specimens were designed to develop the full strength of the connected plate. Group II specimens

were designed such that failure would occur by shearing of the weld. For Group III specimens the weld length was so designed that whether failure would occur in the weld or in the plate could not be predicted with assurance.

The main parameters and test results are summarized in Table 3, and load-deformation curves for two of the welded connections are shown in Fig. 7. Failures are described as Type a (tension) or Type b (weld shear) or a combination of a and b. Conclusions may be summarized as follows:

1. Comparison of σ_{tt}/σ_t for connections that failed in tension shows that a longitudinal fillet welded connection in low ductility steel can be designed to develop the full strength of the plate.

2. A and S steels are "weldable" in the sense that no noticeable defects in the weld of the specimen were observed.

3. When the lap length of the connection is not long enough to develop the full strength of the plate then failure occurs by shearing of the weld. In this case the weld is capable of developing its full shear strength corresponding to the tensile strength as specified by ASTM specifications.

4. The behavior of a low ductility steel specimen is easier to predict than that of the high ductility one, because very little out of plane distortion occurs in low ductility steel specimens. On the other hand in high ductility specimens, where there is a considerable spread between yield and tensile strength, in and out of plane distortions are considerable.

5. In these connections no annealing effects from weld heat were detected; that is, all strength properties were predictable from materials properties before welding.

These conclusions refer to A and S steels. Tests on welded connections of low ductility B-steel will be carried out shortly; the small thickness of the available B-steel may make for difficulties in this respect.

6. Finite Element Analysis

The finite element approach can be used to solve continuum mechanics problems in the plastic range. A solution will be sought for a rectangular plate under tension with a central hole or other stress concentration using stress-strain characteristics of a low ductility steel. By solution one means that the strain state in the plastic and elastic region is calculated for the specimen under consideration, and the extent of the plastic zone around the hole is established for successively increasing loads. The analysis should show whether the effect of a stress raiser is wiped out, i.e. whether the cross-section at the hole completely plastifies. If so, the strength of the tension member is essentially unaffected by the stress concentration and the ductility is adequate. To establish a lower bound on the required local ductility of the material, one calculates the plastic strain at the hole when the element at the edge of the plate just enters the plastic region.

This situation will also be investigated by experimental means using the same geometry of rectangular plate with a

central hole. Two 1/4" foil strain gages can be attached (in the longitudinal direction); one at the hole and the other at the edge. When the gage at the edge of the plate enters the plastic region, the reading of the gage at the hole is the minimum local ductility required for the given material.

The same type of investigation can be carried out for other types of stress concentration.

References

(1) Light Gage Cold Formed Design Manual, American Iron and Steel Institute, 1962 Edition.

(2) Oliver, D. A.; "Proposed New Criteria of Ductility From a New Law Connecting the Percentage Elongation with Size of Test Piece", Inst. of Mech. Engineers, Vol. II, 1928.

(3) Winter, G.; "Tests on Bolted Connections in Light Gage Steel". Proc. ASCE, Vol. 82, Paper No. 920, March 1956.

(4) Popowich, D. W.; "Three-Bolt In-Line Connections with Low Ductility Light-Gage Steel". Report 2, Cornell University, Ithaca, N.Y., February 1969.

(5) Dhalla, A. K., and Errera, S. J.; "Influence of Ductility on the Structural Behavior of Light-Gage Cold-Formed Steel Members", First Progress Report, Cornell University, Ithaca, N.Y., Feb. 1968.

(6) Dhalla, A. K.; "Influence of Ductility on the Structural Behavior of Light-Gage Cold-Formed Steel Members", Second Progress Report, Cornell University, Ithaca, N.Y., Oct. 1968.

TABLE 1

Comparative Study of Ductility Characteristics of A, B and S Steels

Ductility Parameters	20B-Av. B-Steel	12S-L3 S-Steel *	1205-L2 A-Steel *	1605-L3 A-Steel *	16PA-L1 A-Annealed-Steel *
Elongation in 2", (%)	4.38	5.13	5.58	6.84	52.20
Reduction in area (%)	56.10	65.20	69.40	59.00	83.80
Tensile/Yield Ratio	1.08	1.01	1.00	1.00	1.48
Elongation in 1/4" (including neck)(%)	15.55	38.40	44.40	35.20	85.60
Elongation in 2 1/2" (excluding neck) (%)	2.74+	0.33	0.40	1.28	38.00
K	20.50	45.00	46.00	45.00	120.00
a	-0.579	-0.974	-0.983	-0.795	-0.335

Note: * The values reported in these columns are taken from Table 7 of Second Progress Report.

+ This value is for % elongation in 2", excluding neck.

TABLE 2

Typical Results of Tension Tests on Rectangular Plates With Holes

(A, S and B Steels)

Spec. Designation	GEORMETRICAL DIMENSIONS				MAT'L PROPERTIES		EXPERIMENTAL RESULTS				
	Dia. of Hole	Width of Plate	$\frac{d}{s}$	No. of Holes	σ_t	Elong. in 1/4" G.L.	P_{ult}	$\frac{P_{ult}}{A_{net}} = \sigma_{tt}$	Elong. in 1/4" G.L.	$\frac{\sigma_{tt}}{\sigma_t}$	Total Member Deformation
	(in)	(in)			(ksi)	(%)	(kips)	(ksi)	%		(in)
12S-T-L2	9/16	2.50	0.225	one	72.8	44.0	14.50	71.4		0.98	
7S-T-T3	9/16	1.25	0.500	one	91.0	47.0	11.40	91.1		1.00	
1210-T-L2	1/2	4.25	0.118	Three	74.6	49.0	30.70	75.5	37.2	1.01	0.19
1205-T-L4	1/2	4.25	0.118	Three	72.2	47.0	32.20	79.4	28.6	1.10	0.11
20-B-L8	1/2	4.25	0.118	Three	81.7	15.5	12.80	90.0	12.9	1.10	0.06
					σ_y	σ_t	P_y	P_{ult}	σ_{ty}	σ_{tt}	
12FA-T-L12	1/2	4.25	0.118	one	27.4	43.9 72.3	11.0	17.0	27.4	42.4	0.96

TABLE 3

Results of Longitudinal Lap Welded Connection Tests

(A, S and B Steels)

Spec. Designation	SPEC. GEOM.		MAT'L PROPERTY		EXPERIMENTAL RESULTS					
	Width of Plate b_n (in)	Lap Length L (in)	Tensile Stress σ_t (ksi)	Electrode Tensile Stress σ_{ta} (ksi)	Ult. Load P_{ult} (kips)	Ult. Tensile Stress in Plate σ_{tt} (ksi)	Ult. Tensile Stress in Weld σ_{tu} (ksi)	Mode of Failure (type)	$\frac{\sigma_{tt}}{\sigma_t}$	$\frac{\sigma_{tu}}{\sigma_{ta}}$
7S-W70-L1	2.50	3.00	83.3	70.0	37.25	81.5	83.1	b	0.98	1.18
7S-W70-L2	2.50	5.00	83.3	70.0	38.90	85.0	52.5	a	1.02	0.75
7S-W100-L3	2.50	3.25	83.3	100.0	38.30	83.7	78.6	a	1.00	0.78
12S-W100-L4	3.00	3.25	82.5	100.0	24.90	78.8	88.4	a	0.96	0.88
1205-W100-L5	3.00	3.25	84.1	100.0	25.80	79.0	89.4	a	0.94	0.89
1605-W100-L6	3.00	3.75	98.0	100.0	16.60	87.8	86.8	a	0.89	0.87
12FA-W70-L7	4.00	3.75	45.0	70.0	16.80	39.9	51.0	a	0.88	0.73
7S-W100-L8	2.50	2.25	83.3	100.0	33.80	73.8	100.8	b	0.88	1.01
12S-W100-L9	3.00	2.25	82.5	100.0	19.40	60.8	99.5	b	0.74	0.99
1205-W100-L10	3.00	2.25	84.1	100.0	16.40	50.2	82.5	b	0.60	0.82
1605-W100-L11	3.00	2.75	98.0	100.0	14.30	75.7	101.8	b	0.77	1.02
12FA-W70-L12	4.00	1.50	44.6	70.0	9.80	22.7	74.0	a+b	0.51	1.05
7S-W100-L13	2.50	2.75	83.3	100.0	37.50	82.0	91.2	a	0.98	0.91
12S-W100-L14	3.00	2.75	82.5	100.0	22.25	70.0	93.6	b	0.85	0.94
1205-W100-L15	3.00	2.75	84.1	100.0	23.80	70.5	98.0	b	0.84	0.98
1605-W100-L16	3.00	3.25	98.0	100.0	16.20	85.7	97.5	b	0.87	0.97
12FA-W70-L17	4.00	2.00	44.6	70.0	11.80	28.2	66.6	a	0.63	0.95

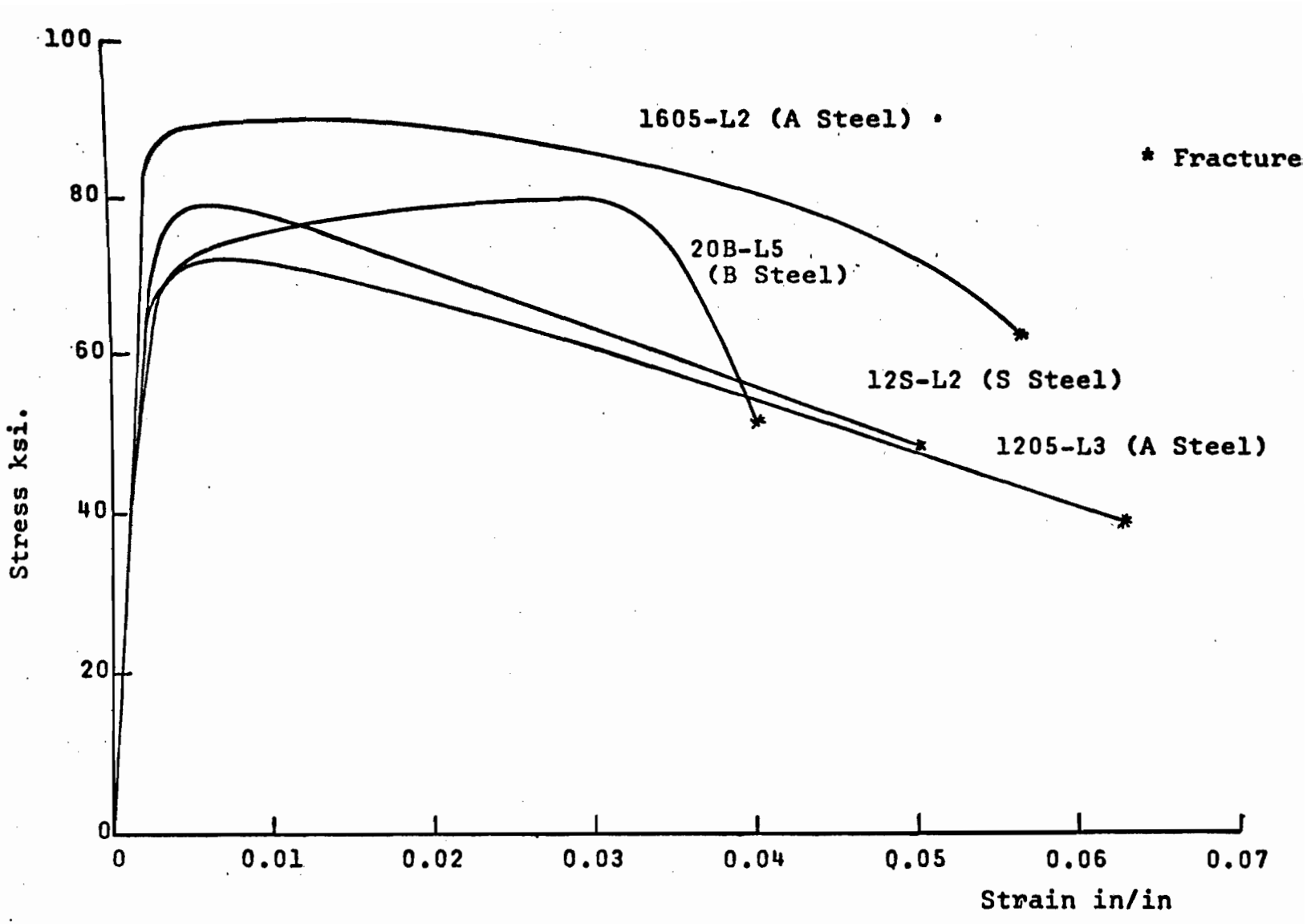

FIG. 1 COMPLETE STRESS STRAIN CURVES OF A, S AND B STEEL.

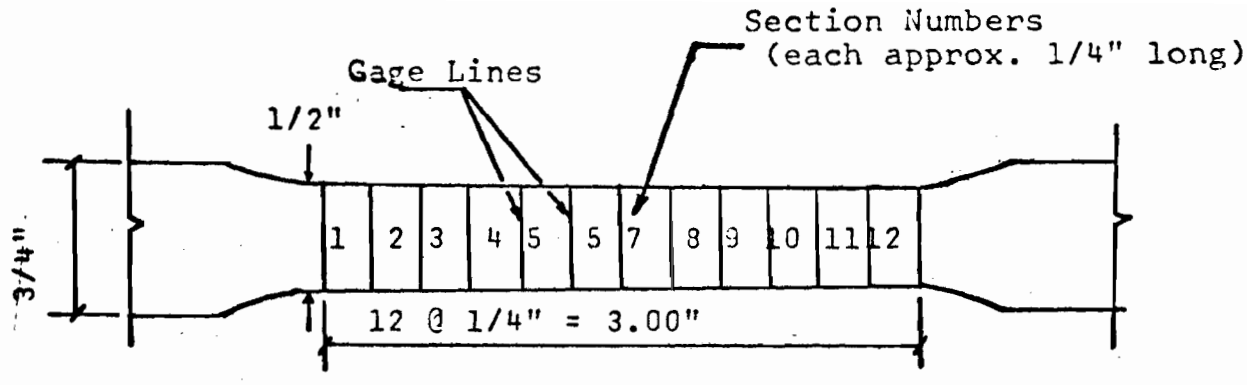

FIG. 2a. SKETCH OF A STANDARD TENSION COUPON

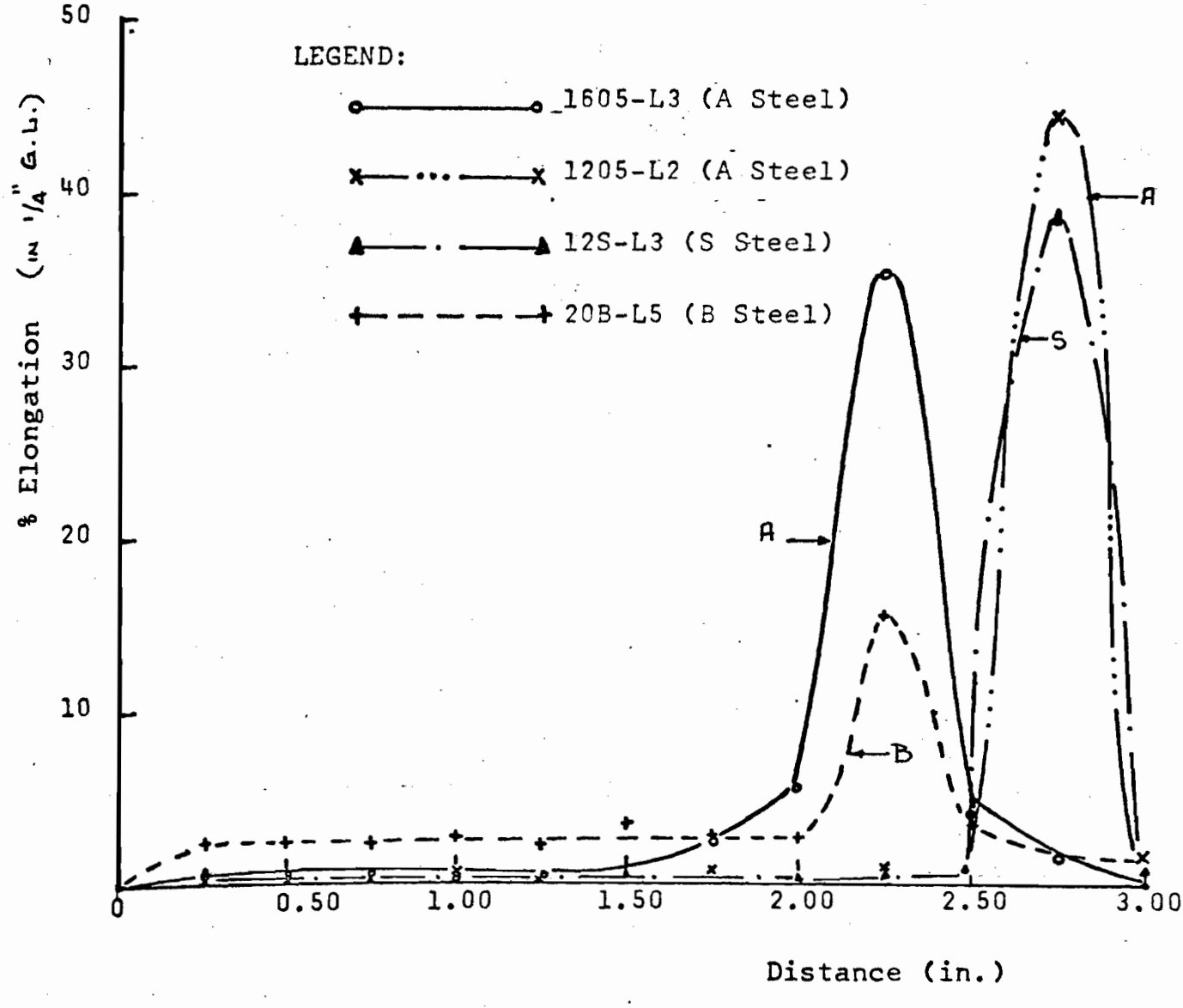

FIG. 2b. DISTRIBUTION OF LONGITUDINAL STRAIN IN TENSION COUPON (after fracture)

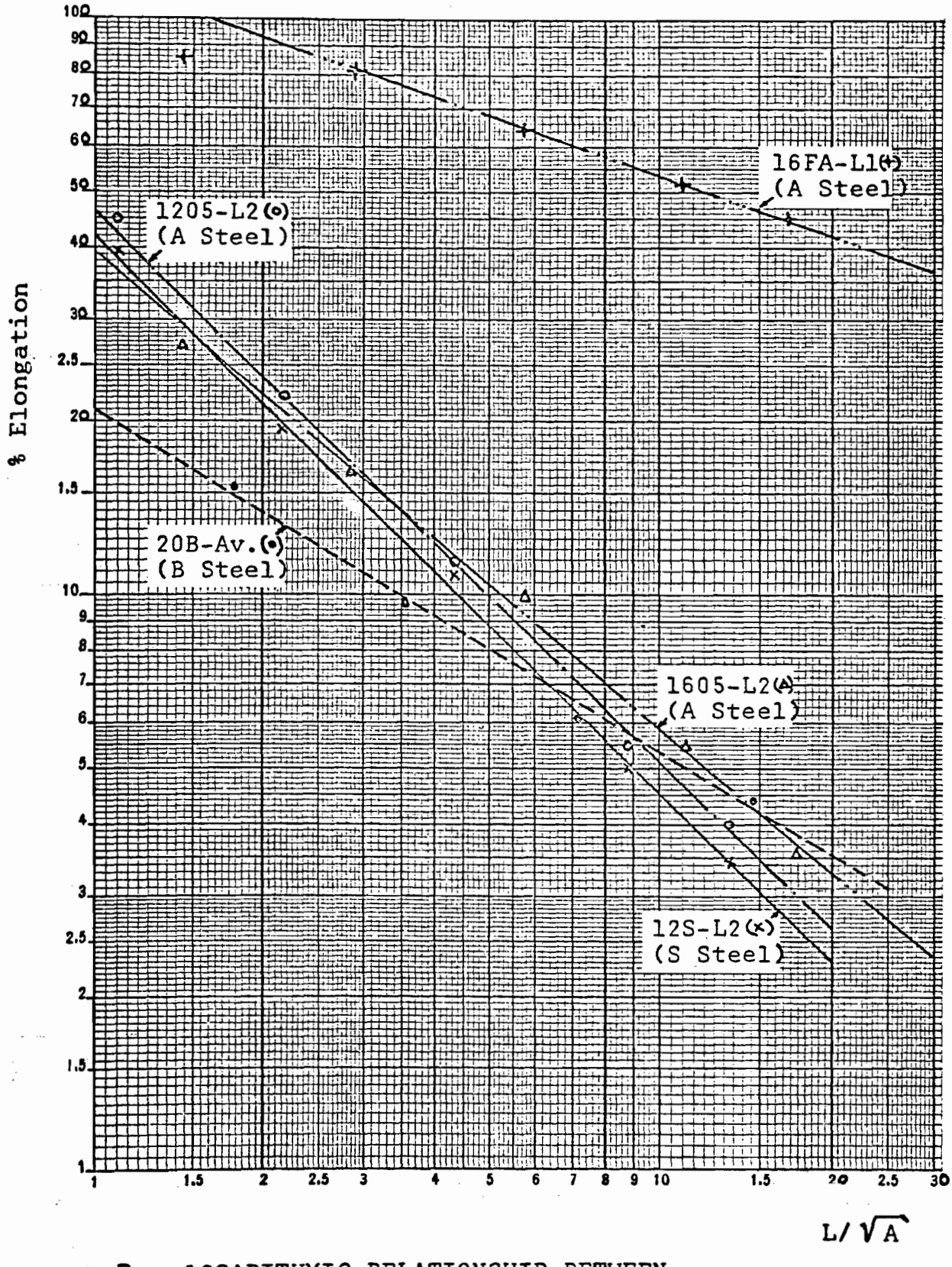

FIG. 3. LOGARITHMIC RELATIONSHIP BETWEEN ELONGATION AND $L/\sqrt{A}$ FOR A, S AND B STEEL

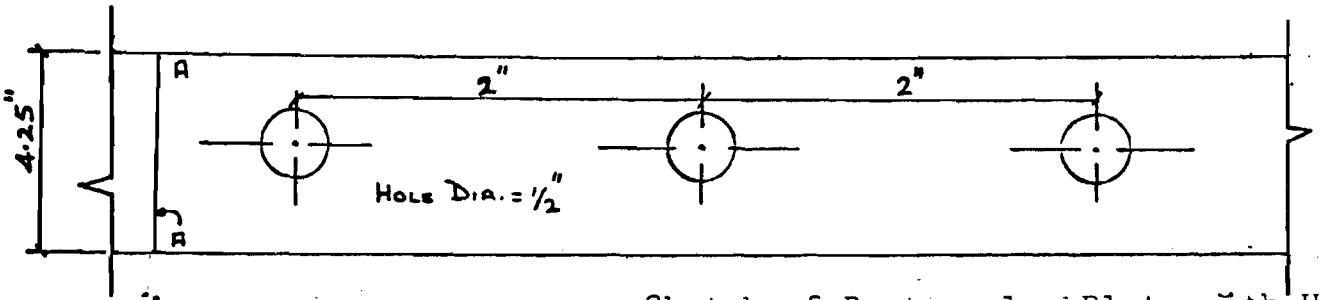

Sketch of Rectangular Plate with Holes

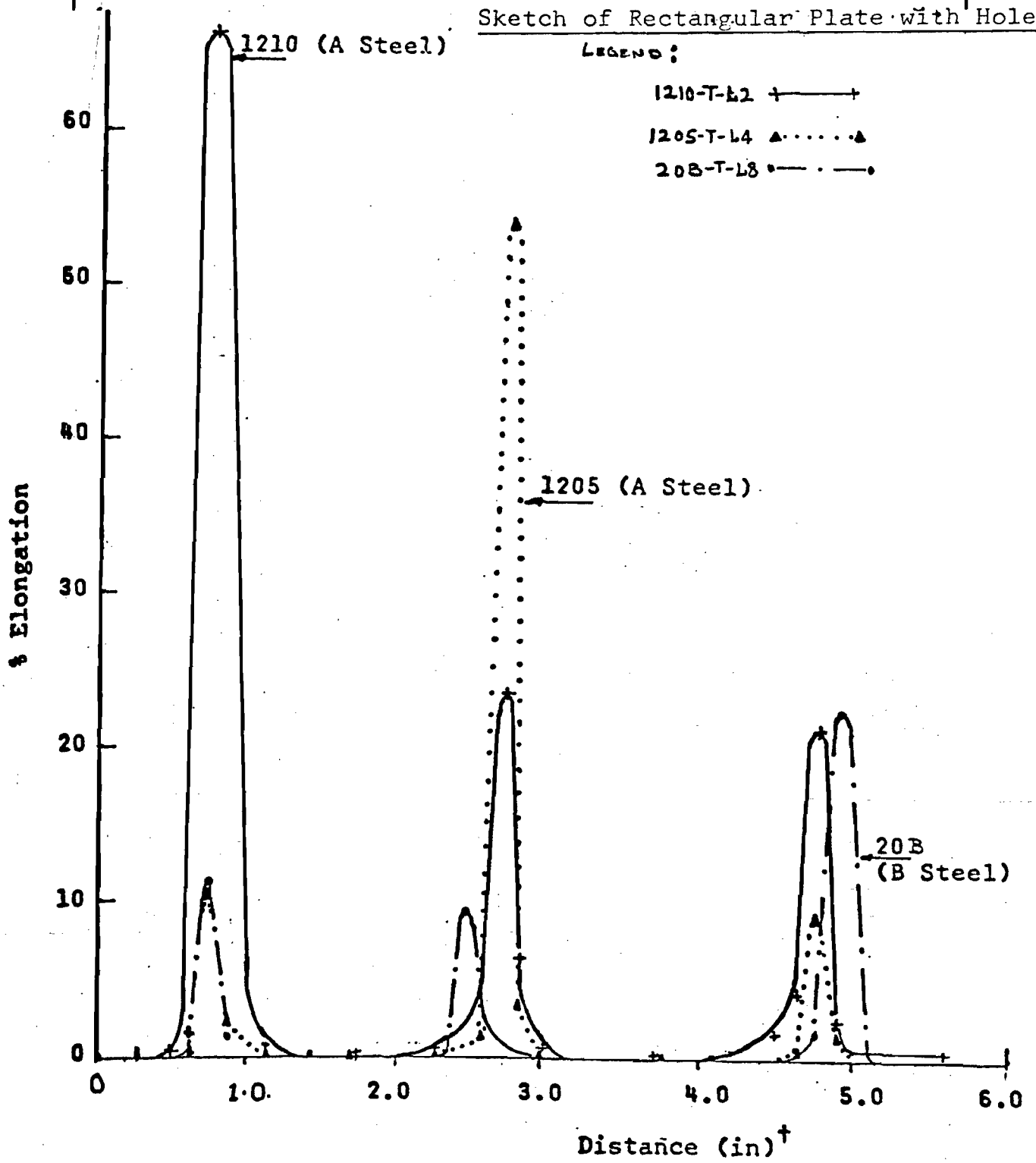

FIG 4 LONGITUDINAL STRAIN DISTRIBUTION (AFTER FRACTURE) IN RECTANGULAR PLATE WITH HOLES

†Distance measured from Line A-A (See Sketch Above)

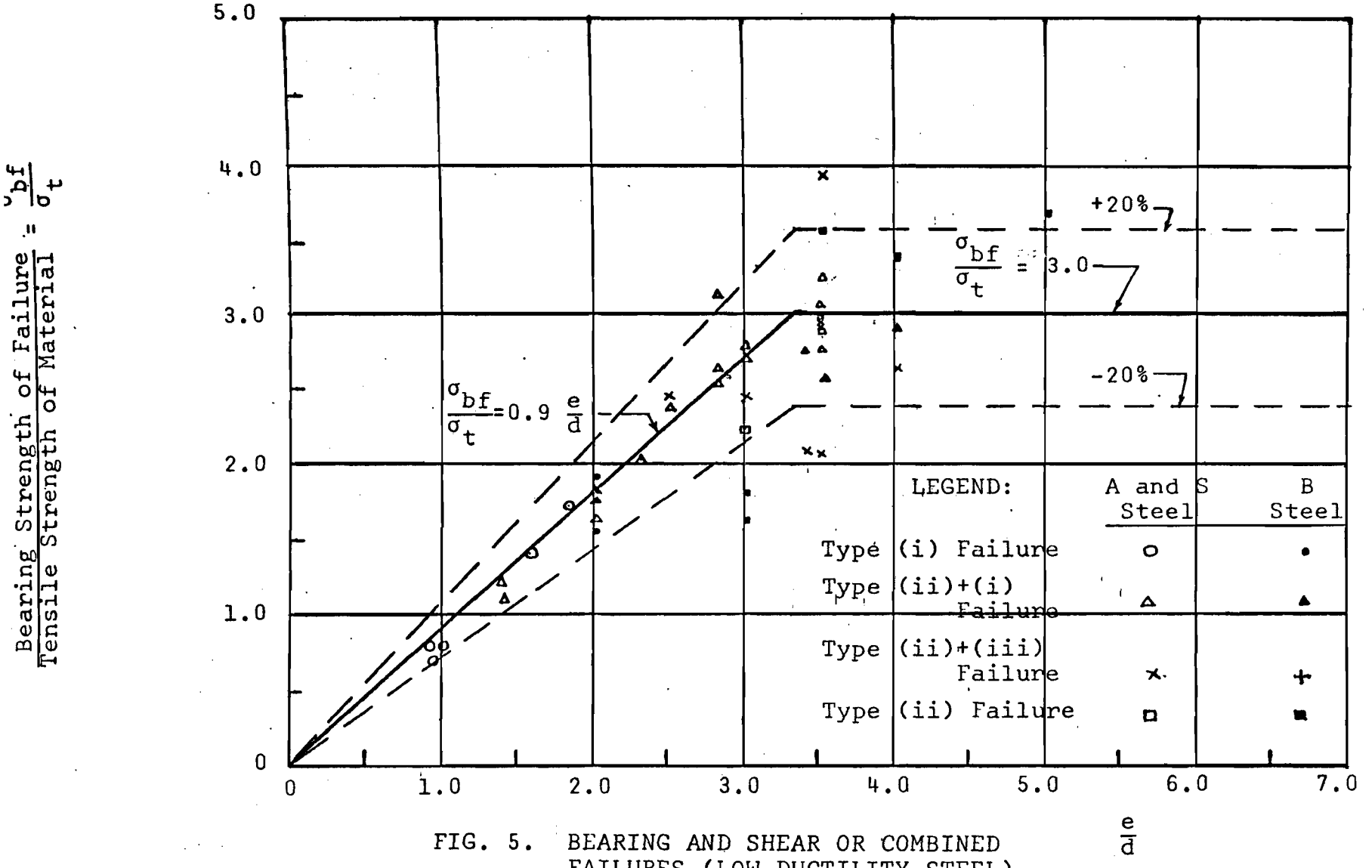

FIG. 5. BEARING AND SHEAR OR COMBINED FAILURES (LOW DUCTILITY STEEL)

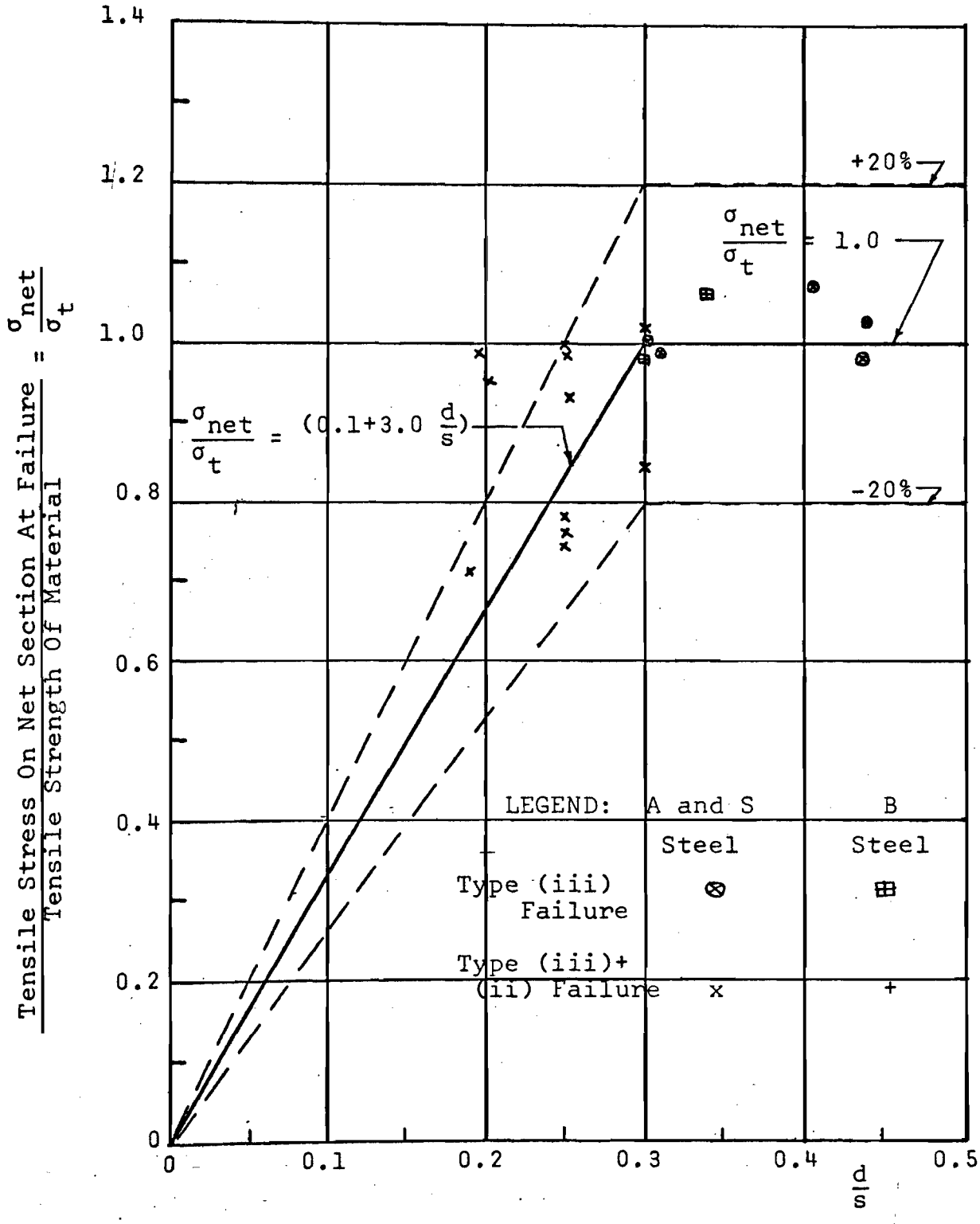

FIG. 6. TRANSVERSE TEARING OR COMBINATION OF BEARING AND TENSION FAILURES (LOW DUCTILITY STEEL)

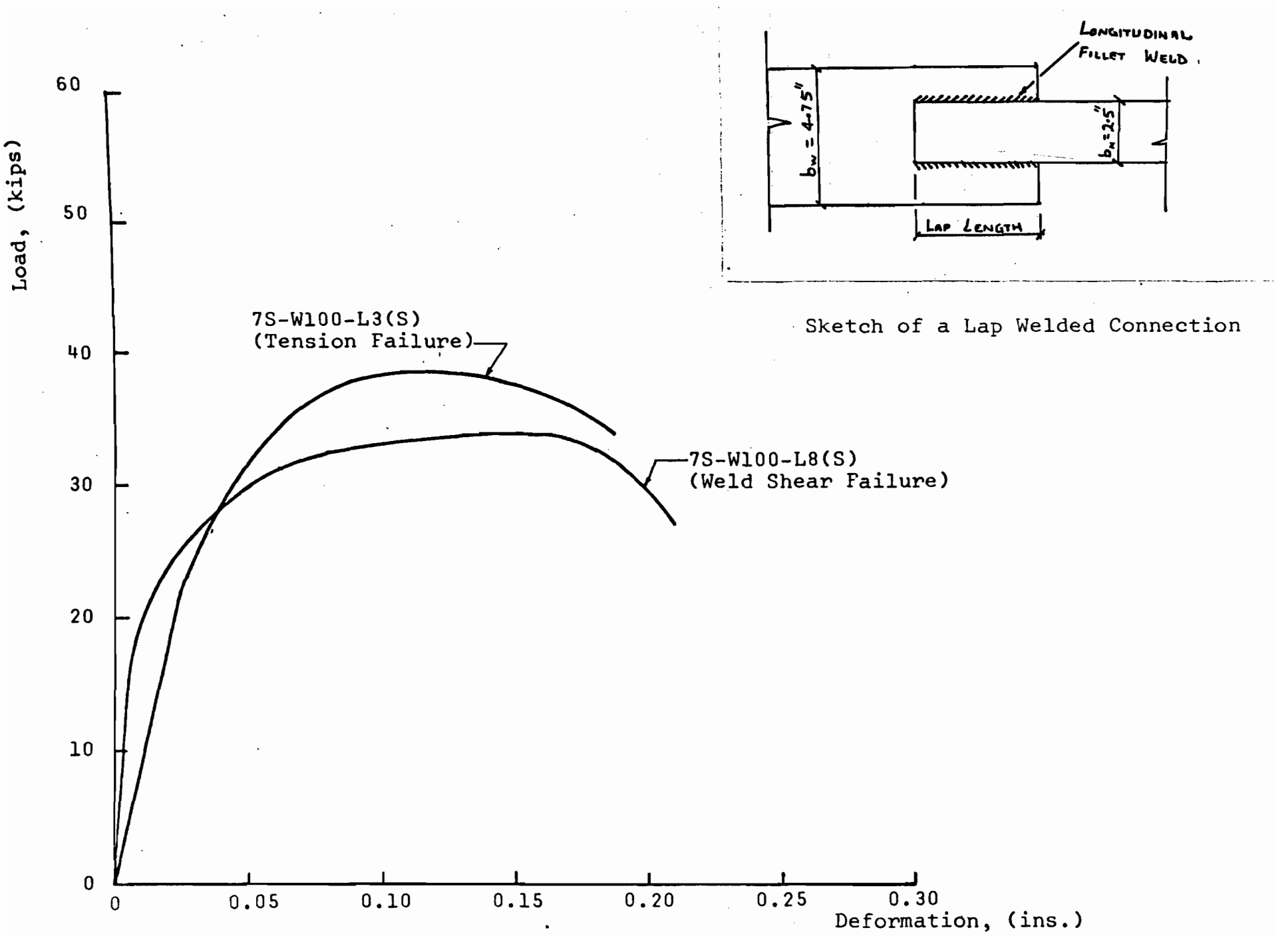

Sketch of a Lap Welded Connection

FIG. 7. LOAD-DEFORMATION CURVES OF LONGITUDINAL FILLET WELDED SPECIMENS

October 3, 1969

To: Members Technical Committee On Structural Research and Design Specifications

From; G. Winter

Enclosed please find an informal fairly detailed summary of our entire research to date on Influence of Ductility. This summary has been prepared for the meeting in Bethlehem October 10 of our research staff (Dr. Errera, myself and Mr. Dhalla) with Al Oudeusden and members of the Bethlehem staff knowledgeable in these matters.

It is believed that distribution of this summary to members of the Technical Committee will be informative to them and will enhance discussion of this area at Chicago.

Sincerely,

George Winter
1912 Professor of Engineering
Chairman, Dept. of Structural Engineering

Enclosure

cc: W.G. Kirkland

October 2, 1969

To: G. Winter

From: A. K. Dhalla and S. J. Errera

Subject: Influence of Ductility on the Structural Behavior of Cold-Formed Steel Members

Summary of Investigation and

Plans for Immediate Future

Table of Contents

1. Introduction 1
2. Material Properties 1
3. Rectangular Plates with Holes 4
4. Single Bolted Connection Tests 5
5. Longitudinal Fillet-Welded Connections 6
6. Finite Element Analysis 8

References 10

List of Tables:

1. Comparative Study of Ductility Characteristics of A, B, and S Steel
2. Typical Results of Tension Tests on Rectangular Plate with Holes
3. Results of Longitudinal Lap Welded Connection Tests

List of Figures:

1. Complete Stress Strain Curves of A, B, and S Steel
2. Distribution of Longitudinal Strain in Tension Coupon
3. Logarithmic Relationship Between Elongation and $L/\sqrt{A}$ for A, S and B Steel.
4. Longitudinal Strain Distribution After Fracture in Rectangular Plate with Holes.
5. Bearing and Shear or Combined Failures (Low Ductility Steel).
6. Transverse Tearing or Combination of Bearing and Tension Failure (Low Ductility Steel).
7. Load-Deformation Curve of Longitudinal Fillet Welded Specimens.

1. Introduction

In order to determine the "suitability of steel"[1] for cold-formed construction one needs to know, in addition to other mechanical properties of the material, performance characteristics such as ductility, formability and weldability. Ductility is the ability of a material to undergo large plastic deformations without fracture. It reduces the harmful effect of stress concentrations, permits large local strains without serious damage, and helps achieve uniform stress or load distribution in connections.

There are different tests specified by ASTM to measure ductility, the chief of them being the percent elongation after fracture in a specified gage length, usually 2" or 8". The minimum acceptable for structural use, according to ASTM standards, varies a great deal. Two of the low ductility steels used in this investigation were specially rolled and made available by the manufacturers. These are designated as A and S steels, and had between 5 and 10 percent elongation in 2" gage length, well below the "ductility" required by ASTM for structural steels in general use in load carrying members. The third steel investigated to date is a 20 gage commercial low ductility steel, ASTM A-446 Grade E, herein designated as Steel B, with a specified minimum elongation of 1.5% in 2". Grade E steel is used primarily for cold formed panels.

2. Material Properties

The parameters which can be used to define the ductility

of steel were discussed in the Second Progress Report. These include elongation in 2", reduction in area, tensile-yield strength ratio, elongation in 1/4", and elongation in some gage length which excludes the fracture zone. These parameters were measured from standard tension tests wherein the coupons were prepared and tested in accordance with ASTM Specification E8-65T. The A and S steel coupon test results were presented in the first and second progress reports. B steel coupons were tested subsequently.

Typical complete stress-strain curves for 12 and 16 gage A steel, 12 gage S steel and 20 gage B steel are shown in Fig. 1. An important fact indicated by the figure is that B steel has a strain hardening range while the other two steels do not. The B steel shows about 4% elongation in 2", which is considerably more than the 1.5% required by ASTM for the A-446 Grade E. Fig. 2 shows the distribution of longitudinal strains in typical coupons of each of the steels.

In the earlier tests of A and S steels it was observed that though the elongation in 2" G.L. was around 5 to 8 percent, the elongation in 1/4" G.L. was around 30 to 45 percent. Hence the measure of ductility was separated into two parts; one was designated as local ductility and the other as overall ductility. The total percentage strain is given by the following equation[2]:

$$e = K \left(\frac{L}{\sqrt{A}}\right)^{\alpha} \qquad (1)$$

where e = the percent elongation in gage length L

A = cross sectional area of the specimen

K and α = constants related to local and overall ductility, respectively

One advantage of the above relationship is that the constants K and α are independent of the size and shape of the test specimen used.

Table 1 presents ductility parameters obtained from representative standard tension coupon tests of A, S and B steels, wherein percent reduction of area, percent elongation in 1/4" G.L. and K are indicators of local ductility of the material, while tensile-to-yield ratio, percent elongation in 2 1/2" G.L. excluding neck, and α are indicators of overall ductility of the material. Higher algebraic values indicate greater ductility in all cases. Comparison of the algebraic values given in Table 1 indicates that A and S steels have more local ductility and less overall ductility than that obtained in B steel.

Fig. 3 is a graph of Eq. 1 for each of the steels using the values of K and α from Table 1, and includes also the results for full annealed A steel taken from the Second Progress Report. In Fig. 3 higher values of the intercept on the elongation axis indicate greater local ductility, and flatter slopes indicate greater overall ductility. Table 1 and Figs. 2 and 3 all indicate that B steel has less local ductility than the low ductility A or S steels; but B steel has greater overall ductility.

The overall ductility of B steel is a consequence of its strain-hardenability. This permits sufficient strain hardening at that portion or portions of the member at which localized first yielding begins, so that yielding spreads to other portions of the specimen rather than causing necking at the location of initial yielding.

3. Rectangular Plates with Holes

Tests of rectangular plates of A, S and B steel with one or more holes in line of stress showed that these plates developed their full tensile strength as calculated on the net cross sectional area; that is

$$\frac{\sigma_{tt}}{\sigma_t} \geq 1 \qquad (2)$$

where σ_{tt} = tensile stress calculated on the net area at fracture

σ_t = tensile strength of coupon in uniaxial tension

Typical results are given in Table 2. The local ductility determined from tests of plates with holes compares reasonably well with the local ductility measured in the coupon tests. For A steel the average elongation in 1/4" G.L. at the hole in the plate was approximately 32 percent, while that of the tension coupon was 48 percent. For B steel elongation in 1/4" G.L. in the tension coupon was 15.5 percent, while at the hole in the rectangular plate it was 12.9 percent. Fig. 4 shows the longitudinal strain distribution for plates of A and B steel with three holes in line of stress. The greater local ductility of the A steel is again evident.

The above tests indicate that the effects of the elastic stress concentration produced by a hole are eventually wiped out due to the good local ductility of these "low ductility" steels.

4. Single Bolted Connection Tests

Single bolted connection tests were conducted using each of the project steels. The experimental set up and the presentation of results are similar to those given by Winter[3] in an earlier paper. The types of failure and form of the prediction equations also are similar to those obtained from Winter's tests which were performed on high ductility steels.

Variables considered in the program in addition to the type of steel used were: edge distance e, bolt diameter d, sheet thickness t, plate width s, and coupon tensile strength σ_t. The connection failures are divided into three main types:

(i) Longitudinal shearing of the plate along two practically parallel planes whose distance is equal to the bolt diameter

(ii) Bearing failure with considerable elongation of the hole and material "piling up" in front of the bolt

(iii) Transverse tension-tearing across the plate

Test results for the low ductility steels are presented in Fig. 5 for bearing, shear and combined failures, and in Fig. 6 for tension and combined failures. The failure loads can be represented by the following equations:

$$P_{shear} = P_{sh} = 0.9\ e\ \sigma_t\ t \tag{4}$$

$$P_{bearing} = P_b = 3.0\ \sigma_t\ dt \tag{5}$$

$$P_{tension} = P_t = (0.1 + 3\ \frac{d}{s})\ \sigma_t\ A_{net} \leq \sigma_t\ A_{net} \tag{6}$$

where A_{net} = net cross sectional area of the plate through center of the hole

σ_t = tensile strength of the material as obtained from the coupon test

One of the main differences in the behavior of Winter's tests and the current ones is that the bearing strength of the low ductility material is a lower multiple of σ_t (by about 20%) than previously obtained for high ductility connection specimens. On the other hand, the expression for tension failure of connections of low ductility steel is identical to Winter's expression for high ductility steels. Tests of three-bolt in-line connections with low ductility steel gave similar results[4].

Dimensional analysis has been used in an attempt to refine the strength prediction of bolted connections under mixed modes of failure; this study is continuing.

5. Longitudinal Fillet-Welded Connections

Tests of longitudinal fillet welded connections using A and S steel have been conducted. Variables considered in the program were: lap length L, thickness of material t, and type of steel. The connections were designed to fall into three groups. Group I specimens were designed to develop the full strength of the connected plate. Group II specimens

were designed such that failure would occur by shearing of the weld. For Group III specimens the weld length was so designed that whether failure would occur in the weld or in the plate could not be predicted with assurance.

The main parameters and test results are summarized in Table 3, and load-deformation curves for two of the welded connections are shown in Fig. 7. Failures are described as Type a (tension) or Type b (weld shear) or a combination of a and b. Conclusions may be summarized as follows:

1. Comparison of σ_{tt}/σ_t for connections that failed in tension shows that a longitudinal fillet welded connection in low ductility steel can be designed to develop the full strength of the plate.

2. A and S steels are "weldable" in the sense that no noticeable defects in the weld of the specimen were observed.

3. When the lap length of the connection is not long enough to develop the full strength of the plate then failure occurs by shearing of the weld. In this case the weld is capable of developing its full shear strength corresponding to the tensile strength as specified by ASTM specifications.

4. The behavior of a low ductility steel specimen is easier to predict than that of the high ductility one, because very little out of plane distortion occurs in low ductility steel specimens. On the other hand in high ductility specimens, where there is a considerable spread between yield and tensile strength, in and out of plane distortions are considerable.

5. In these connections no annealing effects from weld heat were detected; that is, all strength properties were predictable from materials properties before welding.

These conclusions refer to A and S steels. Tests on welded connections of low ductility B-steel will be carried out shortly; the small thickness of the available B-steel may make for difficulties in this respect.

6. Finite Element Analysis

The finite element approach can be used to solve continuum mechanics problems in the plastic range. A solution will be sought for a rectangular plate under tension with a central hole or other stress concentration using stress-strain characteristics of a low ductility steel. By solution one means that the strain state in the plastic and elastic region is calculated for the specimen under consideration, and the extent of the plastic zone around the hole is established for successively increasing loads. The analysis should show whether the effect of a stress raiser is wiped out, i.e. whether the cross-section at the hole completely plastifies. If so, the strength of the tension member is essentially unaffected by the stress concentration and the ductility is adequate. To establish a lower bound on the required local ductility of the material, one calculates the plastic strain at the hole when the element at the edge of the plate just enters the plastic region.

This situation will also be investigated by experimental means using the same geometry of rectangular plate with a

central hole. Two 1/4" foil strain gages can be attached (in the longitudinal direction); one at the hole and the other at the edge. When the gage at the edge of the plate enters the plastic region, the reading of the gage at the hole is the minimum local ductility required for the given material.

The same type of investigation can be carried out for other types of stress concentration.

References

(1) Light Gage Cold Formed Design Manual, American Iron and Steel Institute, 1962 Edition.

(2) Oliver, D. A.; "Proposed New Criteria of Ductility From a New Law Connecting the Percentage Elongation with Size of Test Piece", Inst. of Mech. Engineers, Vol. II, 1928.

(3) Winter, G.; "Tests on Bolted Connections in Light Gage Steel". Proc. ASCE, Vol. 82, Paper No. 920, March 1956.

(4) Popowich, D. W.; "Three-Bolt In-Line Connections with Low Ductility Light-Gage Steel". Report 2, Cornell University, Ithaca, N.Y., February 1969.

(5) Dhalla, A. K., and Errera, S. J.; "Influence of Ductility on the Structural Behavior of Light-Gage Cold-Formed Steel Members", First Progress Report, Cornell University, Ithaca, N.Y., Feb. 1968.

(6) Dhalla, A. K.; "Influence of Ductility on the Structural Behavior of Light-Gage Cold-Formed Steel Members", Second Progress Report, Cornell University, Ithaca, N.Y., Oct. 1968.

TABLE 1

Comparative Study of Ductility Characteristics of A, B and S Steels

Ductility Parameters	20B-Av. B-Steel	12S-L3 S-Steel *	1205-L2 A-Steel *	1605-L3 A-Steel *	16FA-L1 A-Annealed-Steel *
Elongation in 2", (%)	4.38	5.13	5.58	6.84	52.20
Reduction in area (%)	56.10	65.20	69.40	59.00	83.80
Tensile/Yield Ratio	1.08	1.01	1.00	1.00	1.48
Elongation in 1/4" (including neck)(%)	15.55	38.40	44.40	35.20	85.60
Elongation in 2 1/2" (excluding neck) (%)	2.74±	0.33	0.40	1.28	38.00
K	20.50	45.00	46.00	45.00	120.00
α	-0.579	-0.974	-0.983	-0.795	-0.335

Note: * The values reported in these columns are taken from Table 7 of Second Progress Report.

± This value is for % elongation in 2", excluding neck.

TABLE 2

Typical Results of Tension Tests on Rectangular Plates With Holes

(A, S and B Steels)

Spec. Designation	GEORMETRICAL DIMENSIONS				MAT'L PROPERTIES		EXPERIMENTAL RESULTS				
	Dia. of Hole	Width of Plate	$\frac{d}{s}$	No. of Holes	σ_t	Elong. in 1/4" G.L.	P_{ult}	$\frac{P_{ult}}{A_{net}} = \sigma_{tt}$	Elong. in 1/4" G.L.	$\frac{\sigma_{tt}}{\sigma_t}$	Total Member Deformation
	(in)	(in)			(ksi)	(%)	(kips)	(ksi)	%		(in)
12S-T-L2	9/16	2.50	0.225	one	72.8	44.0	14.50	71.4		0.98	
7S-T-T3	9/16	1.25	0.500	one	91.0	47.0	11.40	91.1		1.00	
1210-T-L2	1/2	4.25	0.118	Three	74.6	49.0	30.70	75.5	37.2	1.01	0.19
1205-T-L4	1/2	4.25	0.118	Three	72.2	47.0	32.20	79.4	28.6	1.10	0.11
20-B-L8	1/2	4.25	0.118	Three	81.7	15.5	12.80	90.0	12.9	1.10	0.06
					σ_y σ_t		P_y P_{ult}	σ_{ty} σ_{tt}			
12FA-T-L12	1/2	4.25	0.118	one	27.4 43.9	72.3	11.0 17.0	27.4 42.4		0.96	

TABLE 3

Results of Longitudinal Lap Welded Connection Tests

(A, S and B Steels)

Spec. Designation	SPEC. GEOM. Width of Plate b_n (in)	SPEC. GEOM. Lap Length L (in)	MAT'L PROPERTY Tensile Stress σ_t (ksi)	MAT'L PROPERTY Electrode Tensile Stress σ_{ta} (ksi)	EXPERIMENTAL RESULTS Ult. Load P_{ult} (kips)	Ult. Tensile Stress in Plate σ_{tt} (ksi)	Ult. Tensile Stress in Weld σ_{tu} (ksi)	Mode of Failure (type)	$\frac{\sigma_{tt}}{\sigma_t}$	$\frac{\sigma_{tu}}{\sigma_{ta}}$
7S-W70-L1	2.50	3.00	83.3	70.0	37.25	81.5	83.1	b	0.98	1.18
7S-W70-L2	2.50	5.00	83.3	70.0	38.90	85.0	52.5	a	1.02	0.75
7S-W100-L3	2.50	3.25	83.3	100.0	38.30	83.7	78.6	a	1.00	0.78
12S-W100-L4	3.00	3.25	82.5	100.0	24.90	78.8	88.4	a	0.96	0.88
1205-W100-L5	3.00	3.25	84.1	100.0	25.80	79.0	89.4	a	0.94	0.89
1605-W100-L6	3.00	3.75	98.0	100.0	16.60	87.8	86.8	a	0.89	0.87
12FA-W70-L7	4.00	3.75	45.0	70.0	16.80	39.9	51.0	a	0.88	0.73
7S-W100-L8	2.50	2.25	83.3	100.0	33.80	73.8	100.8	b	0.88	1.01
12S-W100-L9	3.00	2.25	82.5	100.0	19.40	60.8	99.5	b	0.74	0.99
1205-W100-L10	3.00	2.25	84.1	100.0	16.40	50.2	82.5	b	0.60	0.82
1605-W100-L11	3.00	2.75	98.0	100.0	14.30	75.7	101.8	b	0.77	1.02
12FA-W70-L12	4.00	1.50	44.6	70.0	9.80	22.7	74.0	a+b	0.51	1.05
7S-W100-L13	2.50	2.75	83.3	100.0	37.50	82.0	91.2	a	0.98	0.91
12S-W100-L14	3.00	2.75	82.5	100.0	22.25	70.0	93.6	b	0.85	0.94
1205-W100-L15	3.00	2.75	84.1	100.0	23.80	70.5	98.0	b	0.84	0.98
1605-W100-L16	3.00	3.25	98.0	100.0	16.20	85.7	97.5	b	0.87	0.97
12FA-W70-L17	4.00	2.00	44.6	70.0	11.80	28.2	66.6	a	0.63	0.95

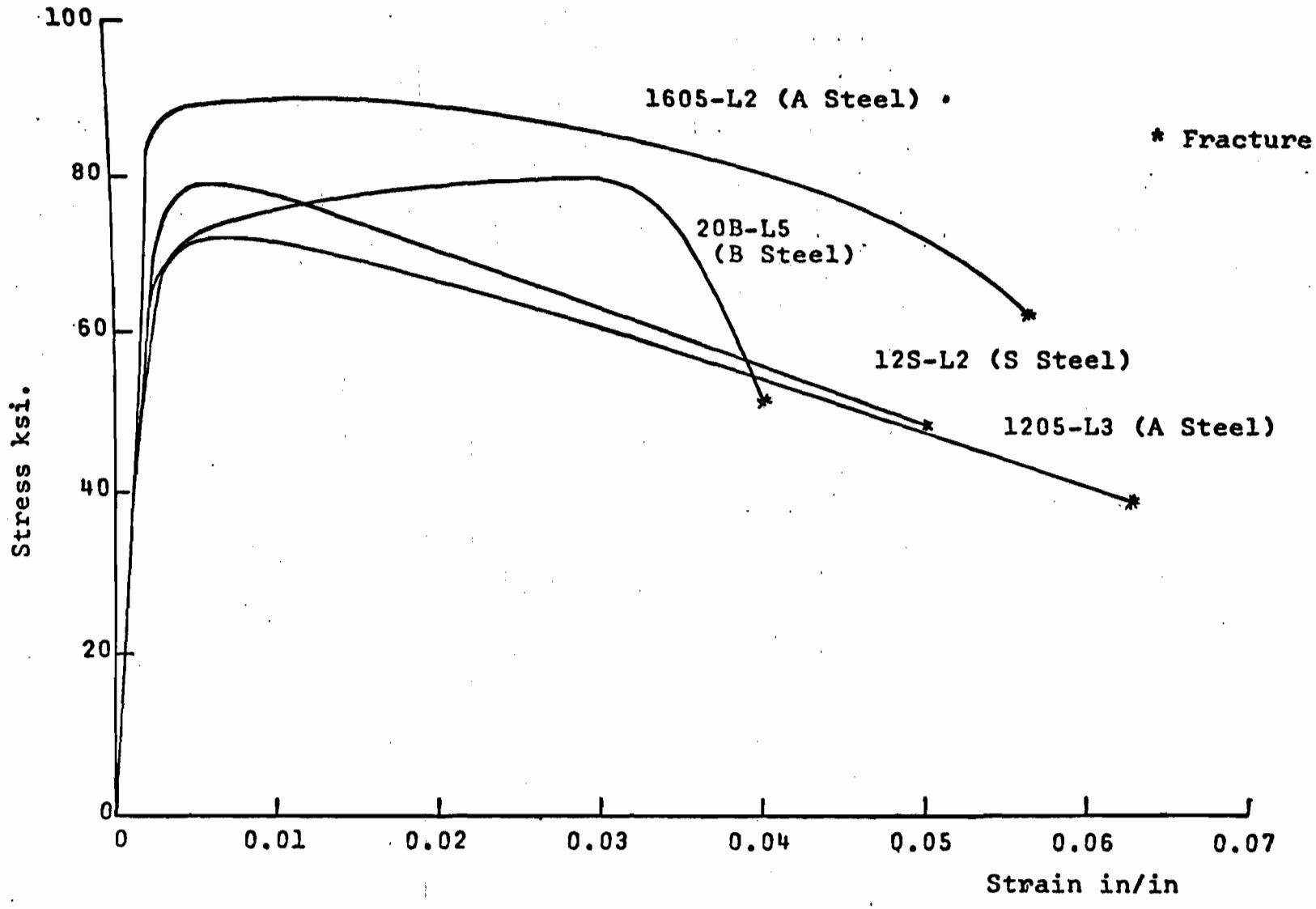

FIG. 1 COMPLETE STRESS STRAIN CURVES OF A, S AND B STEEL.

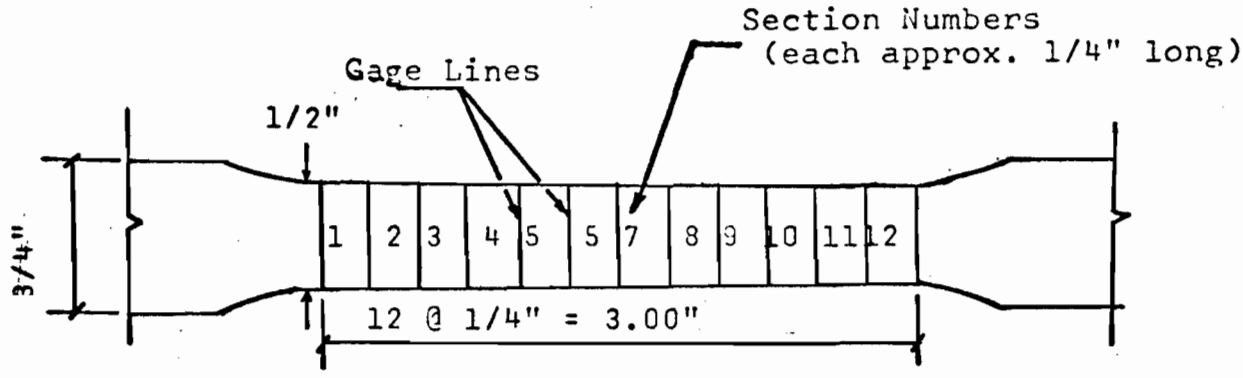

FIG. 2a. SKETCH OF A STANDARD TENSION COUPON

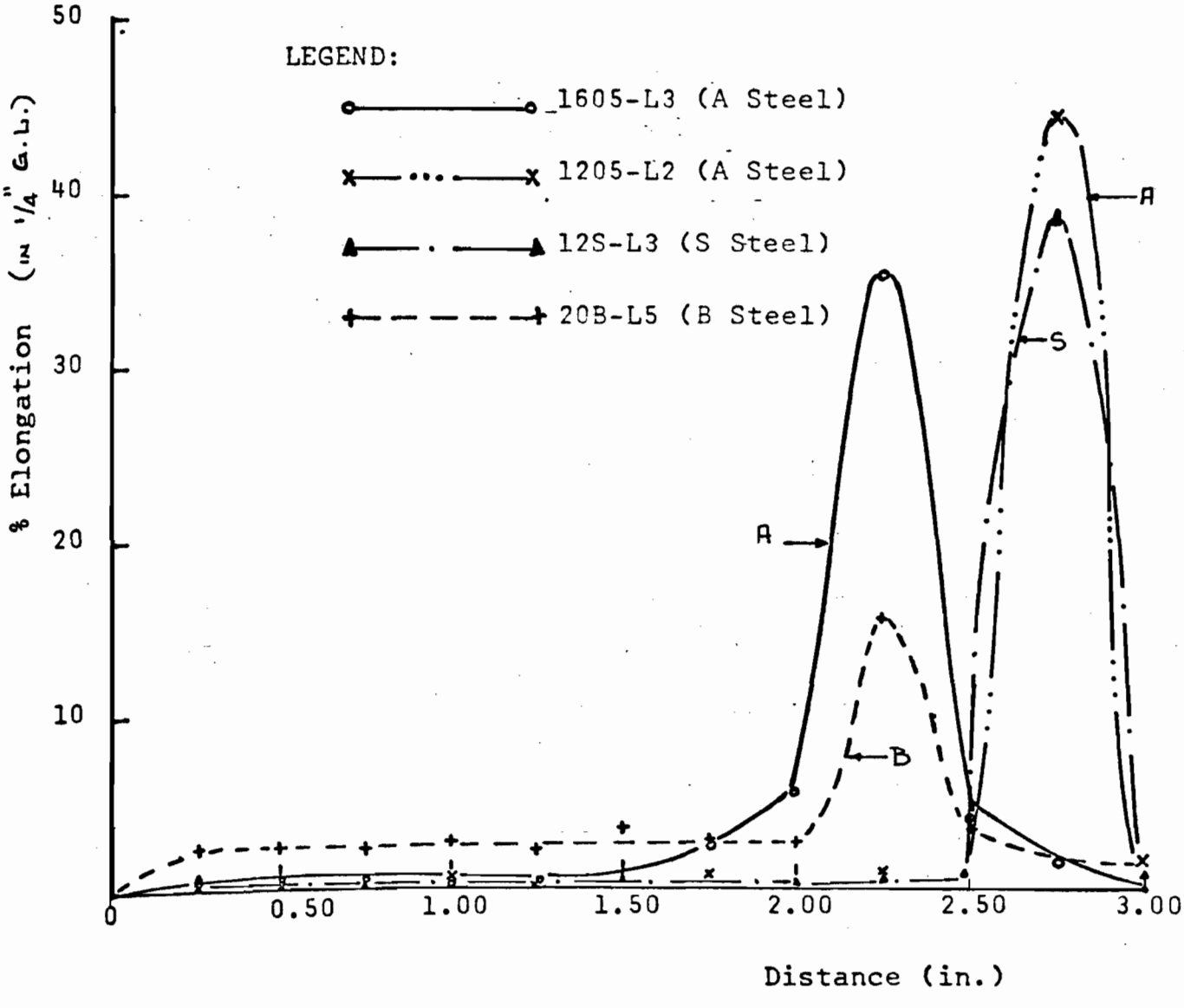

FIG. 2b. DISTRIBUTION OF LONGITUDINAL STRAIN IN TENSION COUPON (after fracture)

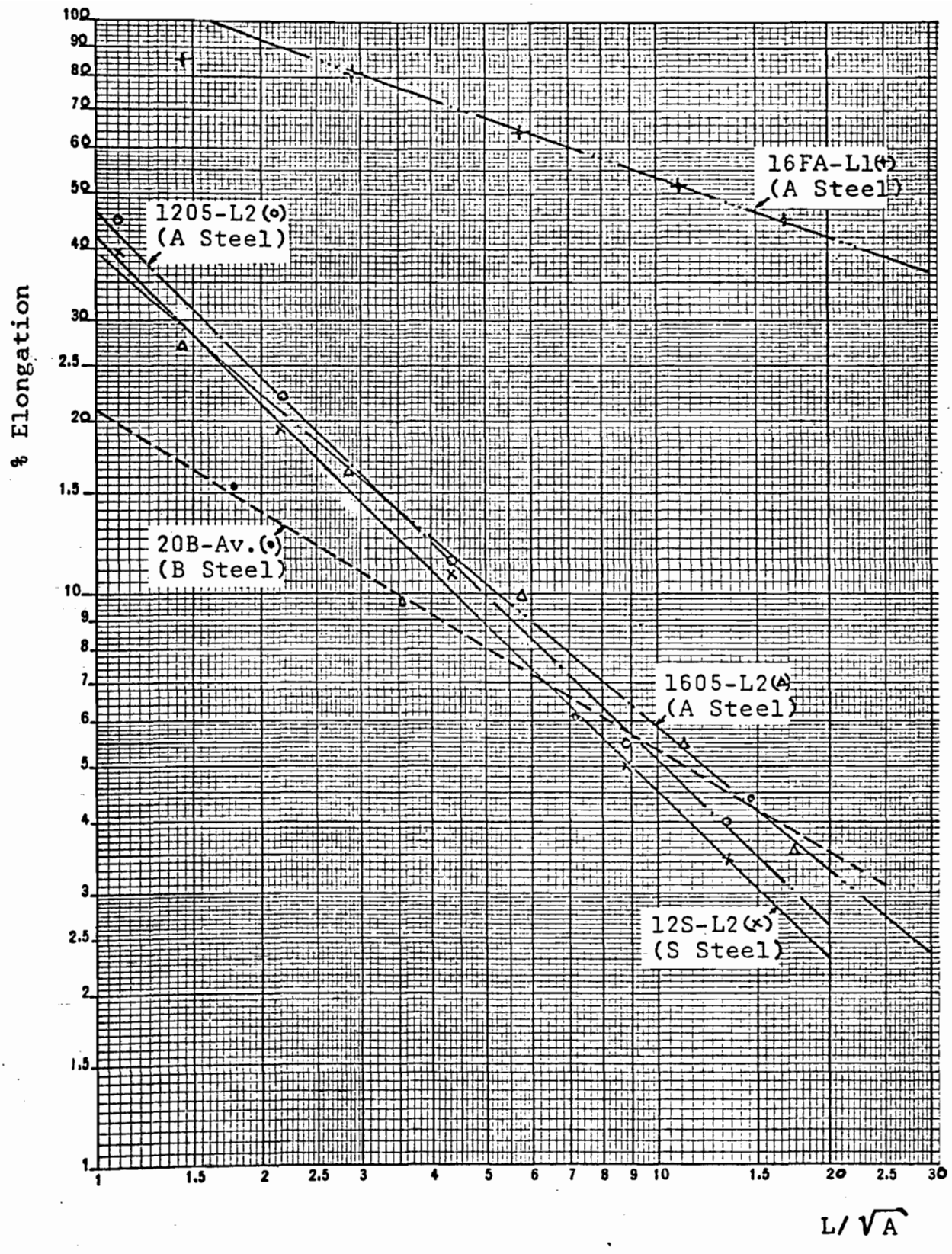

FIG. 3. LOGARITHMIC RELATIONSHIP BETWEEN ELONGATION AND $L/\sqrt{A}$ FOR A, S AND B STEEL

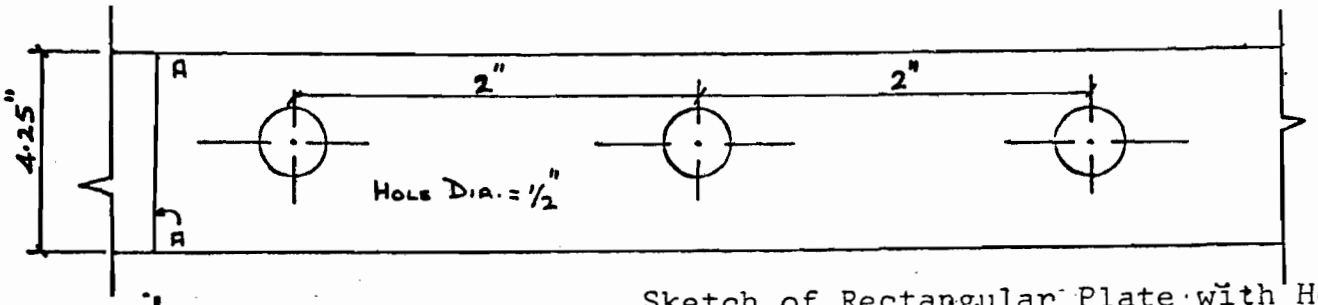

Sketch of Rectangular Plate with Holes

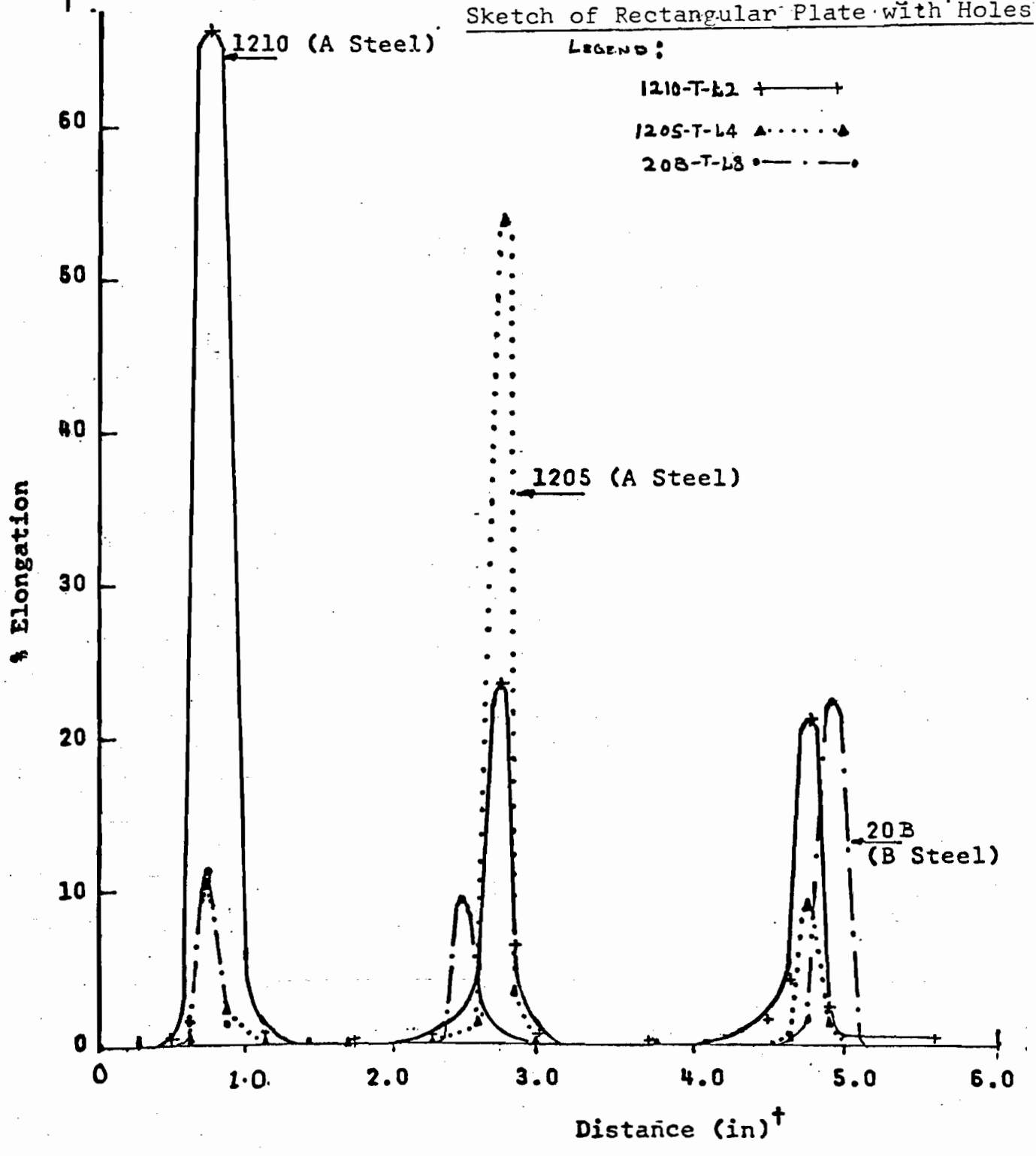

FIG 4 LONGITUDINAL STRAIN DISTRIBUTION (AFTER FRACTURE) IN RECTANGULAR PLATE WITH HOLES

†Distance measured from Line A-A (See Sketch Above)

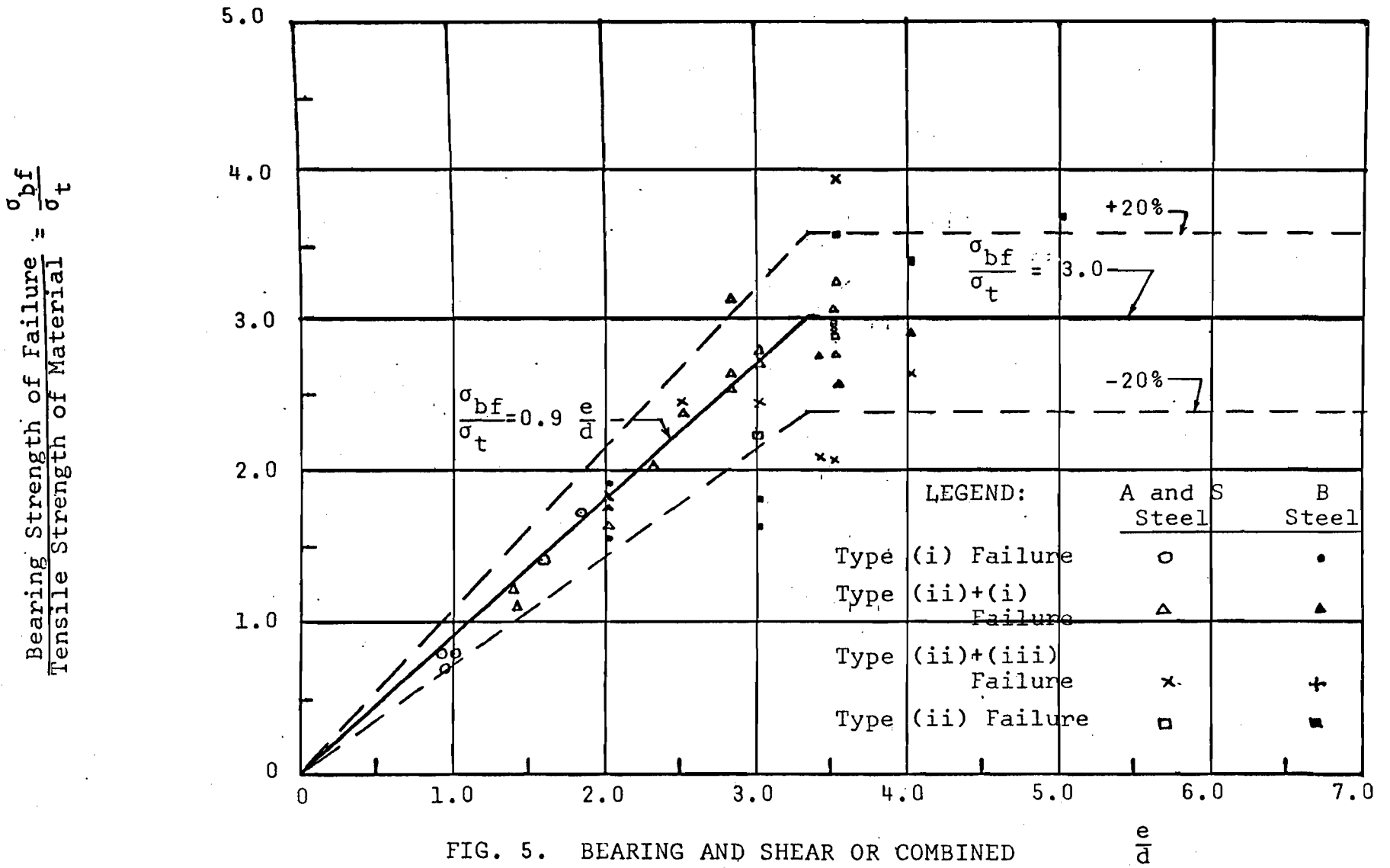

FIG. 5. BEARING AND SHEAR OR COMBINED FAILURES (LOW DUCTILITY STEEL)

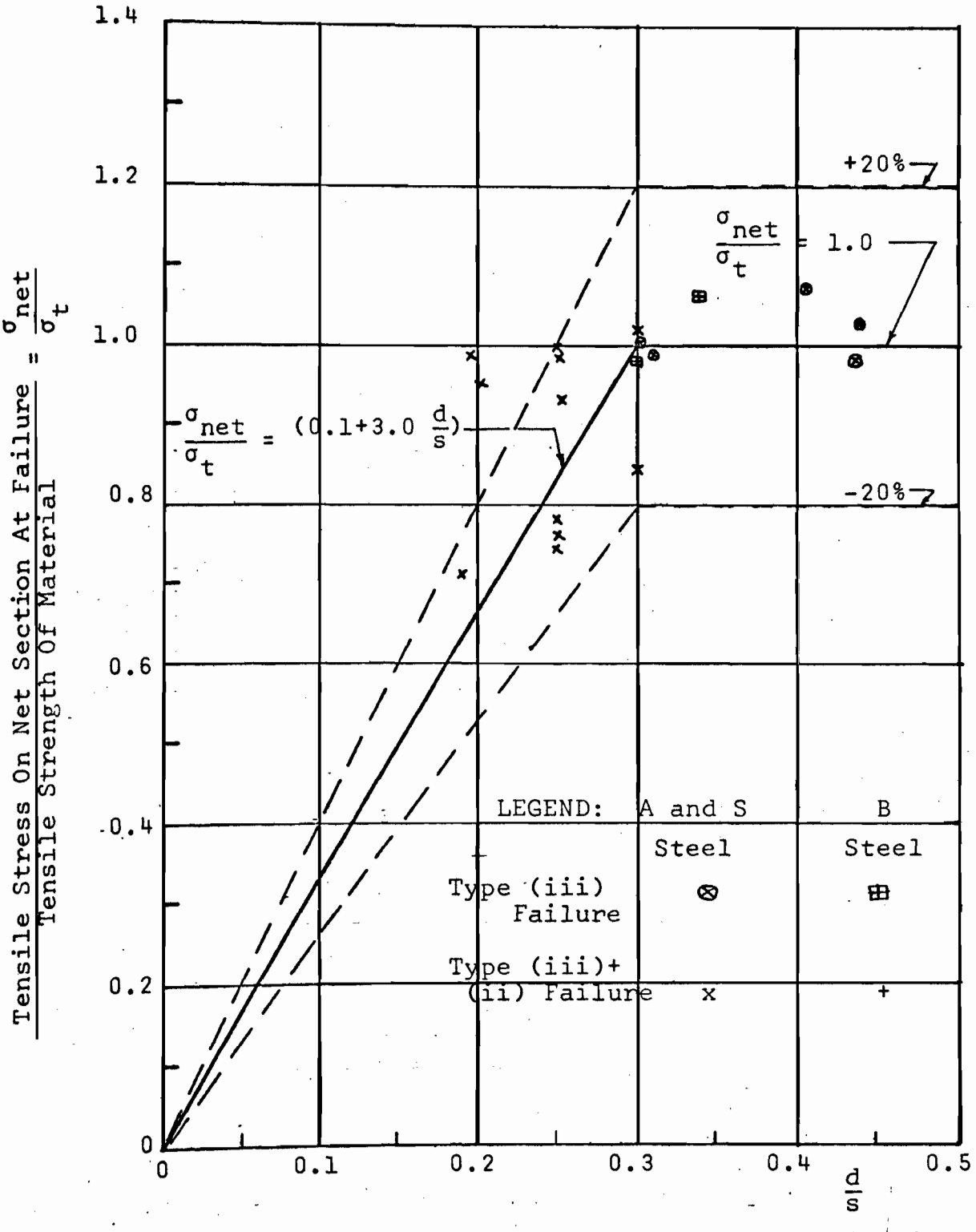

FIG. 6. TRANSVERSE TEARING OR COMBINATION OF BEARING AND TENSION FAILURES (LOW DUCTILITY STEEL)

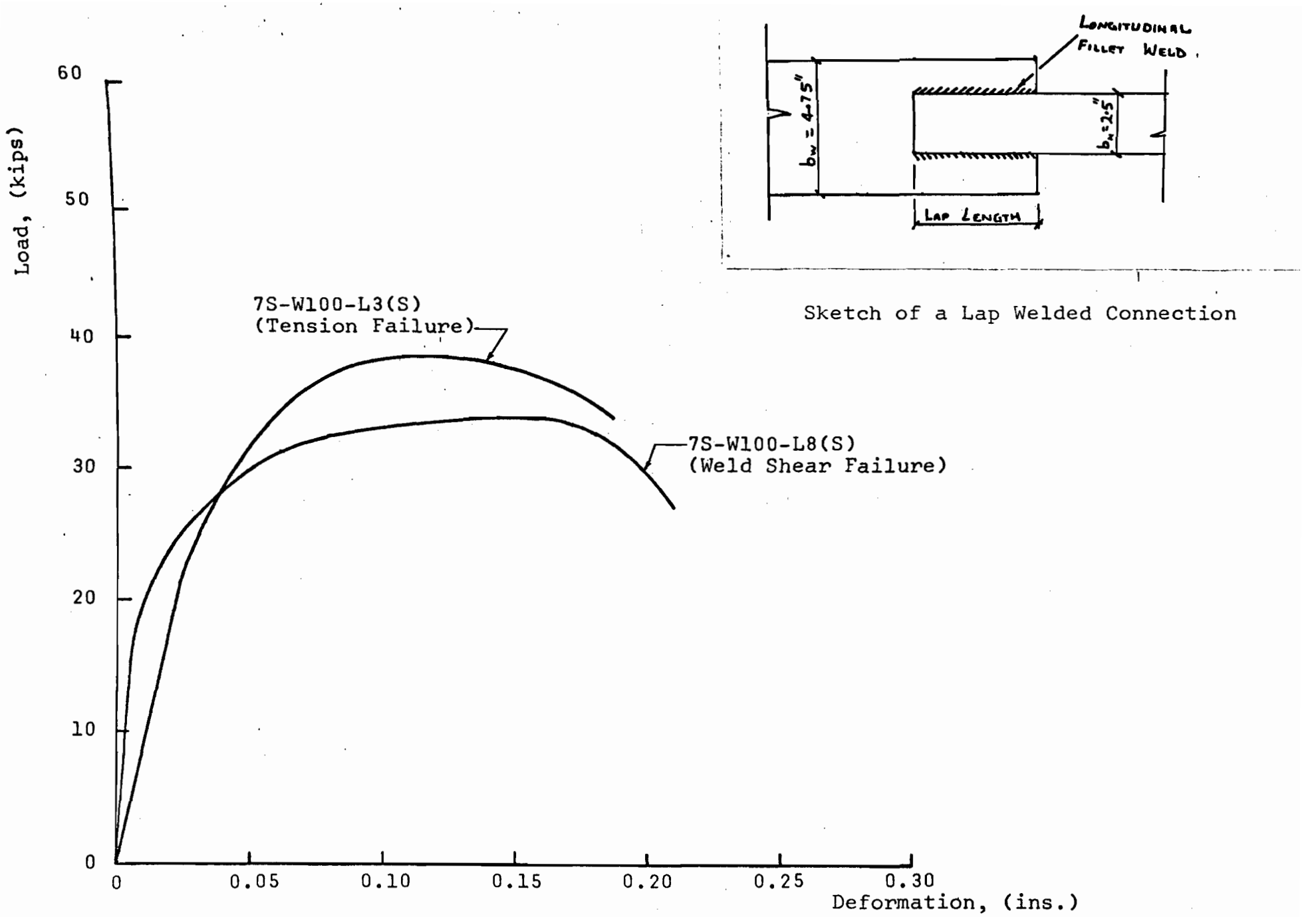

Sketch of a Lap Welded Connection

FIG. 7. LOAD-DEFORMATION CURVES OF LONGITUDINAL FILLET WELDED SPECIMENS

October 3, 1969

To: Members Technical Committee On Structural Research and Design Specifications

From; G. Winter

Enclosed please find an informal fairly detailed summary of our entire research to date on Influence of Ductility. This summary has been prepared for the meeting in Bethlehem October 10 of our research staff (Dr. Errera, myself and Mr. Dhalla) with Al Oudeusden and members of the Bethlehem staff knowledgeable in these matters.

It is believed that distribution of this summary to members of the Technical Committee will be informative to them and will enhance discussion of this area at Chicago.

Sincerely,

George Winter
1912 Professor of Engineering
Chairman, Dept. of Structural Engineering

Enclosure

cc: W.G. Kirkland

October 2, 1969

To: G. Winter

From: A. K. Dhalla and S. J. Errera

Subject: Influence of Ductility on the Structural Behavior of Cold-Formed Steel Members

Summary of Investigation and

Plans for Immediate Future

Table of Contents

1. Introduction 1
2. Material Properties 1
3. Rectangular Plates with Holes 4
4. Single Bolted Connection Tests 5
5. Longitudinal Fillet-Welded Connections 6
6. Finite Element Analysis 8

References 10

List of Tables:

1. Comparative Study of Ductility Characteristics of A, B, and S Steel
2. Typical Results of Tension Tests on Rectangular Plate with Holes
3. Results of Longitudinal Lap Welded Connection Tests

List of Figures:

1. Complete Stress Strain Curves of A, B, and S Steel
2. Distribution of Longitudinal Strain in Tension Coupon
3. Logarithmic Relationship Between Elongation and $L/\sqrt{A}$ for A, S and B Steel.
4. Longitudinal Strain Distribution After Fracture in Rectangular Plate with Holes.
5. Bearing and Shear or Combined Failures (Low Ductility Steel).
6. Transverse Tearing or Combination of Bearing and Tension Failure (Low Ductility Steel).
7. Load-Deformation Curve of Longitudinal Fillet Welded Specimens.

1. Introduction

In order to determine the "suitability of steel"[1] for cold-formed construction one needs to know, in addition to other mechanical properties of the material, performance characteristics such as ductility, formability and weldability. Ductility is the ability of a material to undergo large plastic deformations without fracture. It reduces the harmful effect of stress concentrations, permits large local strains without serious damage, and helps achieve uniform stress or load distribution in connections.

There are different tests specified by ASTM to measure ductility, the chief of them being the percent elongation after fracture in a specified gage length, usually 2" or 8". The minimum acceptable for structural use, according to ASTM standards, varies a great deal. Two of the low ductility steels used in this investigation were specially rolled and made available by the manufacturers. These are designated as A and S steels, and had between 5 and 10 percent elongation in 2" gage length, well below the "ductility" required by ASTM for structural steels in general use in load carrying members. The third steel investigated to date is a 20 gage commercial low ductility steel, ASTM A-446 Grade E, herein designated as Steel B, with a specified minimum elongation of 1.5% in 2". Grade E steel is used primarily for cold formed panels.

2. Material Properties

The parameters which can be used to define the ductility

of steel were discussed in the Second Progress Report. These include elongation in 2", reduction in area, tensile-yield strength ratio, elongation in 1/4", and elongation in some gage length which excludes the fracture zone. These parameters were measured from standard tension tests wherein the coupons were prepared and tested in accordance with ASTM Specification E8-65T. The A and S steel coupon test results were presented in the first and second progress reports. B steel coupons were tested subsequently.

Typical complete stress-strain curves for 12 and 16 gage A steel, 12 gage S steel and 20 gage B steel are shown in Fig. 1. An important fact indicated by the figure is that B steel has a strain hardening range while the other two steels do not. The B steel shows about 4% elongation in 2", which is considerably more than the 1.5% required by ASTM for the A-446 Grade E. Fig. 2 shows the distribution of longitudinal strains in typical coupons of each of the steels.

In the earlier tests of A and S steels it was observed that though the elongation in 2" G.L. was around 5 to 8 percent, the elongation in 1/4" G.L. was around 30 to 45 percent. Hence the measure of ductility was separated into two parts; one was designated as local ductility and the other as overall ductility. The total percentage strain is given by the following equation[2]:

$$e = K \left(\frac{L}{\sqrt{A}}\right)^{\alpha} \qquad (1)$$

where e = the percent elongation in gage length L

A = cross sectional area of the specimen

K and α = constants related to local and overall ductility, respectively

One advantage of the above relationship is that the constants K and α are independent of the size and shape of the test specimen used.

Table 1 presents ductility parameters obtained from representative standard tension coupon tests of A, S and B steels, wherein percent reduction of area, percent elongation in 1/4" G.L. and K are indicators of local ductility of the material, while tensile-to-yield ratio, percent elongation in 2 1/2" G.L. excluding neck, and α are indicators of overall ductility of the material. Higher algebraic values indicate greater ductility in all cases. Comparison of the algebraic values given in Table 1 indicates that A and S steels have more local ductility and less overall ductility than that obtained in B steel.

Fig. 3 is a graph of Eq. 1 for each of the steels using the values of K and α from Table 1, and includes also the results for full annealed A steel taken from the Second Progress Report. In Fig. 3 higher values of the intercept on the elongation axis indicate greater local ductility, and flatter slopes indicate greater overall ductility. Table 1 and Figs. 2 and 3 all indicate that B steel has less local ductility than the low ductility A or S steels; but B steel has greater overall ductility.

The overall ductility of B steel is a consequence of its strain-hardenability. This permits sufficient strain hardening at that portion or portions of the member at which localized first yielding begins, so that yielding spreads to other portions of the specimen rather than causing necking at the location of initial yielding.

3. Rectangular Plates with Holes

Tests of rectangular plates of A, S and B steel with one or more holes in line of stress showed that these plates developed their full tensile strength as calculated on the net cross sectional area; that is

$$\frac{\sigma_{tt}}{\sigma_t} \geq 1 \qquad (2)$$

where σ_{tt} = tensile stress calculated on the net area at fracture

σ_t = tensile strength of coupon in uniaxial tension

Typical results are given in Table 2. The local ductility determined from tests of plates with holes compares reasonably well with the local ductility measured in the coupon tests. For A steel the average elongation in 1/4" G.L. at the hole in the plate was approximately 32 percent, while that of the tension coupon was 48 percent. For B steel elongation in 1/4" G.L. in the tension coupon was 15.5 percent, while at the hole in the rectangular plate it was 12.9 percent. Fig. 4 shows the longitudinal strain distribution for plates of A and B steel with three holes in line of stress. The greater local ductility of the A steel is again evident.

The above tests indicate that the effects of the elastic stress concentration produced by a hole are eventually wiped out due to the good local ductility of these "low ductility" steels.

4. Single Bolted Connection Tests

Single bolted connection tests were conducted using each of the project steels. The experimental set up and the presentation of results are similar to those given by Winter[3] in an earlier paper. The types of failure and form of the prediction equations also are similar to those obtained from Winter's tests which were performed on high ductility steels.

Variables considered in the program in addition to the type of steel used were: edge distance e, bolt diameter d, sheet thickness t, plate width s, and coupon tensile strength σ_t. The connection failures are divided into three main types:

(i) Longitudinal shearing of the plate along two practically parallel planes whose distance is equal to the bolt diameter

(ii) Bearing failure with considerable elongation of the hole and material "piling up" in front of the bolt

(iii) Transverse tension-tearing across the plate

Test results for the low ductility steels are presented in Fig. 5 for bearing, shear and combined failures, and in Fig. 6 for tension and combined failures. The failure loads can be represented by the following equations:

$$P_{shear} = P_{sh} = 0.9\ e\ \sigma_t\ t \tag{4}$$

$$P_{bearing} = P_b = 3.0\ \sigma_t\ dt \tag{5}$$

$$P_{tension} = P_t = (0.1 + 3\ \frac{d}{s})\ \sigma_t\ A_{net} \leq \sigma_t\ A_{net} \tag{6}$$

where A_{net} = net cross sectional area of the plate through center of the hole

σ_t = tensile strength of the material as obtained from the coupon test

One of the main differences in the behavior of Winter's tests and the current ones is that the bearing strength of the low ductility material is a lower multiple of σ_t (by about 20%) than previously obtained for high ductility connection specimens. On the other hand, the expression for tension failure of connections of low ductility steel is identical to Winter's expression for high ductility steels. Tests of three-bolt in-line connections with low ductility steel gave similar results[4]

Dimensional analysis has been used in an attempt to refine the strength prediction of bolted connections under mixed modes of failure; this study is continuing.

5. Longitudinal Fillet-Welded Connections

Tests of longitudinal fillet welded connections using A and S steel have been conducted. Variables considered in the program were: lap length L, thickness of material t, and type of steel. The connections were designed to fall into three groups. Group I specimens were designed to develop the full strength of the connected plate. Group II specimens

were designed such that failure would occur by shearing of the weld. For Group III specimens the weld length was so designed that whether failure would occur in the weld or in the plate could not be predicted with assurance.

The main parameters and test results are summarized in Table 3, and load-deformation curves for two of the welded connections are shown in Fig. 7. Failures are described as Type a (tension) or Type b (weld shear) or a combination of a and b. Conclusions may be summarized as follows:

1. Comparison of σ_{tt}/σ_t for connections that failed in tension shows that a longitudinal fillet welded connection in low ductility steel can be designed to develop the full strength of the plate.

2. A and S steels are "weldable" in the sense that no noticeable defects in the weld of the specimen were observed.

3. When the lap length of the connection is not long enough to develop the full strength of the plate then failure occurs by shearing of the weld. In this case the weld is capable of developing its full shear strength corresponding to the tensile strength as specified by ASTM specifications.

4. The behavior of a low ductility steel specimen is easier to predict than that of the high ductility one, because very little out of plane distortion occurs in low ductility steel specimens. On the other hand in high ductility specimens, where there is a considerable spread between yield and tensile strength, in and out of plane distortions are considerable.

5. In these connections no annealing effects from weld heat were detected; that is, all strength properties were predictable from materials properties before welding.

These conclusions refer to A and S steels. Tests on welded connections of low ductility B-steel will be carried out shortly; the small thickness of the available B-steel may make for difficulties in this respect.

6. Finite Element Analysis

The finite element approach can be used to solve continuum mechanics problems in the plastic range. A solution will be sought for a rectangular plate under tension with a central hole or other stress concentration using stress-strain characteristics of a low ductility steel. By solution one means that the strain state in the plastic and elastic region is calculated for the specimen under consideration, and the extent of the plastic zone around the hole is established for successively increasing loads. The analysis should show whether the effect of a stress raiser is wiped out, i.e. whether the cross-section at the hole completely plastifies. If so, the strength of the tension member is essentially unaffected by the stress concentration and the ductility is adequate. To establish a lower bound on the required local ductility of the material, one calculates the plastic strain at the hole when the element at the edge of the plate just enters the plastic region.

This situation will also be investigated by experimental means using the same geometry of rectangular plate with a

central hole. Two 1/4" foil strain gages can be attached (in the longitudinal direction); one at the hole and the other at the edge. When the gage at the edge of the plate enters the plastic region, the reading of the gage at the hole is the minimum local ductility required for the given material.

The same type of investigation can be carried out for other types of stress concentration.

References

(1) Light Gage Cold Formed Design Manual, American Iron and Steel Institute, 1962 Edition.

(2) Oliver, D. A.; "Proposed New Criteria of Ductility From a New Law Connecting the Percentage Elongation with Size of Test Piece", Inst. of Mech. Engineers, Vol. II, 1928.

(3) Winter, G.; "Tests on Bolted Connections in Light Gage Steel". Proc. ASCE, Vol. 82, Paper No. 920, March 1956.

(4) Popowich, D. W.; "Three-Bolt In-Line Connections with Low Ductility Light-Gage Steel". Report 2, Cornell University, Ithaca, N.Y., February 1969.

(5) Dhalla, A. K., and Errera, S. J.; "Influence of Ductility on the Structural Behavior of Light-Gage Cold-Formed Steel Members", First Progress Report, Cornell University, Ithaca, N.Y., Feb. 1968.

(6) Dhalla, A. K.; "Influence of Ductility on the Structural Behavior of Light-Gage Cold-Formed Steel Members", Second Progress Report, Cornell University, Ithaca, N.Y., Oct. 1968.

TABLE 1

Comparative Study of Ductility Characteristics of A, B and S Steels

Ductility Parameters	20B-Av. B-Steel	12S-L3 S-Steel *	1205-L2 A-Steel *	1605-L3 A-Steel *	16FA-L1 A-Annealed-Steel *
Elongation in 2", (%)	4.38	5.13	5.58	6.84	52.20
Reduction in area (%)	56.10	65.20	69.40	59.00	83.80
Tensile/Yield Ratio	1.08	1.01	1.00	1.00	1.48
Elongation in 1/4" (including neck)(%)	15.55	38.40	44.40	35.20	85.60
Elongation in 2 1/2" (excluding neck) (%)	2.74±	0.33	0.40	1.28	38.00
K	20.50	45.00	46.00	45.00	120.00
α	-0.579	-0.974	-0.983	-0.795	-0.335

Note: * The values reported in these columns are taken from Table 7 of Second Progress Report.

± This value is for % elongation in 2", excluding neck.

TABLE 3

Results of Longitudinal Lap Welded Connection Tests

(A, S and B Steels)

Spec. Designation	SPEC. GEOM. Width of Plate b_n (in)	SPEC. GEOM. Lap Length L (in)	MAT'L PROPERTY Tensile Stress σ_t (ksi)	MAT'L PROPERTY Electrode Tensile Stress σ_{ta} (ksi)	EXPERIMENTAL RESULTS Ult. Load P_{ult} (kips)	Ult. Tensile Stress in Plate σ_{tt} (ksi)	Ult. Tensile Stress in Weld σ_{tu} (ksi)	Mode of Failure (type)	$\frac{\sigma_{tt}}{\sigma_t}$	$\frac{\sigma_{tu}}{\sigma_{ta}}$
7S-W70-L1	2.50	3.00	83.3	70.0	37.25	81.5	83.1	b	0.98	1.18
7S-W70-L2	2.50	5.00	83.3	70.0	38.90	85.0	52.5	a	1.02	0.75
7S-W100-L3	2.50	3.25	83.3	100.0	38.30	83.7	78.6	a	1.00	0.78
12S-W100-L4	3.00	3.25	82.5	100.0	24.90	78.8	88.4	a	0.96	0.88
1205-W100-L5	3.00	3.25	84.1	100.0	25.80	79.0	89.4	a	0.94	0.89
1605-W100-L6	3.00	3.75	98.0	100.0	16.60	87.8	86.8	a	0.89	0.87
12FA-W70-L7	4.00	3.75	45.0	70.0	16.80	39.9	51.0	a	0.88	0.73
7S-W100-L8	2.50	2.25	83.3	100.0	33.80	73.8	100.8	b	0.88	1.01
12S-W100-L9	3.00	2.25	82.5	100.0	19.40	60.8	99.5	b	0.74	0.99
1205-W100-L10	3.00	2.25	84.1	100.0	16.40	50.2	82.5	b	0.60	0.82
1605-W100-L11	3.00	2.75	98.0	100.0	14.30	75.7	101.8	b	0.77	1.02
12FA-W70-L12	4.00	1.50	44.6	70.0	9.80	22.7	74.0	a+b	0.51	1.05
7S-W100-L13	2.50	2.75	83.3	100.0	37.50	82.0	91.2	a	0.98	0.91
12S-W100-L14	3.00	2.75	82.5	100.0	22.25	70.0	93.6	b	0.85	0.94
1205-W100-L15	3.00	2.75	84.1	100.0	23.80	70.5	98.0	b	0.84	0.98
1605-W100-L16	3.00	3.25	98.0	100.0	16.20	85.7	97.5	b	0.87	0.97
12FA-W70-L17	4.00	2.00	44.6	70.0	11.80	28.2	66.6	a	0.63	0.95

TABLE 2

Typical Results of Tension Tests on Rectangular Plates With Holes

(A, S and B Steels)

Spec. Designation	GEORMETRICAL DIMENSIONS				MAT'L PROPERTIES		EXPERIMENTAL RESULTS				
	Dia. of Hole	Width of Plate	$\frac{d}{s}$	No. of Holes	σ_t	Elong. in 1/4" G.L.	P_{ult}	$\frac{P_{ult}}{A_{net}} = \sigma_{tt}$	Elong. in 1/4" G.L.	$\frac{\sigma_{tt}}{\sigma_t}$	Total Member Deformation
	(in)	(in)			(ksi)	(%)	(kips)	(ksi)	%		(in)
12S-T-L2	9/16	2.50	0.225	one	72.8	44.0	14.50	71.4		0.98	
7S-T-T3	9/16	1.25	0.500	one	91.0	47.0	11.40	91.1		1.00	
1210-T-L2	1/2	4.25	0.118	Three	74.6	49.0	30.70	75.5	37.2	1.01	0.19
1205-T-L4	1/2	4.25	0.118	Three	72.2	47.0	32.20	79.4	28.6	1.10	0.11
20-B-L8	1/2	4.25	0.118	Three	81.7	15.5	12.80	90.0	12.9	1.10	0.06
					σ_y σ_t		P_y P_{ult}	σ_{ty} σ_{tt}			
12FA-T-L12	1/2	4.25	0.118	one	27.4 43.9	72.3	11.0 17.0	27.4 42.4		0.96	

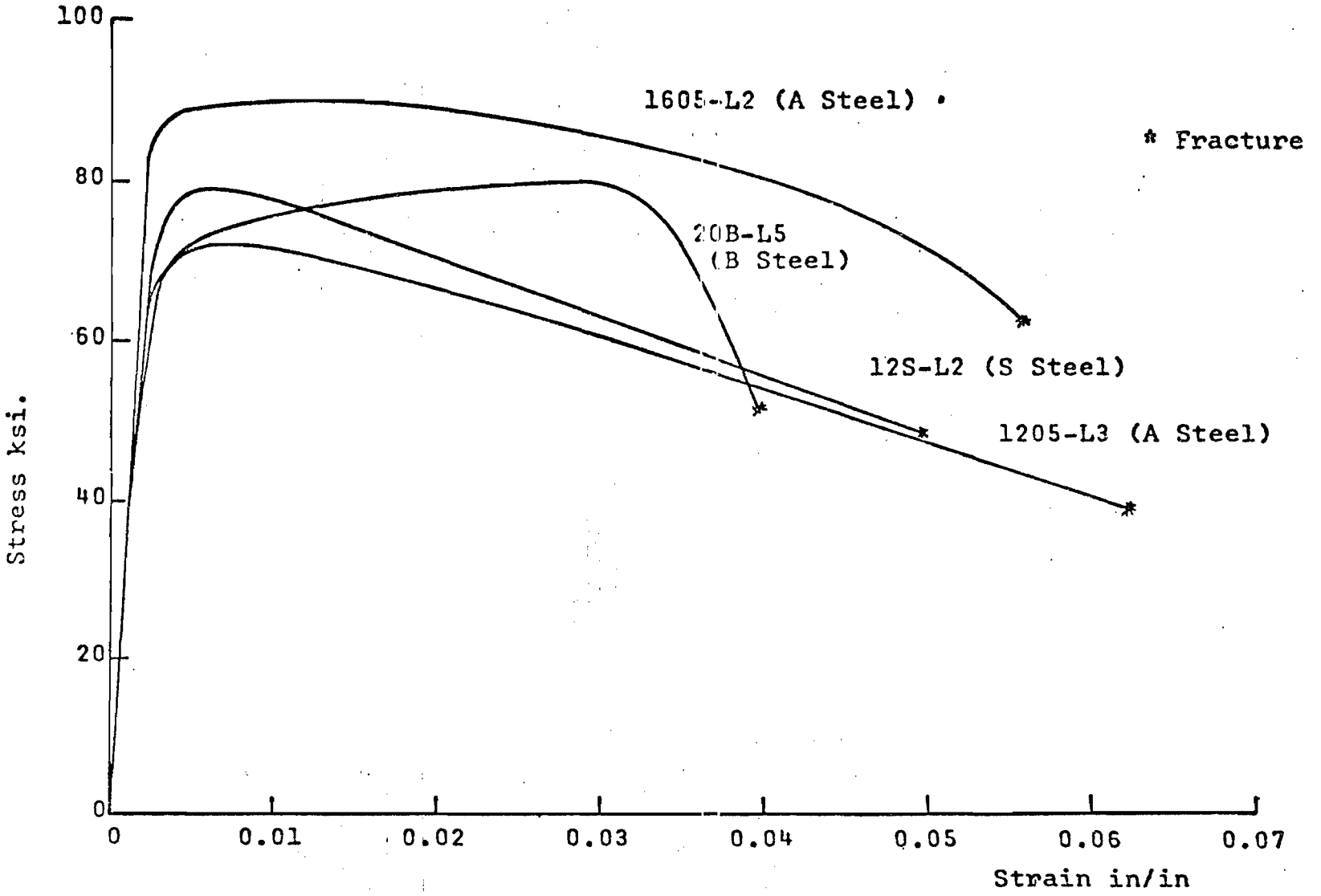

FIG. 1 COMPLETE STRESS STRAIN CURVES OF A, S AND B STEEL.

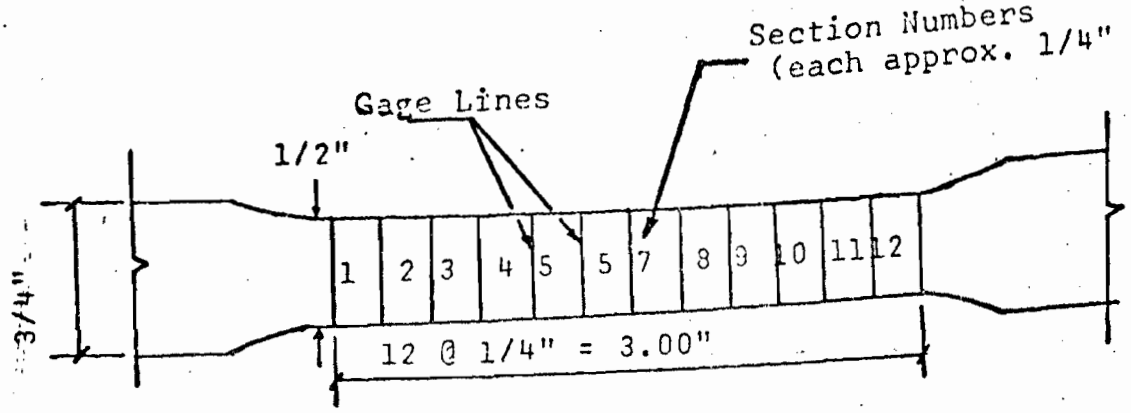

FIG. 2a. SKETCH OF A STANDARD TENSION COUPON

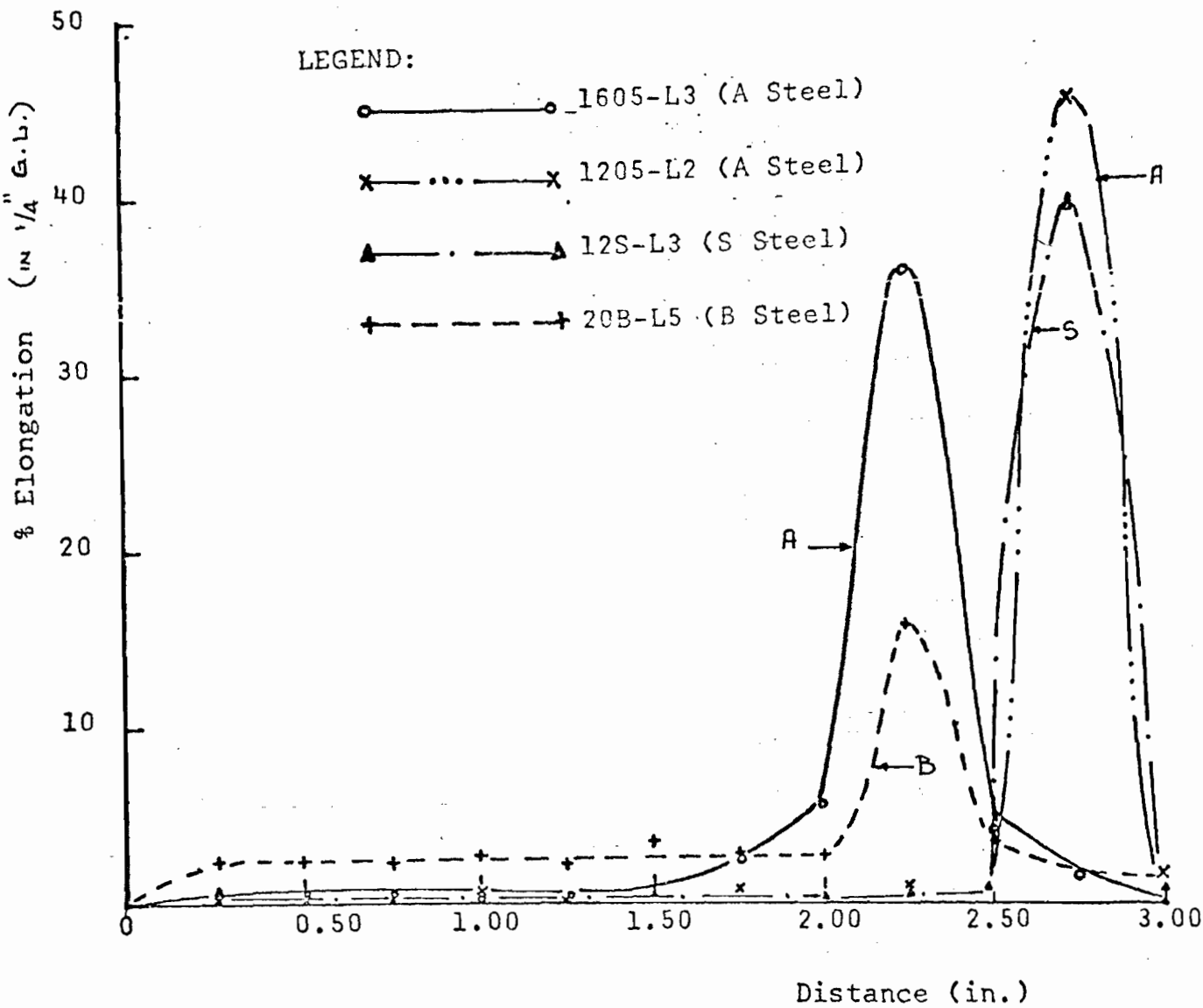

FIG. 2b. DISTRIBUTION OF LONGITUDINAL STRAIN IN TENSION COUPON (after fracture)

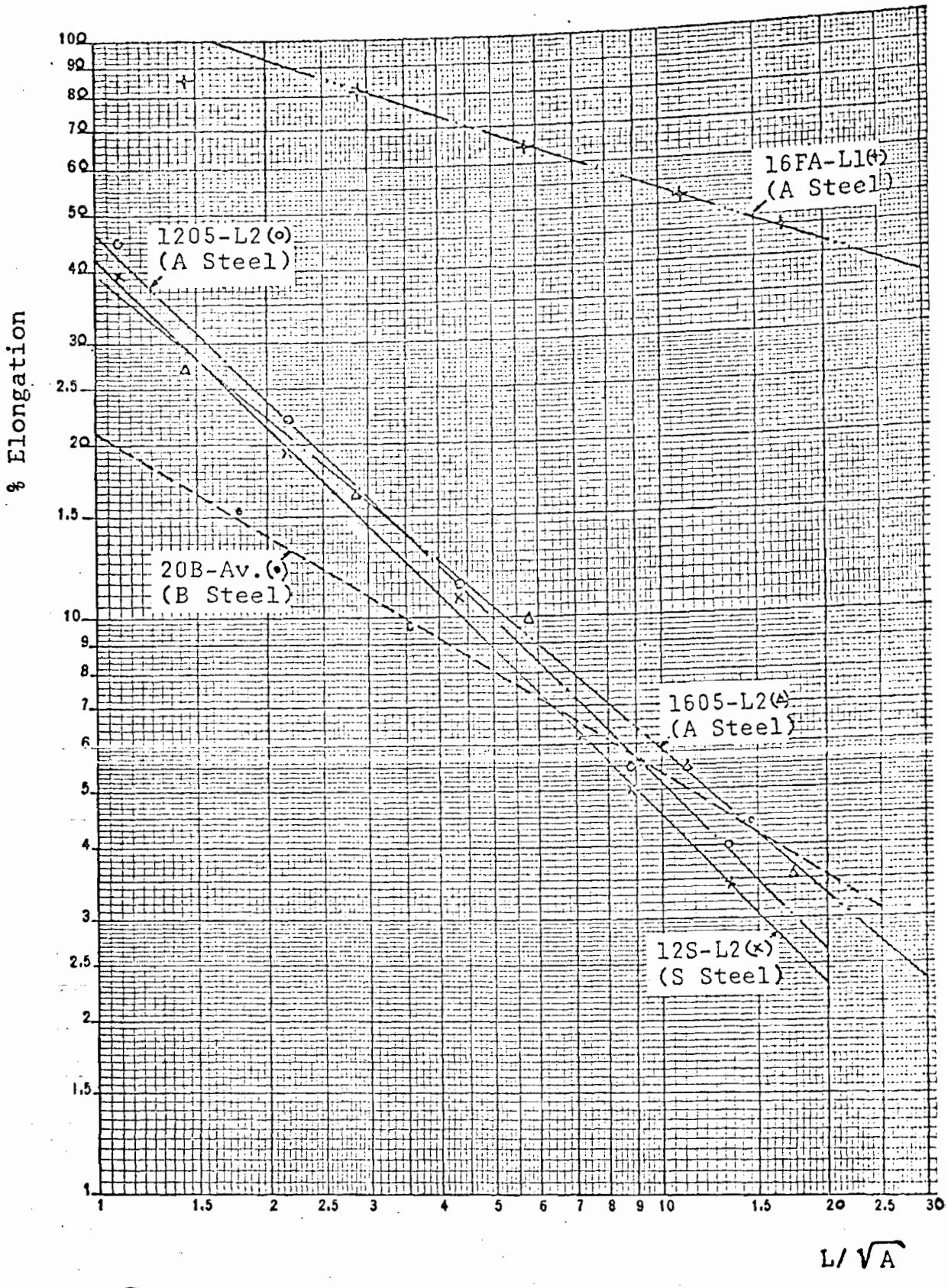

FIG. 3. LOGARITHMIC RELATIONSHIP BETWEEN ELONGATION AND $L/\sqrt{A}$ FOR A, S AND B STEEL

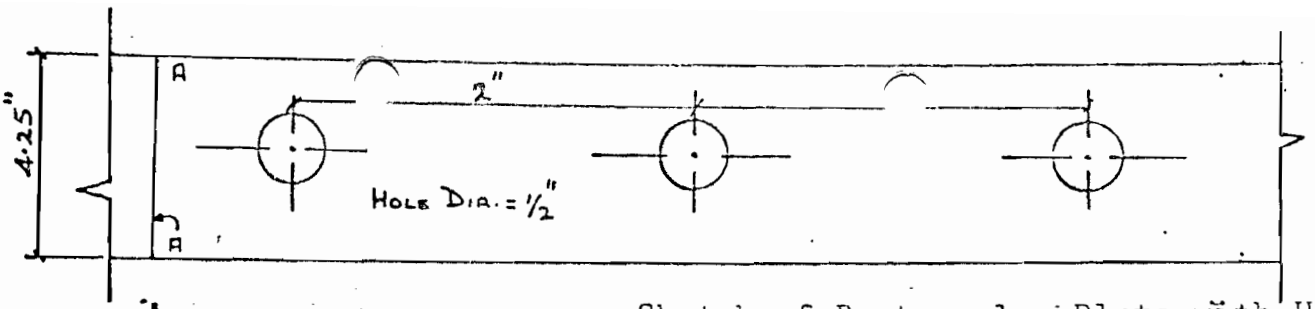

Sketch of Rectangular Plate with Holes

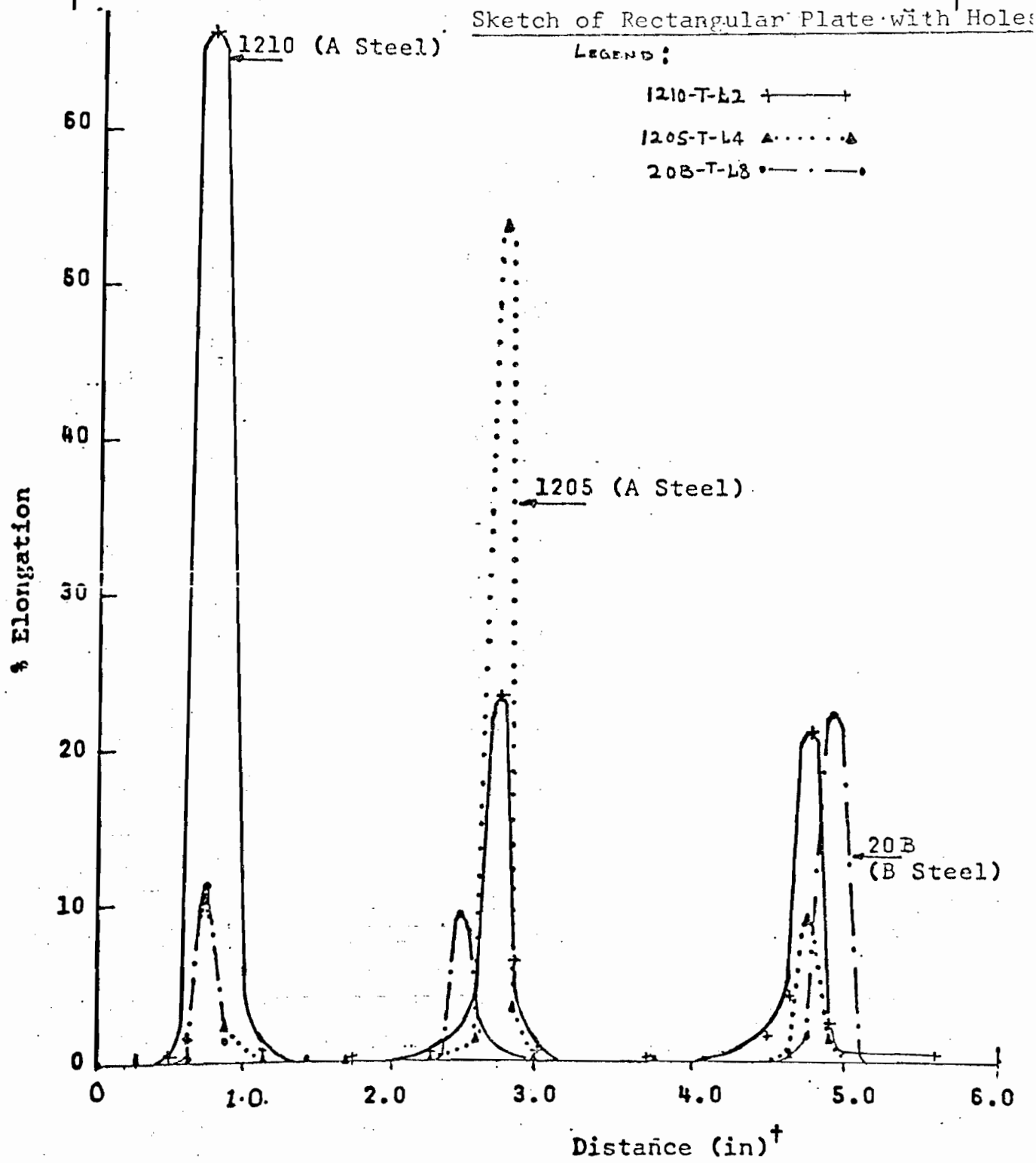

FIG 4 LONGITUDINAL STRAIN DISTRIBUTION (AFTER FRACTURE) IN RECTANGULAR PLATE WITH HOLES

†Distance measured from Line A-A (See Sketch Above)

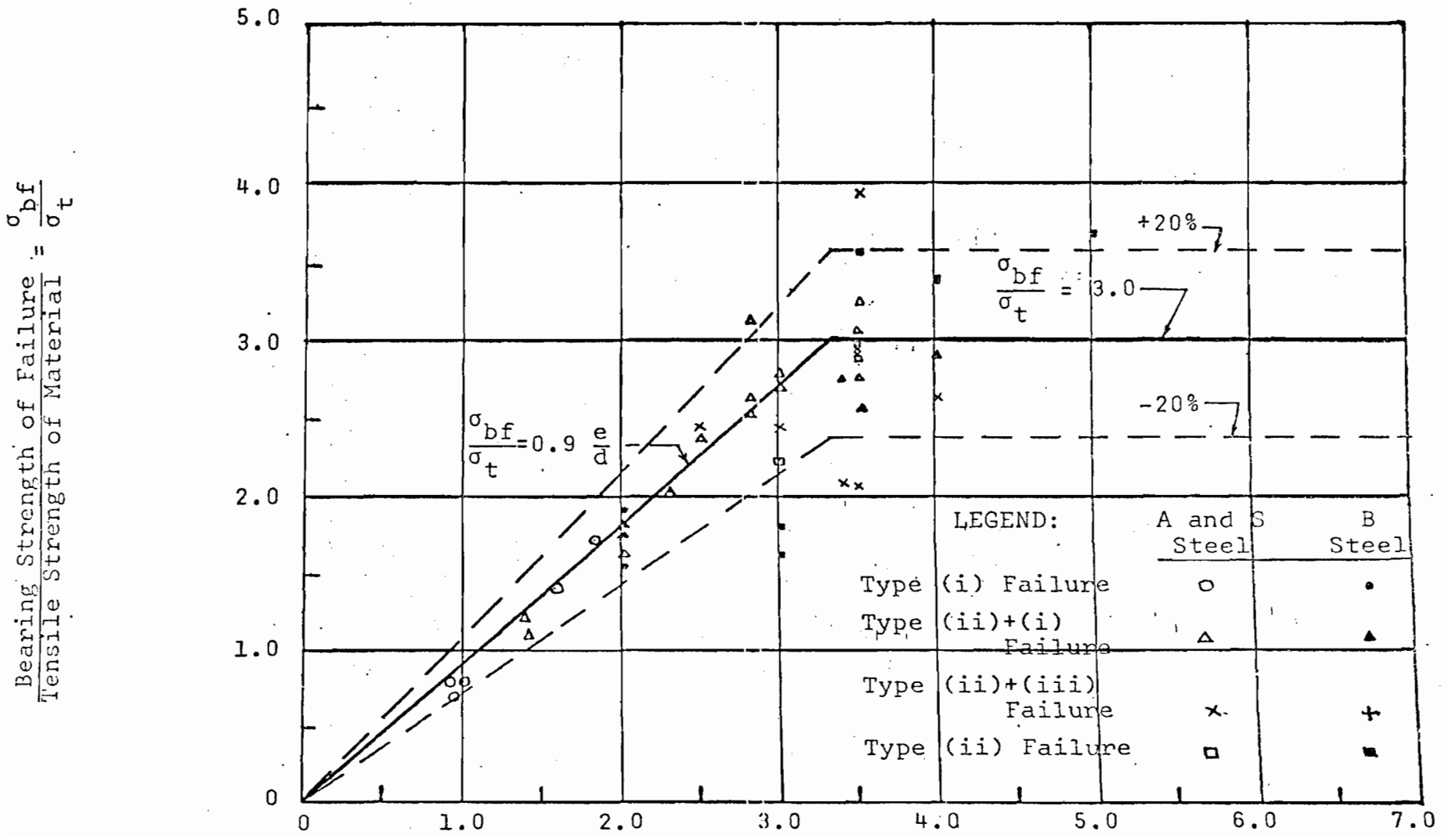

FIG. 5. BEARING AND SHEAR OR COMBINED FAILURES (LOW DUCTILITY STEEL)

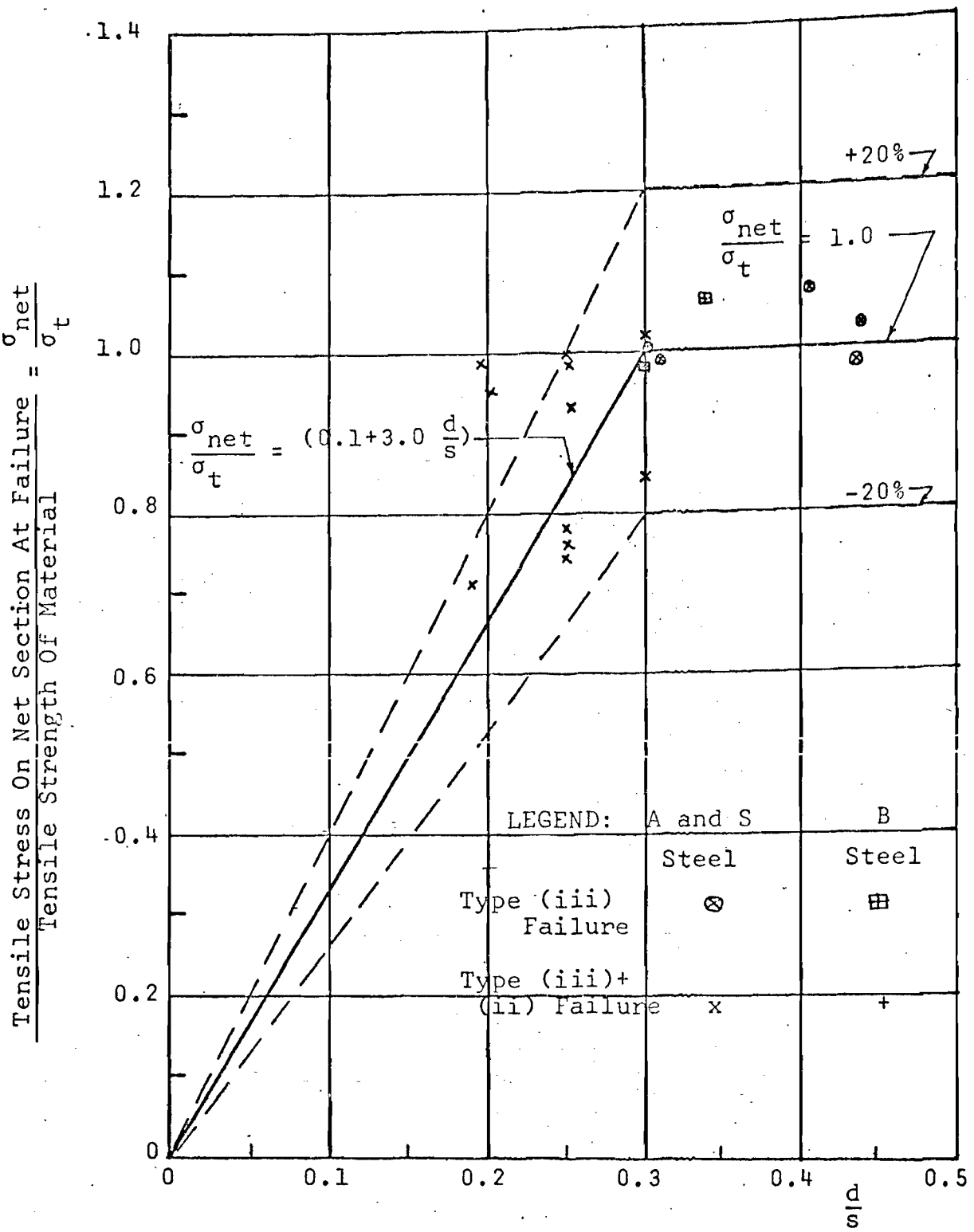

FIG. 6. TRANSVERSE TEARING OR COMBINATION OF BEARING AND TENSION FAILURES (LOW DUCTILITY STEEL)

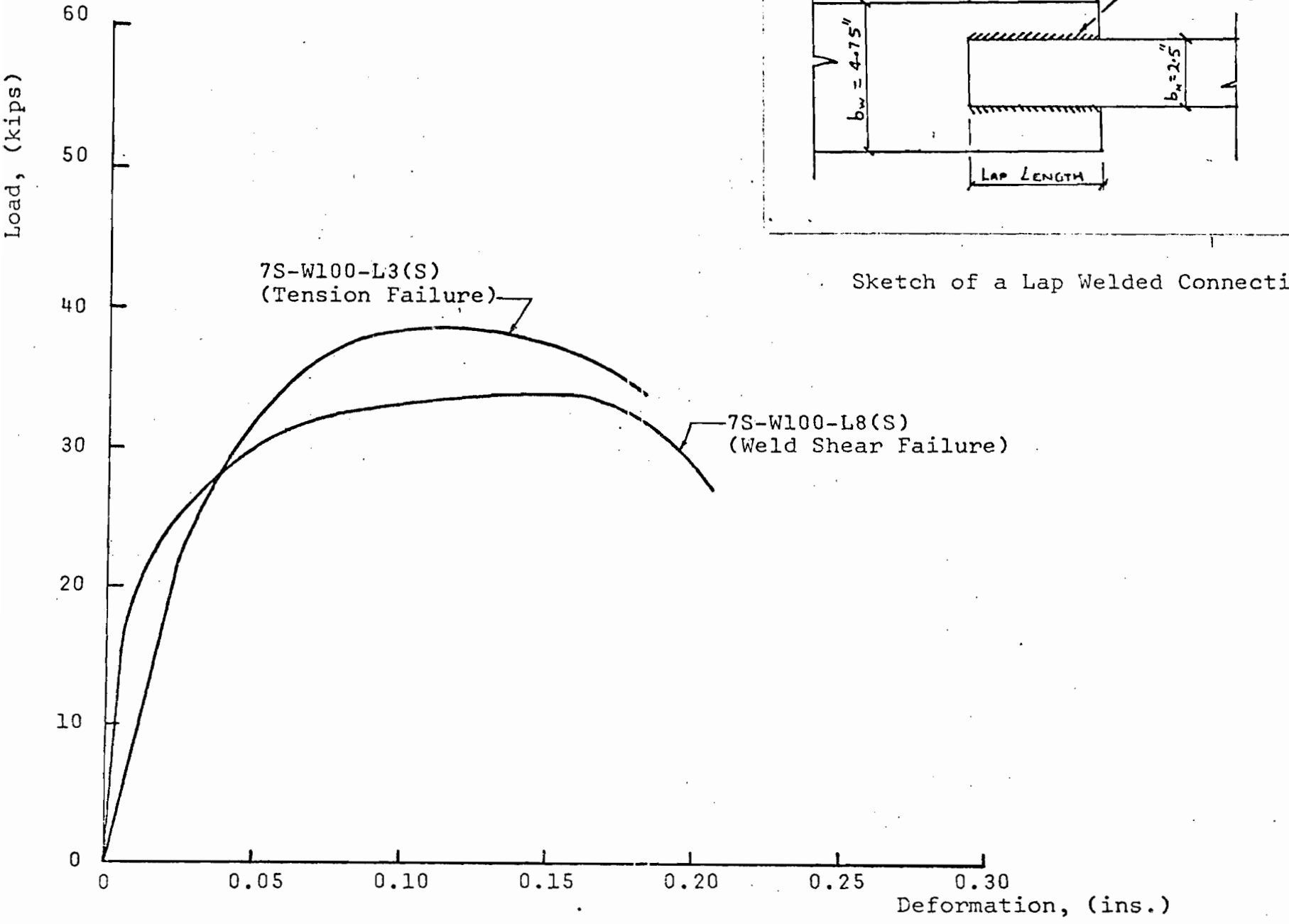

Sketch of a Lap Welded Connection

FIG. 7. LOAD-DEFORMATION CURVES OF LONGITUDINAL FILLET WELDED SPECIMENS